NASA TECHNICAL NOTE

NASA TN D-4011

A STUDY OF BALLISTIC REENTRY TRAJECTORIES AT A VELOCITY of 50 000 FEET PER SECOND (15 240 METERS PER SECOND)

by John T. Suttles and Lucille C. Coltrane

Langley Research Center
Langley Station, Hampton, Va.

NASA TN D-4011

A STUDY OF BALLISTIC REENTRY TRAJECTORIES AT A VELOCITY

OF 50 000 FEET PER SECOND (15 240 METERS PER SECOND)

By John T. Suttles and Lucille C. Coltrane

Langley Research Center
Langley Station, Hampton, Va.

NATIONAL AERONAUTICS AND SPACE ADMINISTRATION

A STUDY OF BALLISTIC REENTRY TRAJECTORIES AT A VELOCITY

OF 50 000 FEET PER SECOND (15 240 METERS PER SECOND)

By John T. Suttles and Lucille C. Coltrane
Langley Research Center

SUMMARY

Results of calculations of ballistic trajectories with an initial velocity of 50 000 ft/sec (15 240 m/sec) are presented for initial reentry angles from about -5° to -25° and for values of the ballistic coefficient from 10 to 200 lbf/ft^2 $\left(479 \text{ to } 9576 \text{ N/m}^2\right)$. The data show the following three types of trajectories: (1) those that pass through the atmosphere and exit to orbit or escape the Earth (skip-out trajectories), (2) those that experience periods of increasing altitude prior to descending to impact (skipping reentry trajectories), and (3) those that have a continuously decreasing altitude to impact (direct reentry trajectories). The altitude-velocity profiles of these ballistic trajectories are compared with the profile of a typical lifting trajectory for a return from a manned interplanetary mission. Results of this comparison indicate that a good ballistic simulation of the initial portion of the altitude-velocity profile of the lifting trajectory can be obtained for a skip-out trajectory with values of the ballistic coefficient between 100 lbf/ft^2 $\left(4788 \text{ N/m}^2\right)$ and 200 lbf/ft^2 $\left(9576 \text{ N/m}^2\right)$. A reasonable simulation can be obtained for a direct reentry trajectory with values of the ballistic coefficient of less than 100 lbf/ft^2 $\left(4788 \text{ N/m}^2\right)$. In a simulation the trajectory dispersions may be significantly reduced for the direct reentries by judicious selection of the values of ballistic coefficient and initial reentry angle whereas, for the skip-out trajectories, acceptable dispersions can be obtained only by requiring high accuracy in the initial reentry angle (i.e., error significantly less than $\pm 1^{\circ}$). It was found that the skipping reentry trajectories have long horizontal ranges and large dispersions. Thus, skipping reentries are to be avoided.

A study was also made of the sensitivity of the ballistic trajectories to velocity errors of ± 500 ft/sec (± 152 m/sec) and to perturbations in the atmospheric density. Results indicate that, whereas the skipping reentry trajectories are quite sensitive to these effects, the skip-out and direct reentry trajectories do not exhibit a significant sensitivity.

INTRODUCTION

Currently one of the primary objectives in the space sciences and aerospace engineering communities is the development of the technology required for the exploration of the planets (ref. 1). Studies (refs. 2 and 3) have shown that a manned mission to Mars would require Earth reentry velocities between 40 000 and 70 000 ft/sec (12 192 and 21 336 m/sec) depending on launch year and trip duration capabilities. As indicated in reference 4, the problem of protecting a spacecraft from the aerodynamic heating environment at these high velocities is considerably more difficult than that encountered in the Apollo program at lunar speeds of about 35 000 ft/sec (10 668 m/sec). The solution of this more difficult problem will require a better definition of the reentry heating environment at hyperbolic speeds and the determination of the performance of materials in this environment. Although some of the required information can be obtained in ground test facilities, it will be necessary to pursue flight test programs. (See ref. 4.)

The purpose of the study reported herein is to examine a series of reentry trajectories and to evaluate various approaches to conducting a flight experiment at 50 000 ft/sec (15 240 m/sec). This value of velocity was chosen since it is used throughout the literature as a typical value for Earth reentry from an interplanetary mission. (See, for example, refs. 3 to 5.) Also pointed out in these references is the necessity for utilizing a lifting reentry trajectory for the Earth reentry phase of a manned interplanetary mission. In a flight experiment it will be desirable to simulate the environment created in the lifting reentry trajectory for a manned spacecraft by using a ballistic reentry. In reference 4 it is suggested that one interesting approach would involve a spin-stabilized spacecraft that reenters at a very shallow angle, passes through the atmosphere, and exits into an escape or orbital trajectory. This approach is in contrast to the more usual type of ballistic reentry in which the spacecraft reenters at a relatively steep angle and has a constantly decreasing altitude until impact. In the present study, trajectory calculations were made for ballistic reentries ranging from the very shallow reentries to the relatively steep reentries in order to determine the limitations of the contrasting approaches to simulating a lifting trajectory.

SYMBOLS

The physical quantities defined in this paper are given first in the U.S. Customary System of Units and parenthetically in the International System of Units (SI). Factors relating the two systems are given in reference 6.

A   reference area, feet^2 $\left(\text{meters}^2\right)$

a_x acceleration along flight path, g units $\left(\text{1g unit} = 9.8 \text{ meters/second}^2\right)$

2

C_D drag coefficient

h_O initial altitude above Earth's surface, feet (meters)

L/D lift-drag ratio

V_O initial Earth relative velocity, feet/second (meters/second)

W weight, pounds force (newtons)

α_O initial azimuth angle, degrees

γ_O initial reentry angle (negative values indicate angles below the local horizontal), degrees

ρ atmospheric density

METHOD

The trajectory data presented were computed on a digital computer utilizing a three-dimensional particle trajectory program which is documented in reference 7. The computations were performed for a rotating, oblate spheroidal Earth, with detailed atmospheric data obtained from reference 8. The initial conditions for the computations were:

$$V_O = 50\ 000 \text{ ft/sec}\quad (15\ 240 \text{ m/sec})$$

$$= 49\ 500 \text{ ft/sec}\quad (15\ 088 \text{ m/sec})$$

$$= 50\ 500 \text{ ft/sec}\quad (15\ 392 \text{ m/sec})$$

$$h_O = 400\ 000 \text{ feet}\quad (121\ 920 \text{ meters})$$

$$\alpha_O = 122.867^O$$

Longitude 16.95^O West

Latitude 7.37^O South

The azimuth and position values were chosen as typical for a reentry occurring near Ascension Island. For the computations the values of γ_O were varied from about -5° to -25° and values of $\dfrac{W}{C_D A}$ were varied from 10 to 200 lbf/ft^2 $\left(479 \text{ to } 9576 \text{ N/m}^2\right)$.

The altitude-velocity profiles of the computed ballistic trajectories were compared with the profile of a typical lifting trajectory for a reentry from a manned interplanetary mission. The typical lifting reentry trajectory was taken from reference 5 and is presented in figure 1. In simulating a lifting reentry with a ballistic reentry, one must concentrate on accomplishing the simulation for a portion of the trajectory only. In this work it has been assumed that the initial portion of the lifting trajectory through pullout is the important portion to simulate. This assumption is based on data presented in reference 5 which indicate that the maximum aerodynamic heating occurs in the initial portion of the trajectory. It should be emphasized that in discussing simulation of the lifting trajectory in this work no regard is given to the simulation of the time histories of trajectory parameters. The conditions for simulation herein are based solely on matching altitude and velocity conditions.

In examining the results of the computations, it is convenient to define three types of trajectories. The trajectory of a spacecraft which reenters at a shallow angle, passes through the atmosphere, and exits into an escape or orbital trajectory is defined in this work as a "skip-out" trajectory. A trajectory which has an initial reentry angle such that oscillations in the altitude occur prior to impact is defined as a "skipping reentry" trajectory. A trajectory with a relatively steep reentry angle so that the altitude decreases continuously to impact is defined as a "direct reentry" trajectory. This nomenclature is used throughout the present report, and the trajectories are illustrated in figure 2.

Most of the calculations were made for an initial velocity of 50 000 ft/sec (15 240 m/sec); however, some calculations were made for initial velocities of 49 500 ft/sec (15 088 m/sec) and 50 500 ft/sec (15 392 m/sec) to determine the effects of velocity errors of ±500 ft/sec (±152 m/sec).

A study was also made of the effects of atmospheric-density perturbations on the reentry trajectories. Values of atmospheric density such as those given in reference 8 are obtained by averaging data for a wide range of conditions. The actual atmospheric densities for a particular location, season of year, and time of day can differ considerably from these averaged values. It is assumed that many of these variables can be eliminated when a flight plan is established; however, values of atmospheric density are subject to unpredictable variations even when a location, season of year, and time of day are known. Values of these unpredictable variations, obtained by consulting the meteorological section at the Eastern Test Range, Patrick Air Force Base, Fla., are presented in figure 3. These values represent estimates based on data obtained up to this time along the meteorological network downrange at the Eastern Test Range. These variations were applied to the values given in reference 8 for some of the computations

to obtain an indication of the effect of atmospheric-density perturbations on the trajectories.

RESULTS AND DISCUSSION

Basic Reentry Trajectory Data

The basic results are presented in figures 4 to 9 in the form of graphs showing altitude-velocity profiles, altitude-range profiles, and time histories of altitude, velocity, acceleration along the fligh path, and dynamic pressure. These results were obtained for an initial velocity of 50 000 ft/sec (15 240 m/sec), for values of γ_0 from about -5° to -25°, and for values of the ballistic coefficient $\frac{W}{C_D A}$ from 10 to 200 lbf/ft² $\left(479 \text{ to } 9576 \text{ N/m}^2\right)$. These data show skip-out, skipping reentry, and direct reentry trajectories. The typical Earth reentry trajectory for a manned lifting spacecraft, given in figure 1, has been reproduced on the altitude-velocity profiles in figure 4 for comparison purposes.

Skipping Reentry Trajectories

Because of the long horizontal range and range sensitivity, shown in the altitude-range profiles in figure 5, much care should be taken to avoid a skipping reentry trajectory in a ballistic flight experiment. For this reason the combinations of the primary variables of this study, γ_0 and $\frac{W}{C_D A}$, which result in skipping reentry trajectories have been defined and presented in figure 10. The boundary between skip-out and skipping reentry trajectories was determined to the nearest 1/8° and the boundary between direct reentry and skipping reentry trajectories was determined to the nearest 1/4°.

Skip-Out Trajectories

As mentioned in the introduction, one interesting approach to simulating a lifting trajectory involves the use of a skip-out ballistic trajectory. For a skip-out trajectory the minimum altitude is important. In figure 11 the minimum altitudes for the trajectories have been taken from figure 4 and plotted against γ_0 for the various values of $\frac{W}{C_D A}$. It is interesting to note that the data for all values of $\frac{W}{C_D A}$ appear on a single curve. These results therefore show that, in order to obtain a particular minimum altitude to correspond to the pullout altitude of a lifting trajectory, there is only one value of γ_0 which could be used. The value of γ_0 for a skip-out ballistic trajectory is therefore dictated only by the desired minimum altitude.

Whereas the desired minimum altitude dictates the values of γ_0 for a skip-out ballistic trajectory, the desired shape of the altitude-velocity profile dictates the selection

of $\dfrac{W}{C_D A}$. The shaping of a skip-out trajectory with $\dfrac{W}{C_D A}$ can be appreciated by comparing in figures 4(d) to 4(g) the lifting trajectory with the skip-out ballistic trajectories for $\gamma_O = -7.0^O$ and for values of $\dfrac{W}{C_D A}$ of 40 lbf/ft^2 $\left(1915 \text{ N/m}^2\right)$, 60 lbf/ft^2 $\left(2873 \text{ N/m}^2\right)$, 100 lbf/ft^2 $\left(4788 \text{ N/m}^2\right)$, and 200 lbf/ft^2 $\left(9576 \text{ N/m}^2\right)$. It is indicated that a good matching of the initial portion of the altitude-velocity profiles can be obtained for values of $\dfrac{W}{C_D A}$ between 100 lbf/ft^2 $\left(4788 \text{ N/m}^2\right)$ and 200 lbf/ft^2 $\left(9576 \text{ N/m}^2\right)$ but not for the lower values.

In examining the data for the skip-out trajectories, it is apparent that these trajectories are very sensitive to changes in γ_O. Since a tolerance in γ_O must be allowed for launch-vehicle inaccuracies, the dispersions in the trajectory due to changes in γ_O must be determined. An indication of these dispersions can be obtained by calculating the slope of the curve in figure 11. The slope of the curve does not change appreciably over the range of data presented, so the slope was computed graphically at a representative altitude of 200 000 feet (60 960 meters). The value obtained (see fig. 11) indicates that the minimum altitude for a skip-out trajectory will vary about 60 000 feet (18 288 meters) for each degree variation in γ_O. Therefore, unless an accuracy in γ_O significantly better than $\pm 1^O$ can be obtained, large dispersions result. It is important to note that the dispersion for a skip-out trajectory can be improved only by improving the accuracy in γ_O.

Direct Reentry Trajectories

It can be seen in figure 4 that for all values of $\dfrac{W}{C_D A}$ less than 100 lbf/ft^2 $\left(4788 \text{ N/m}^2\right)$ a value of γ_O can be selected such that a reasonable simulation of the initial portion of the lifting trajectory can be obtained with a direct reentry ballistic trajectory. For these ballistic reentries the horizontal range and the sensitivity of this range to γ_O and $\dfrac{W}{C_D A}$ are important because of mission requirements such as data acquisition, range safety, and spacecraft recovery. In figure 12 the horizontal range from the reentry point ($h_O = 400 000$ feet (121 920 meters)) to impact for the direct reentry trajectories is presented. The data show that the range is not particularly sensitive to $\dfrac{W}{C_D A}$ but is very sensitive to γ_O at values approaching the skipping reentry condition. It is seen that the magnitude of the range as well as its sensitivity to variations in γ_O can be significantly reduced by selecting values of γ_O steeper than -10°. Therefore, in contrast to the skip-out trajectories, the dispersions of a direct reentry trajectory can not only be reduced by improving the accuracy in γ_O but may also be reduced by a judicious selection of the values of γ_O and $\dfrac{W}{C_D A}$ to achieve the simulation.

Whereas the range and its dispersions can be reduced by selecting relatively steep values of γ_O, the data in figures 13 and 14 show that the dynamic pressure and longitudinal

acceleration can be reduced by selecting relatively shallow values of γ_0. Therefore, if the dynamic pressure or longitudinal acceleration becomes too large, some compromise may be required with the trajectory dispersions. Also shown in figures 13 and 14 is the fact that, whereas $\frac{W}{C_D A}$ has little effect on longitudinal acceleration, the dynamic pressure can be significantly reduced by limiting $\frac{W}{C_D A}$ to small values.

Effect of Velocity Errors

The data in figures 15 to 20 show the effects of increasing and decreasing the initial velocity of 50 000 ft/sec (15 240 m/sec) by 500 ft/sec (152 m/sec). These computations were made for values of γ_0 from about -6° to -25° and for values of $\frac{W}{C_D A}$ of 20 lbf/ft^2 (958 N/m^2) and 60 lbf/ft^2 (2873 N/m^2). These data indicate that only the skipping reentry trajectories exhibit a high sensitivity to these velocity variations. However, the skip-out trajectories are somewhat more sensitive than the direct reentry trajectories.

Effect of Atmospheric-Density Perturbations

In figures 21 to 26 data are presented which show the effects of the atmospheric-density variations shown in figure 3. These computations were made for an initial velocity of 50 000 ft/sec (15 240 m/sec), for values of γ_0 from about -6° to -25°, and for values of $\frac{W}{C_D A}$ of 20 lbf/ft^2 (958 N/m^2) and 60 lbf/ft^2 (2873 N/m^2). These data also indicate that the skip-out trajectories are more sensitive to the density variations than the direct reentry trajectories but that only the skipping reentry trajectories exhibit a high sensitivity.

CONCLUDING REMARKS

The results of computations of ballistic reentry trajectories at a velocity of 50 000 ft/sec (15 240 m/sec) show skip-out, skipping reentry, and direct reentry trajectories. The altitude-velocity profiles of these ballistic trajectories have been compared with the profile of a typical lifting trajectory for the return from a manned interplanetary mission. A good simulation of the initial portion of the profile of the lifting trajectory can be obtained with a skip-out ballistic trajectory. This simulation requires values of the ballistic coefficient of between 100 and 200 lbf/ft^2 (4788 and 9576 N/m^2). In order to reduce the dispersions of these skip-out trajectories, a high degree of accuracy in the initial reentry angle (i.e., error significantly less than ±1°) is required. The results show that the skipping reentry trajectories have long horizontal ranges and large range dispersions, so these trajectories are to be avoided. A reasonable simulation of the initial portion of the altitude-velocity profile of the lifting trajectory can be obtained with

a direct reentry trajectory for values of the ballistic coefficient of less than 100 lbf/ft^2 $(4788 \ N/m^2)$. For the direct reentries the dispersions can be significantly reduced by a judicious selection of values of initial reentry angle and ballistic coefficient for the simulation. In addition, the results of a study of the sensitivity of the trajectories to initial-velocity and density perturbations indicate that, whereas the skipping reentry trajectories are very sensitive to these effects, neither the skip-out nor the direct reentry trajectories exhibit significant sensitivity.

Langley Research Center,
National Aeronautics and Space Administration,
Langley Station, Hampton, Va., February 16, 1967,
124-07-01-41-23.

REFERENCES

1. Anon.: AIAA/AAS Stepping Stones to Mars Meeting, Am. Inst. Aeron. Astronaut., Mar. 1966.

2. Sohn, Robert L.: Manned Mars Trips Using Venus Swingby Modes. Third Manned Space Flight Meeting, Am. Inst . Aeron. Astronaut., Nov. 1964, pp. 330-338.

3. Pritchard, E. Brian: Velocity Requirements and Re-Entry Flight Mechanics for Manned Mars Missions. J. Spacecraft Rockets, vol. 1, no. 6, Nov.-Dec. 1964, pp. 605-610.

4. Roberts, Leonard: Entry Into Planetary Atmospheres. Astronaut. Aeron., vol. 2, no. 10, Oct. 1964, pp. 22-29.

5. Anon.: Study of Heat Shielding Requirements for Manned Mars Landing and Return Missions. 4-74-64-1 (Contract NAS 2-1798), Lockheed Missiles & Space Co., Dec. 1964.

6. Mechtly, E. A.: The International System of Units — Physical Constants and Conversion Factors. NASA SP-7012, 1964.

7. Dennison, A. J.; and Butler, J. F.: Missile and Satellite Systems Program for the I.B.M. 7090. Tech. Inform. Ser. No. 61 SD 170, Missile and Space Vehicle Dept., Gen. Elec. Co., Feb. 1962.

8. Anon.: U.S. Standard Atmosphere, 1962. NASA, U.S. Air Force, and U.S. Weather Bur., Dec. 1962.
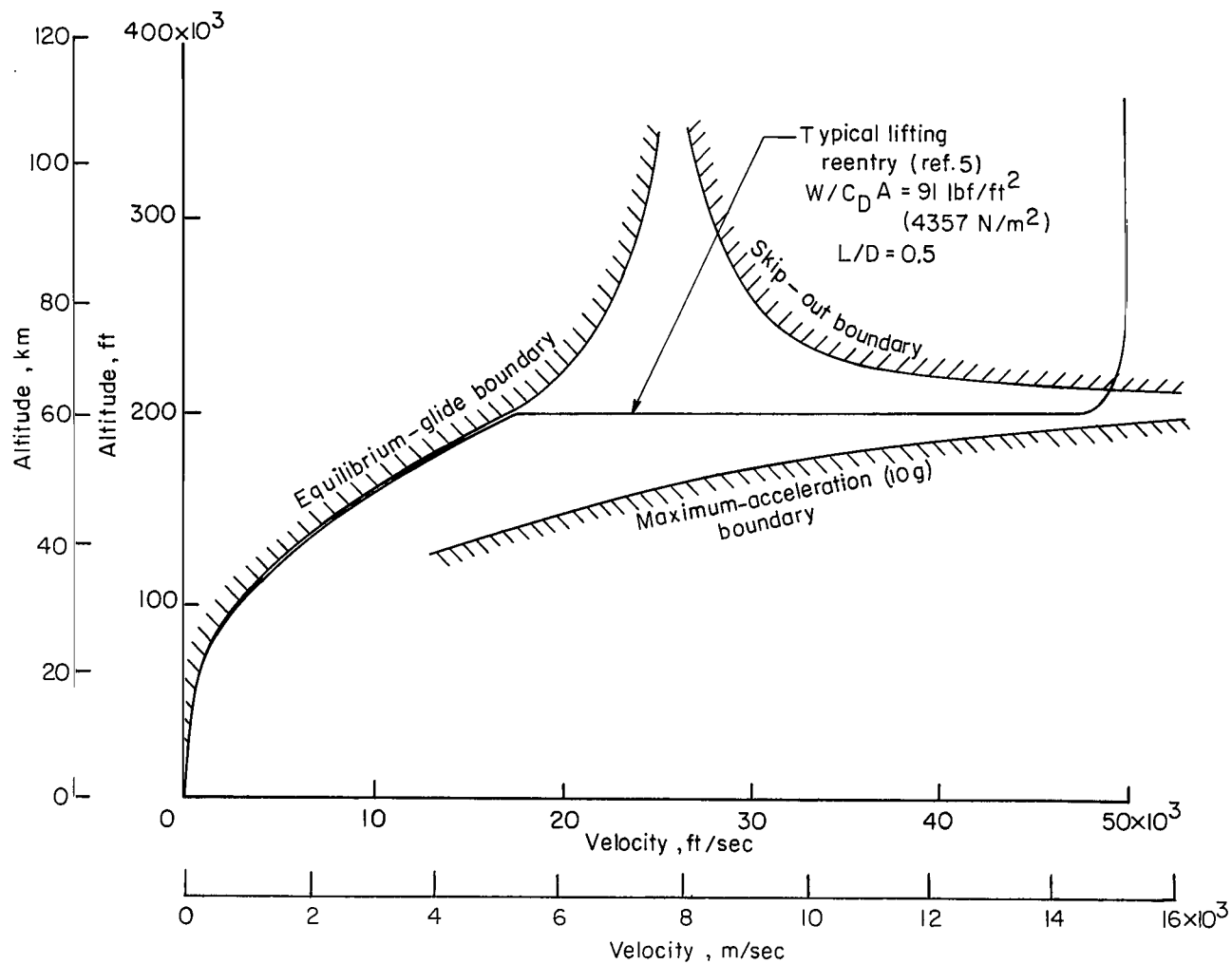
Figure 1.- Typical Earth reentry trajectory for a manned lifting spacecraft (ref. 5).
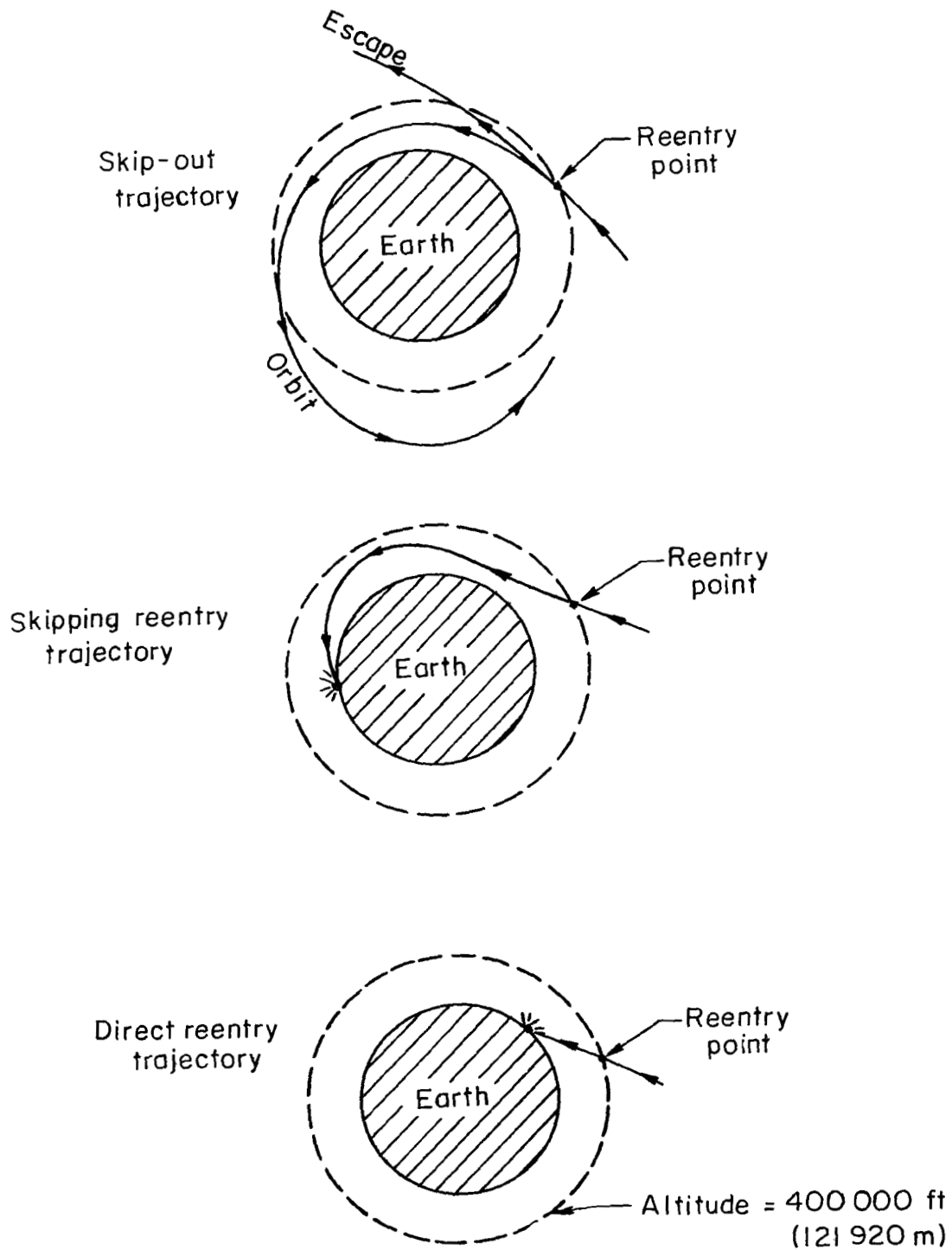
Figure 2.- Various types of reentry trajectories.
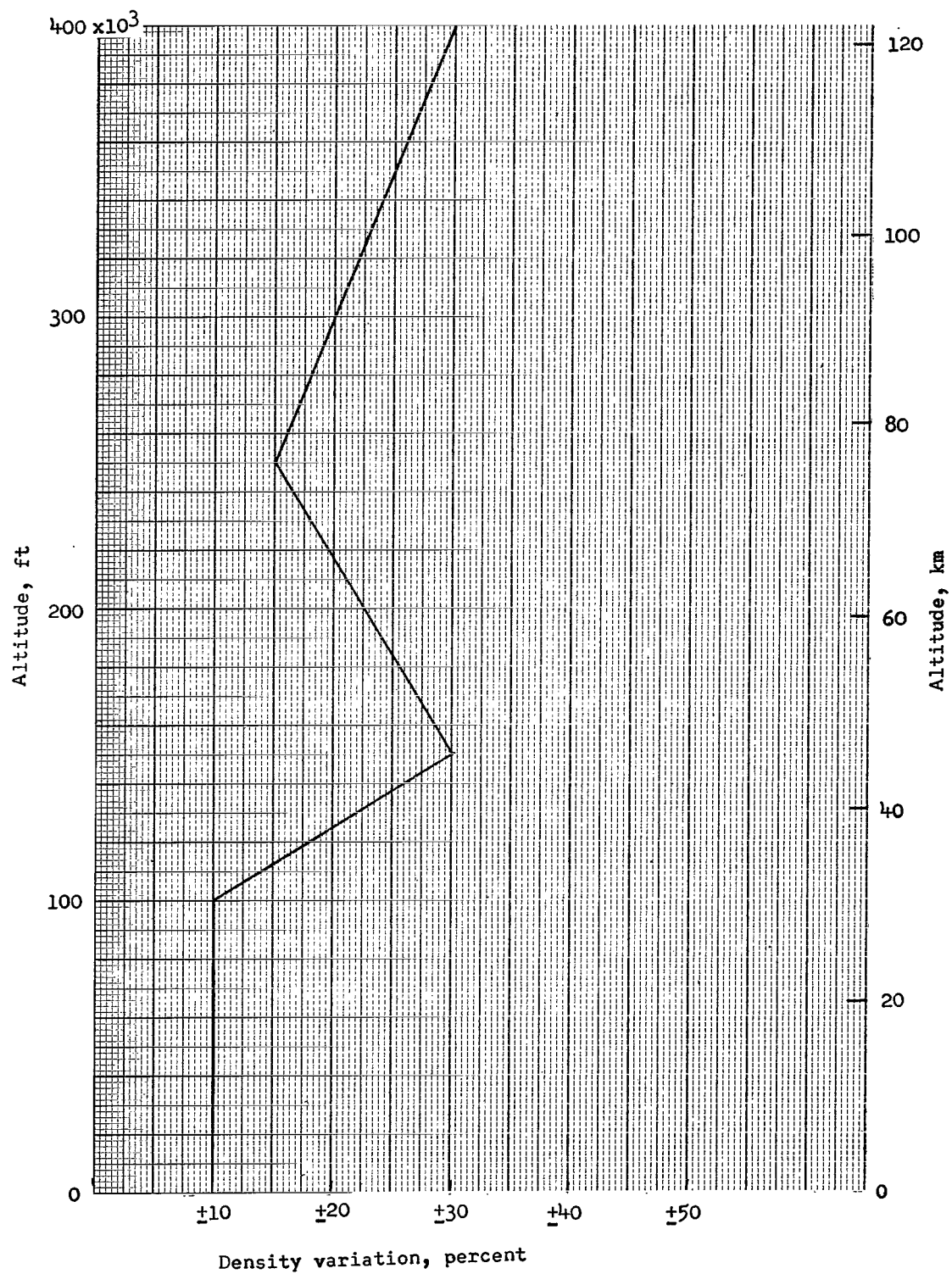
Figure 3.- Density variations applied in the present study to standard values in reference 8.
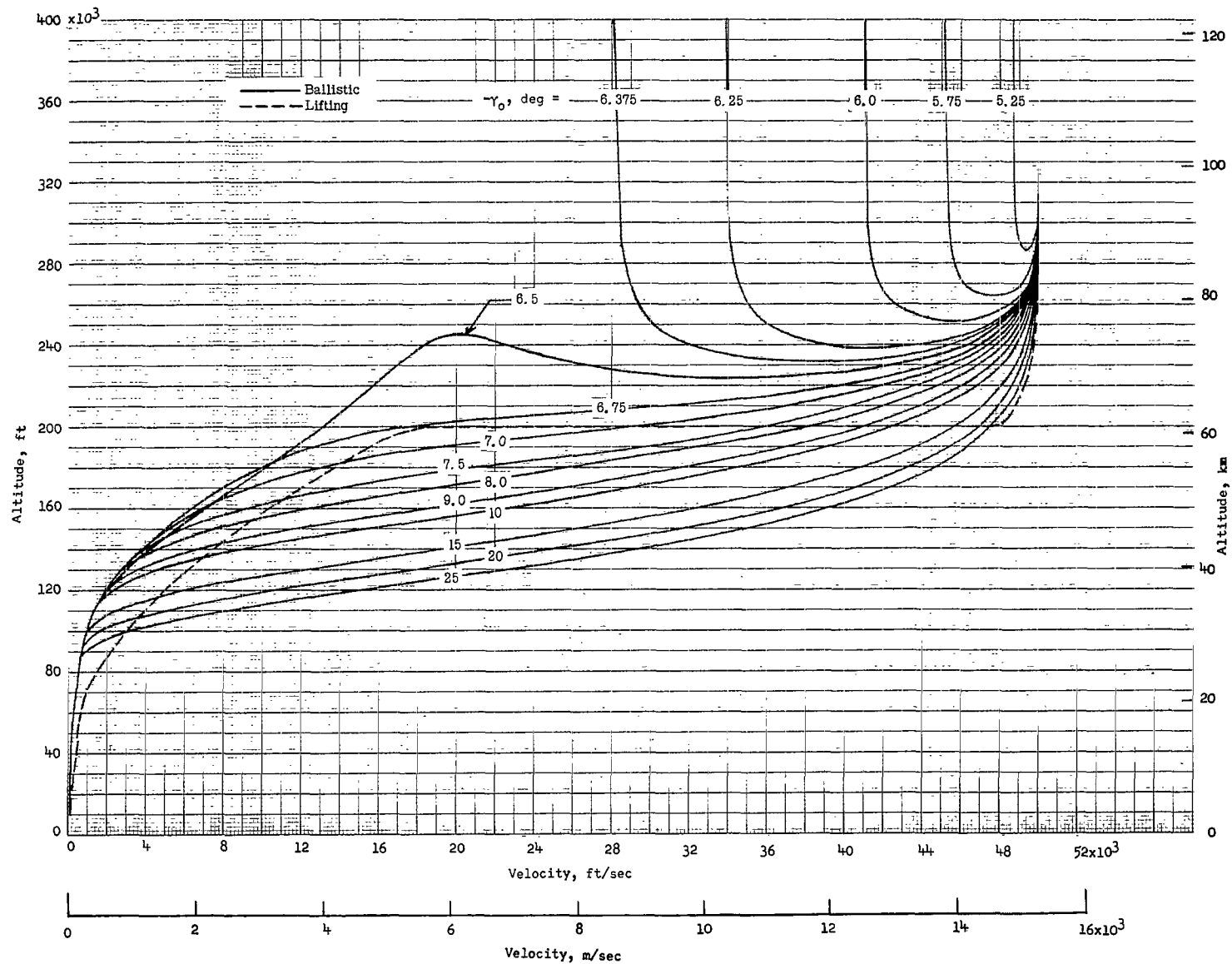
(a) $\dfrac{W}{C_D A} = 10$ lbf/ft^2 $\left(479 \text{ N/m}^2\right)$.

Figure 4.- Effect of initial reentry angle on the altitude-velocity profile for ballistic trajectories. $V_0 = 50\,000$ ft/sec (15 240 m/sec).
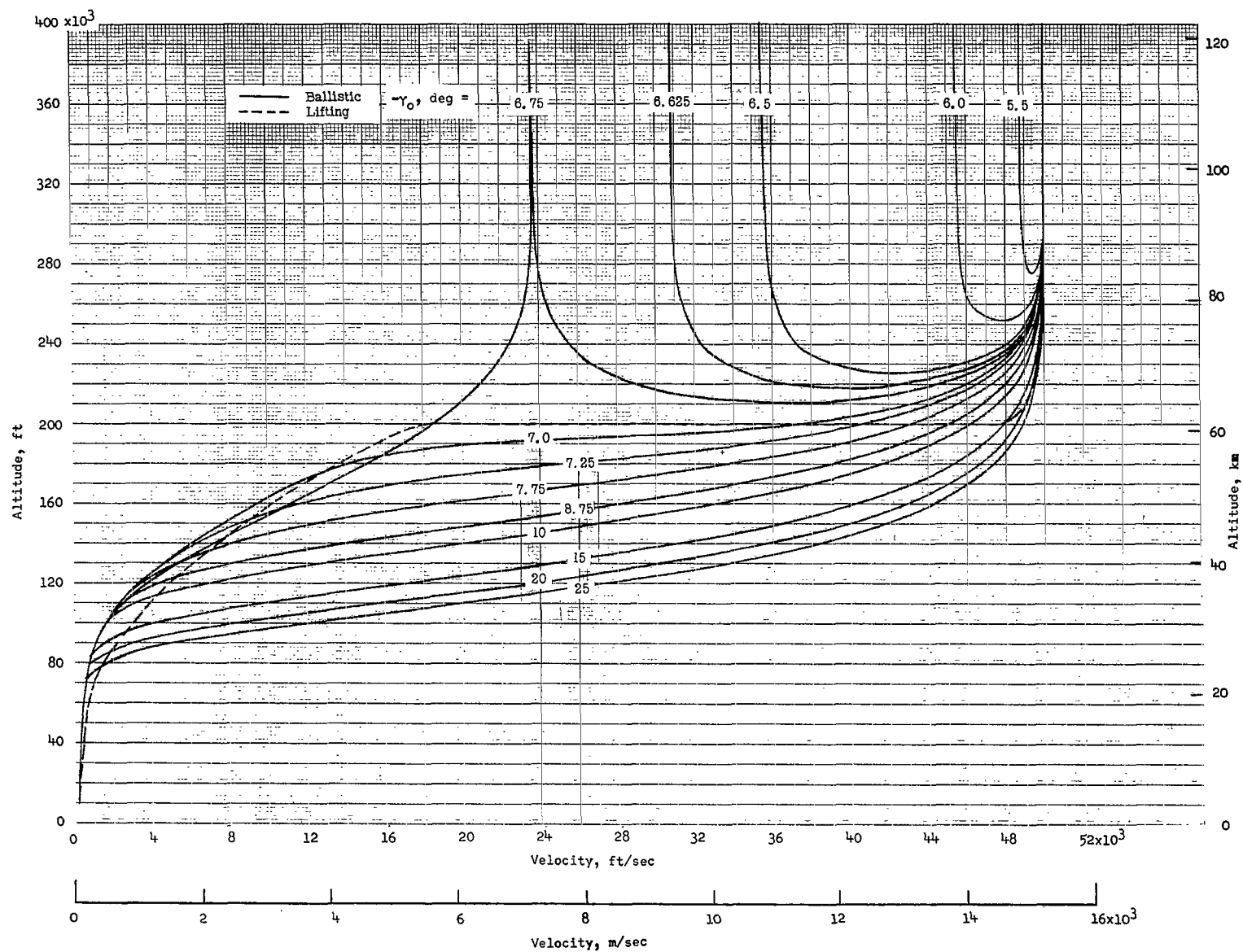
(b) $\frac{W}{C_D A} = 20$ lbf/ft^2 $\left(958 \text{ N/m}^2\right)$.

Figure 4.- Continued.
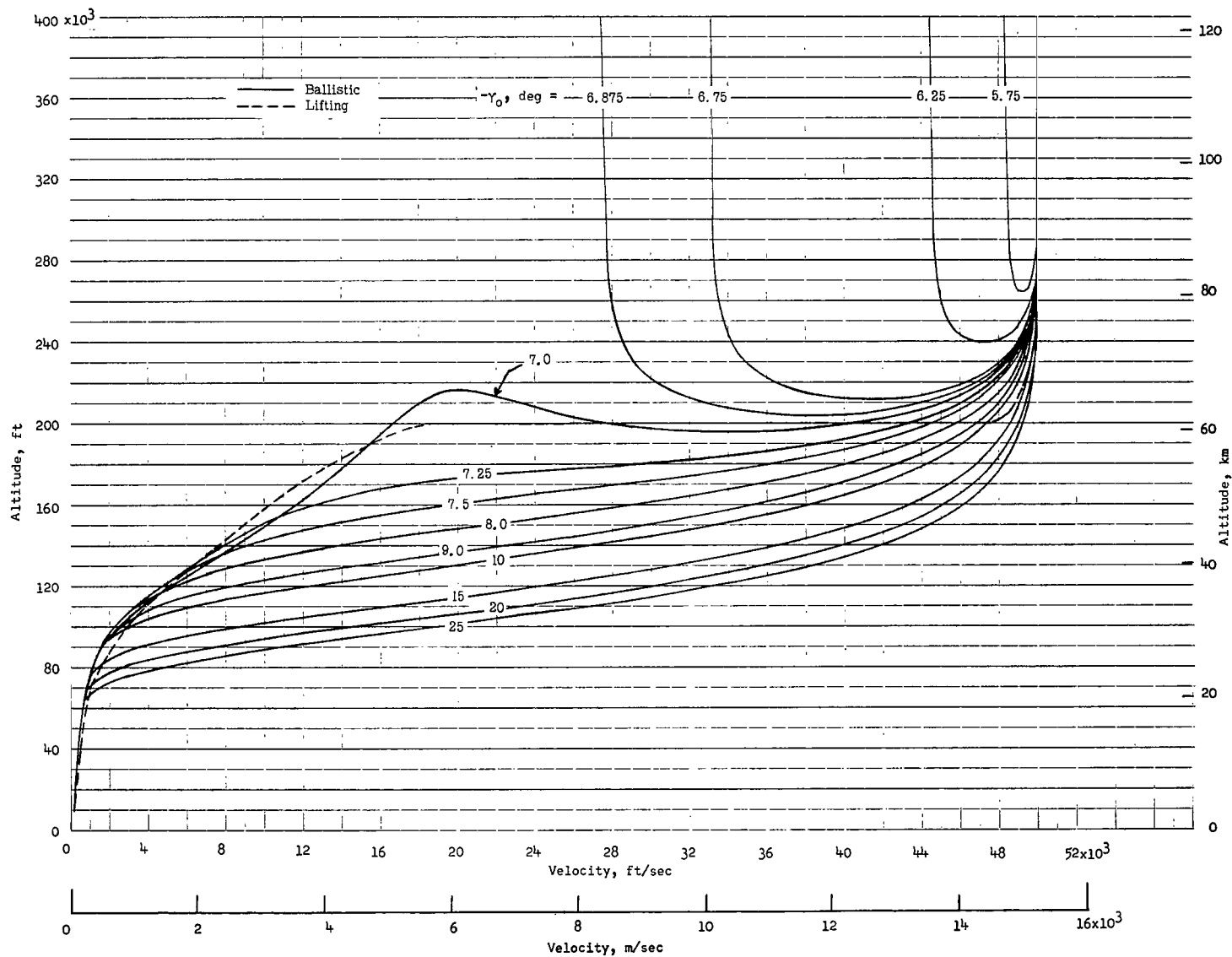
(c) $\frac{W}{C_DA} = 30 \text{ lbf}/\text{ft}^2$ $\left(1436 \text{ N}/\text{m}^2\right)$.

Figure 4.- Continued.

15
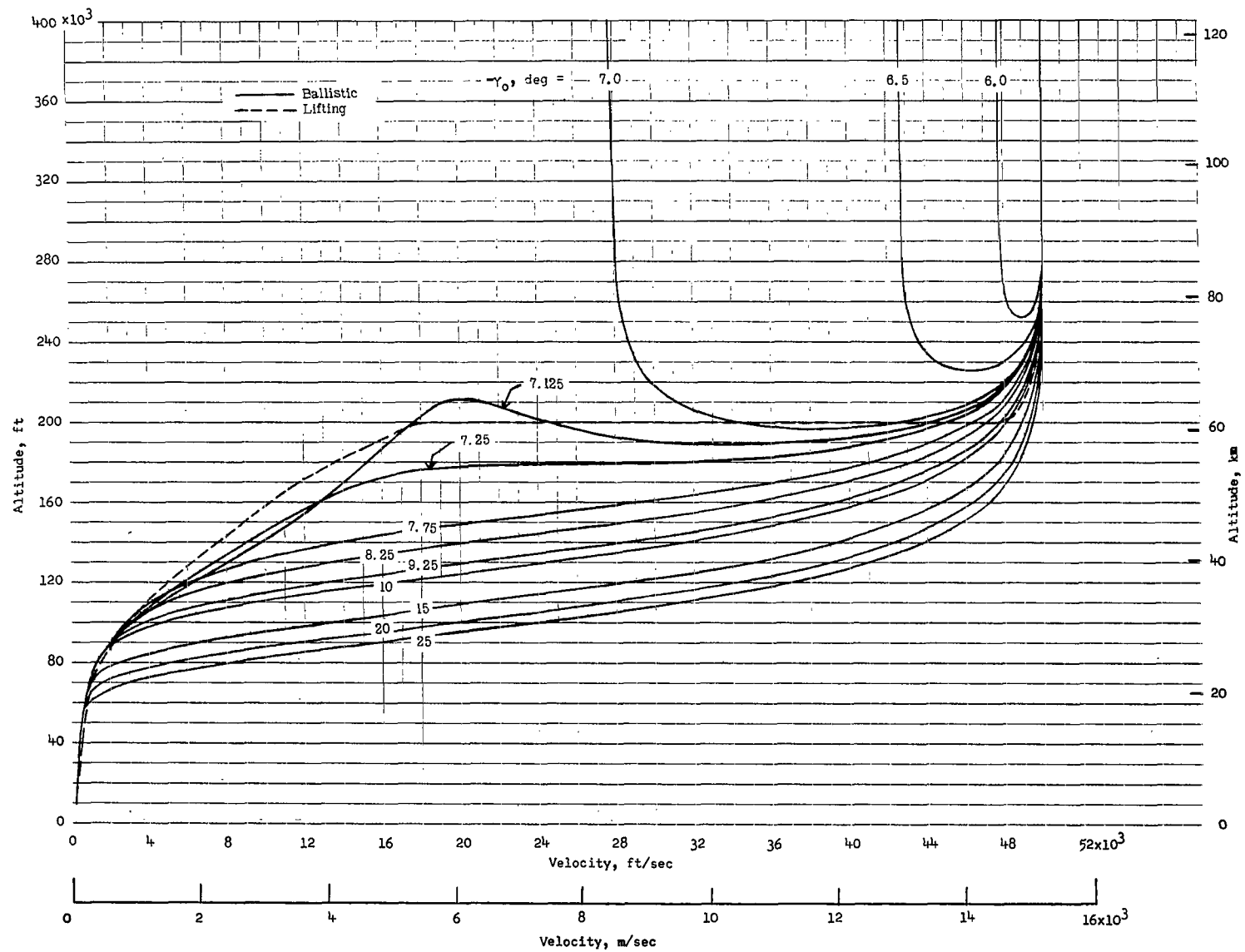
(d) $\dfrac{W}{C_D A} = 40 \text{ lbf/ft}^2 \left(1915 \text{ N/m}^2\right)$.

Figure 4.- Continued.
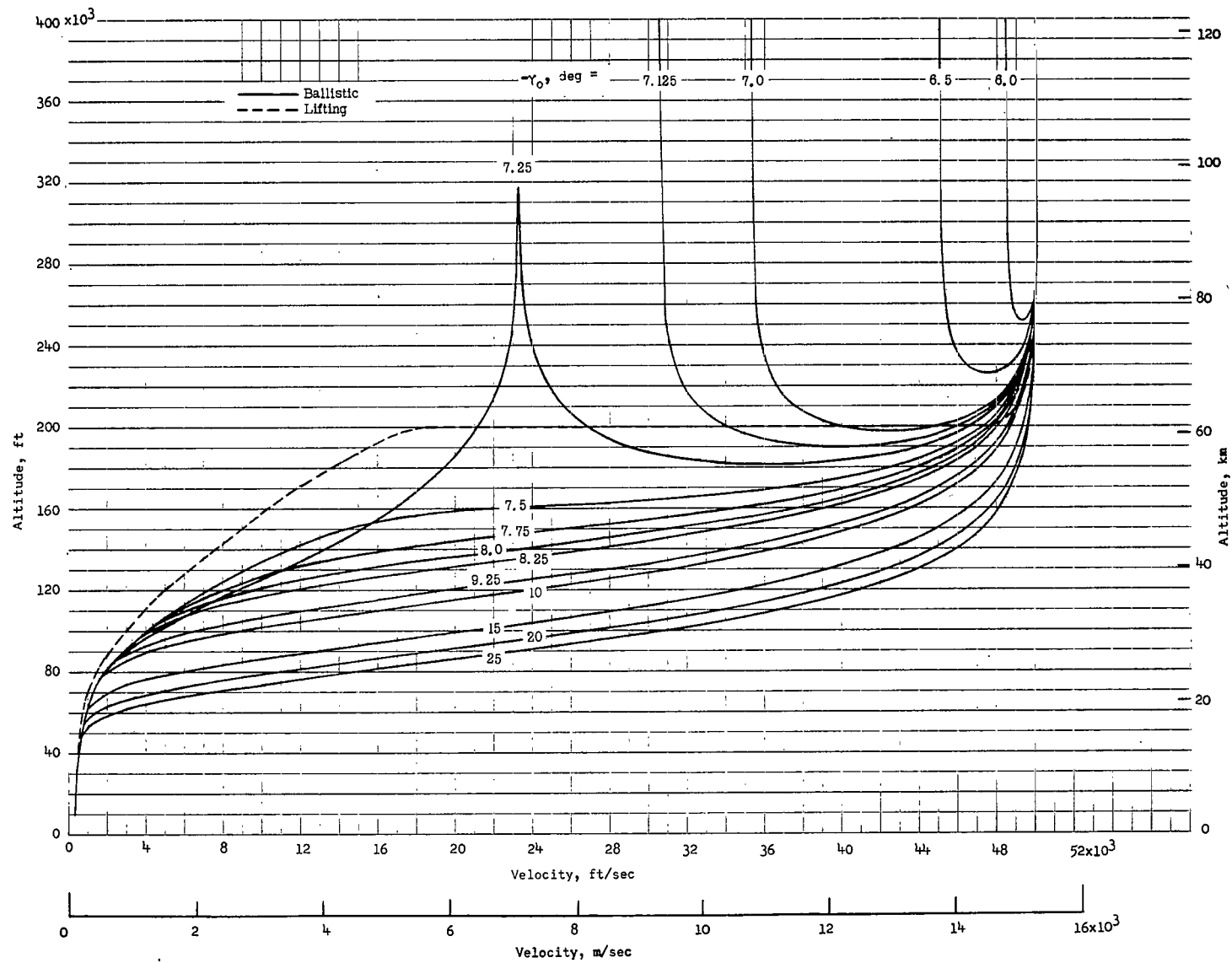
(e) $\frac{W}{C_D A}$ = 60 lbf/ft^2 (2873 N/m^2).

Figure 4.- Continued.
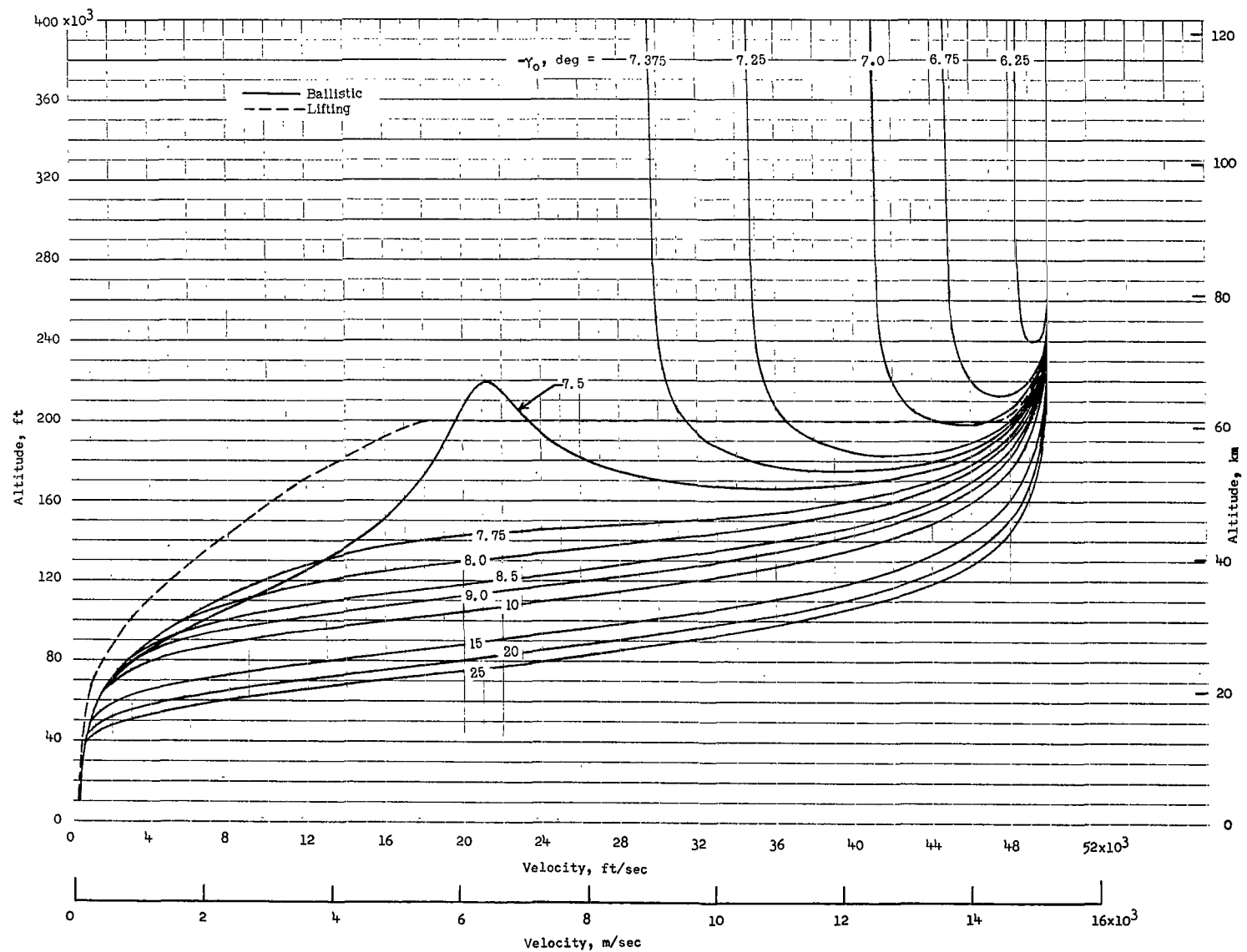
(f) $\frac{W}{C_D A}$ = 100 lbf/ft^2 (4788 N/m^2).

Figure 4.- Continued.
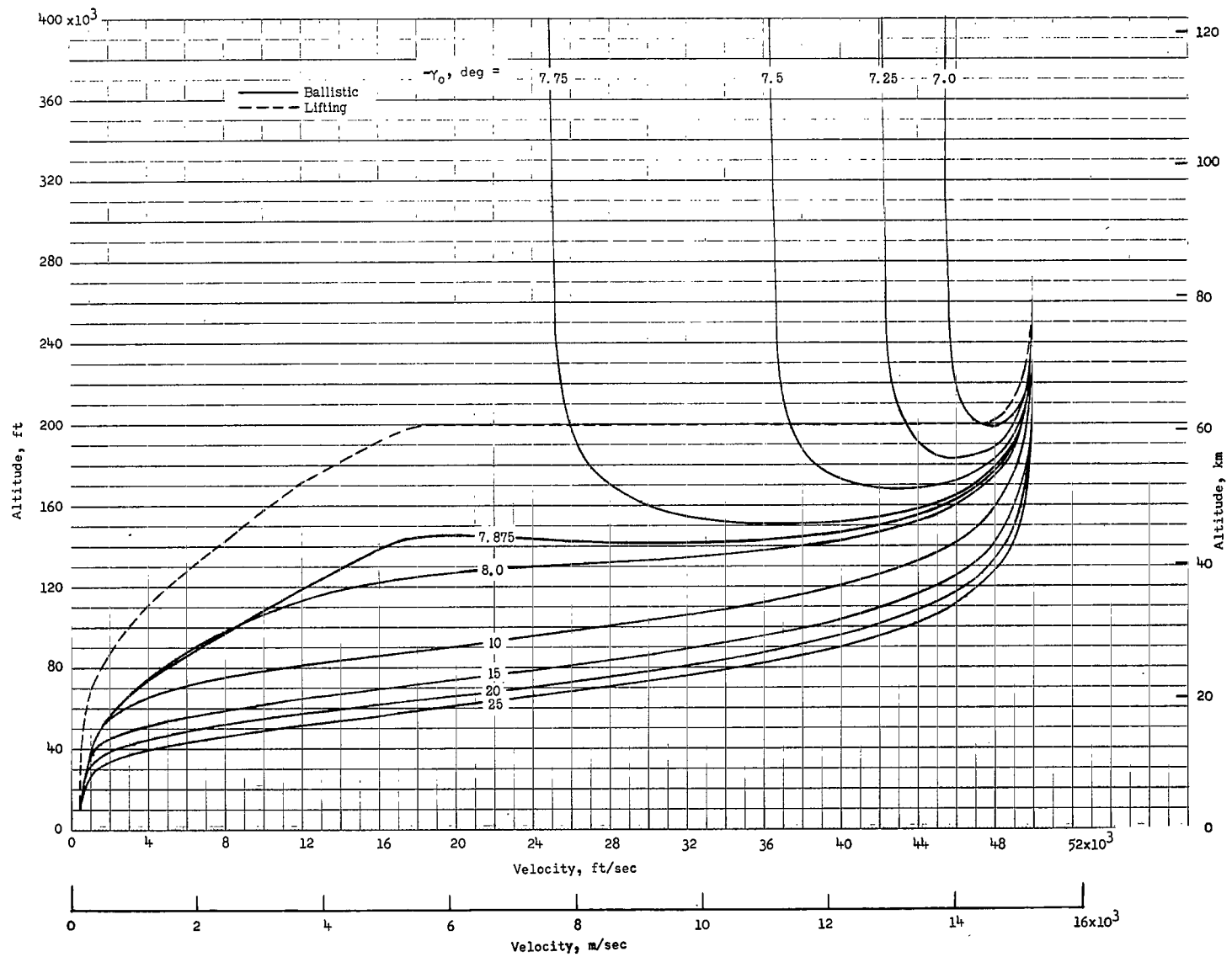
(g) $\frac{W}{C_D A} = 200 \text{ lbf/ft}^2$ (9576 N/m^2).

Figure 4.- Concluded.
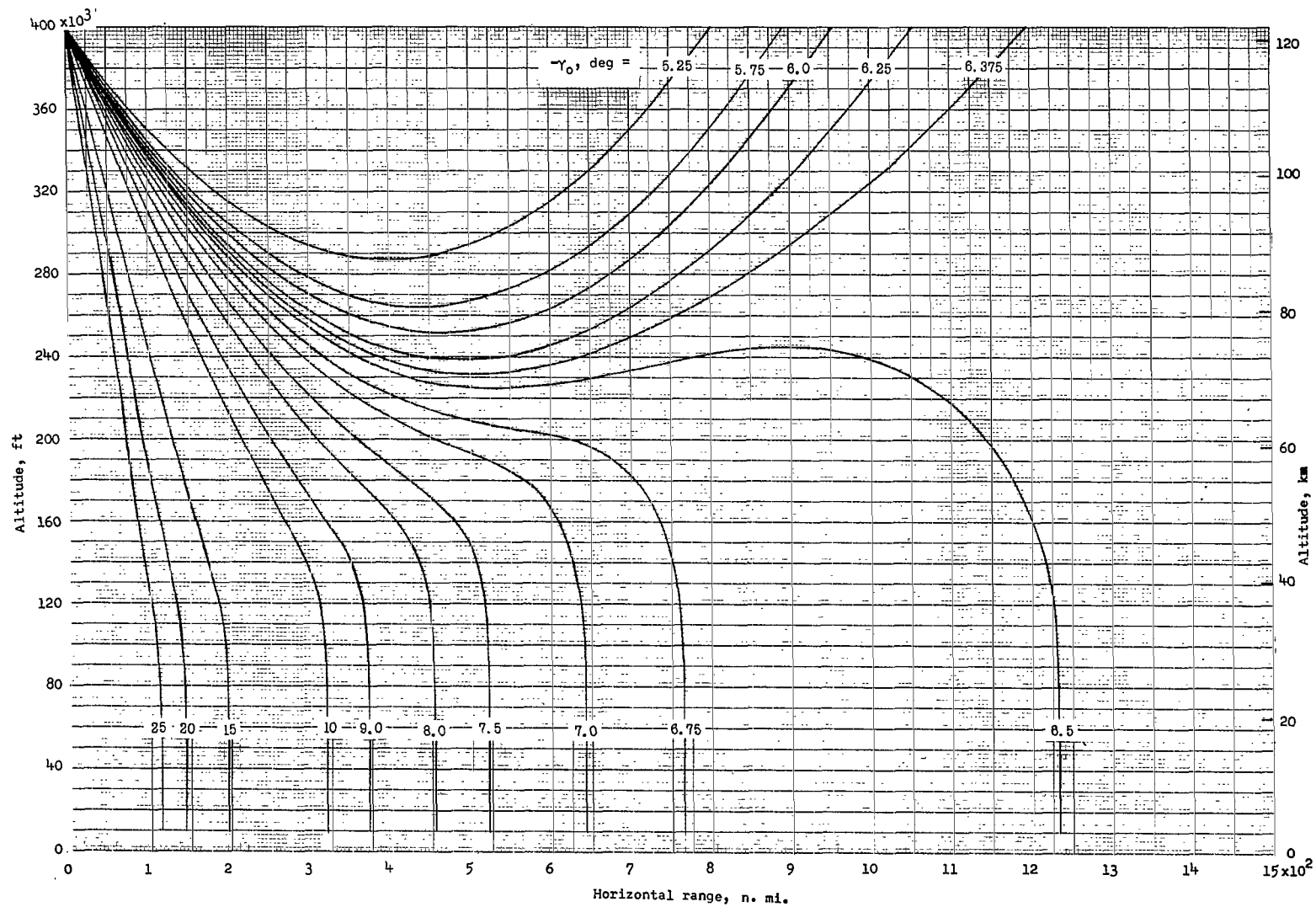
(a) $\dfrac{W}{C_D A} = 10$ lbf/ft^2 $\left(479 \text{ N/m}^2\right)$.

Figure 5.- Effect of intitial reentry angle on the altitude-range profile for ballistic trajectories. $V_0 = 50\ 000$ ft/sec (15 240 m/sec).
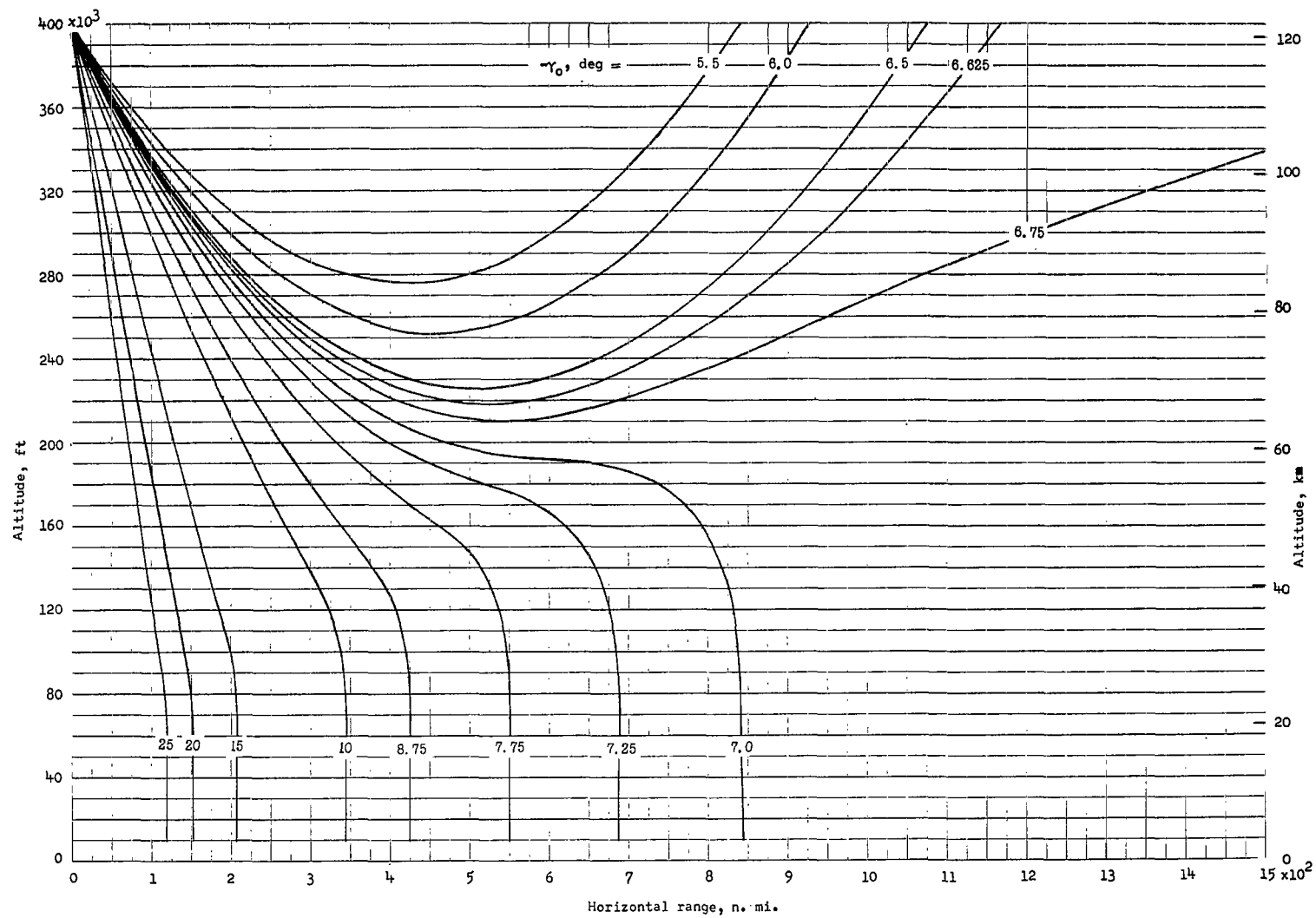
(b) $\frac{W}{C_D A} = 20 \ lbf/ft^2 \ \left(958 \ N/m^2\right)$.

Figure 5.- Continued.
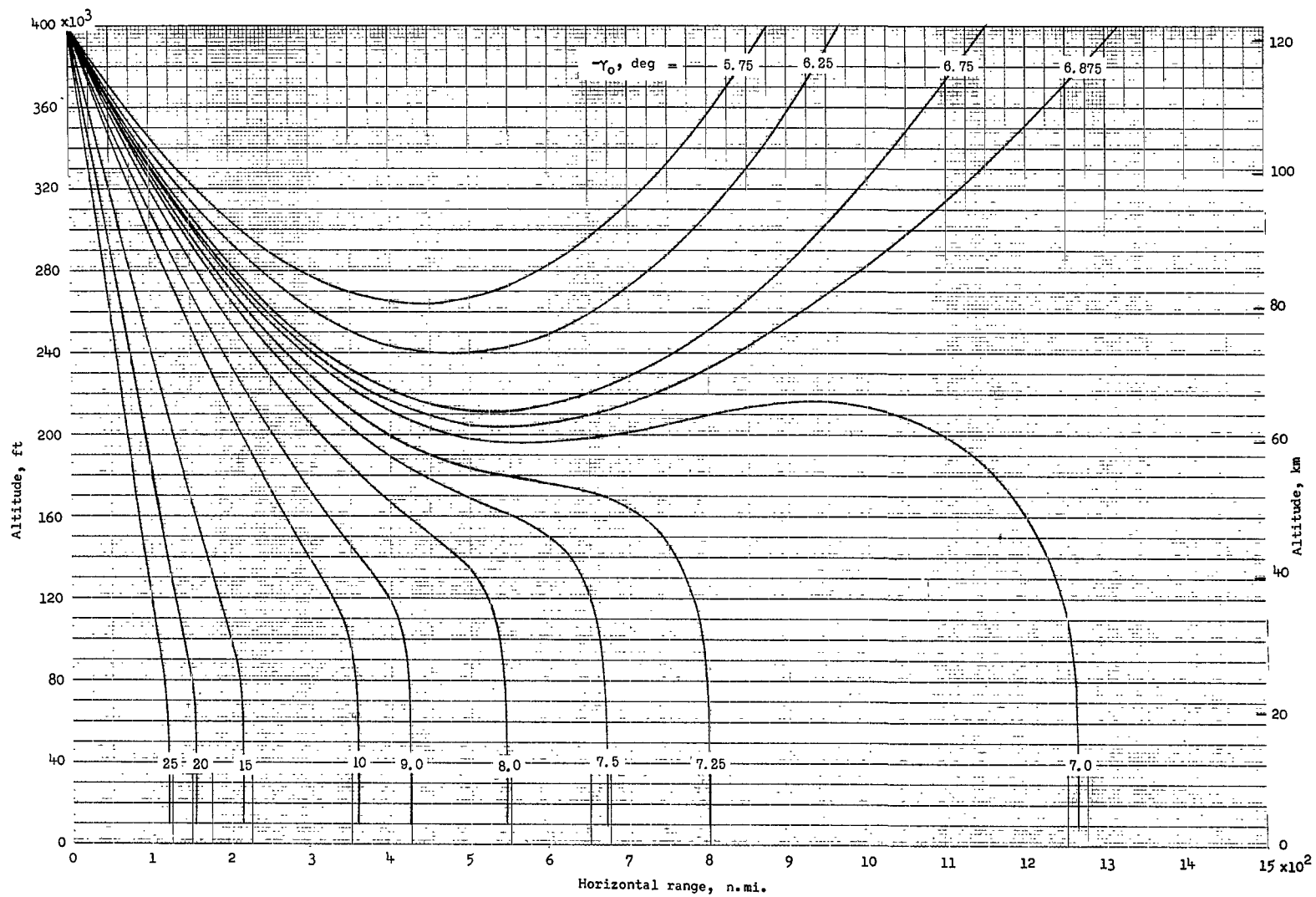
(c) $\frac{W}{C_D A} = 30$ lbf/ft^2 (1436 N/m^2).

Figure 5.- Continued.
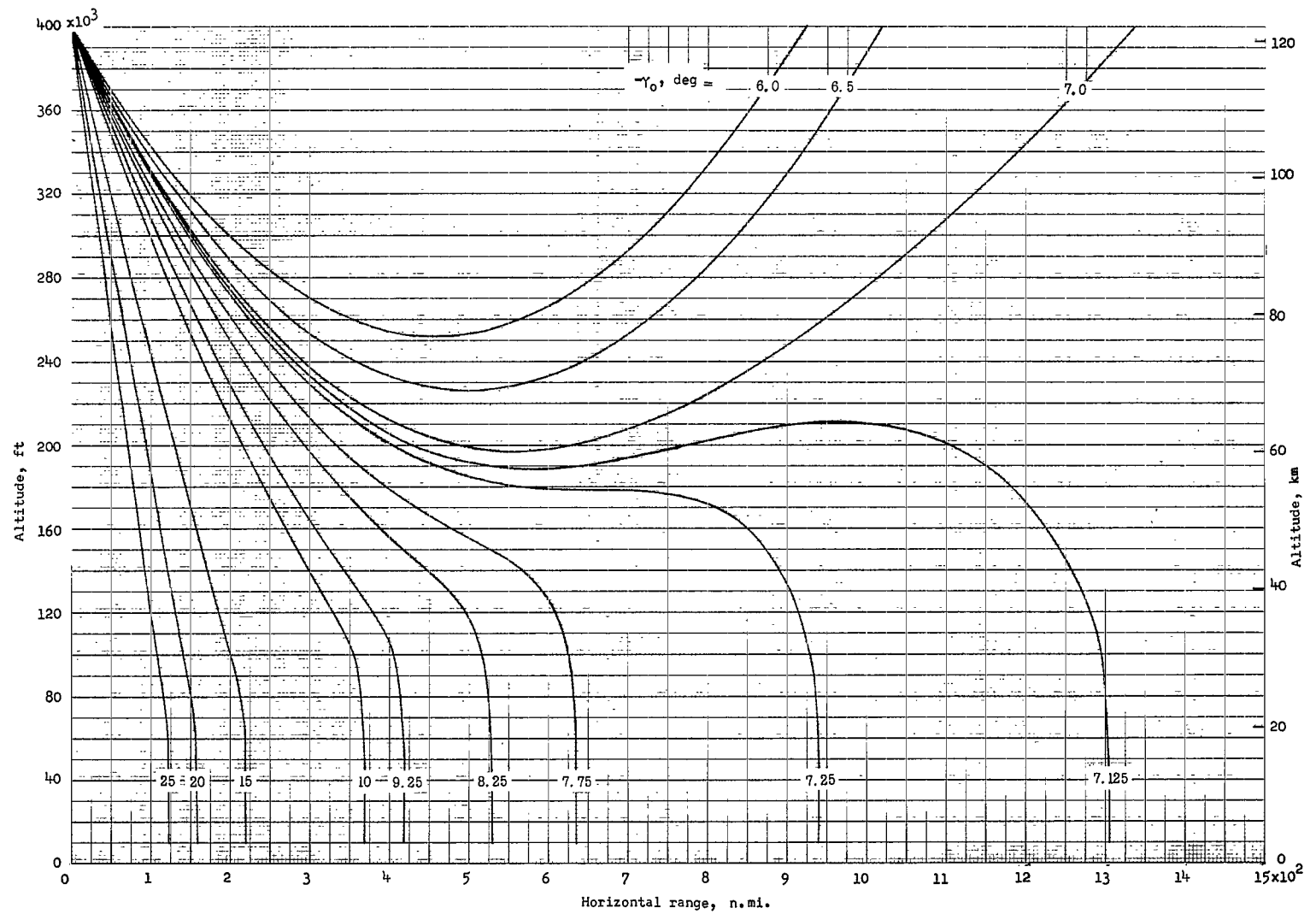
(d) $\frac{W}{C_D A}$ = 40 lbf/ft^2 $\left(1915 \text{ N/m}^2\right)$.

Figure 5.- Continued.
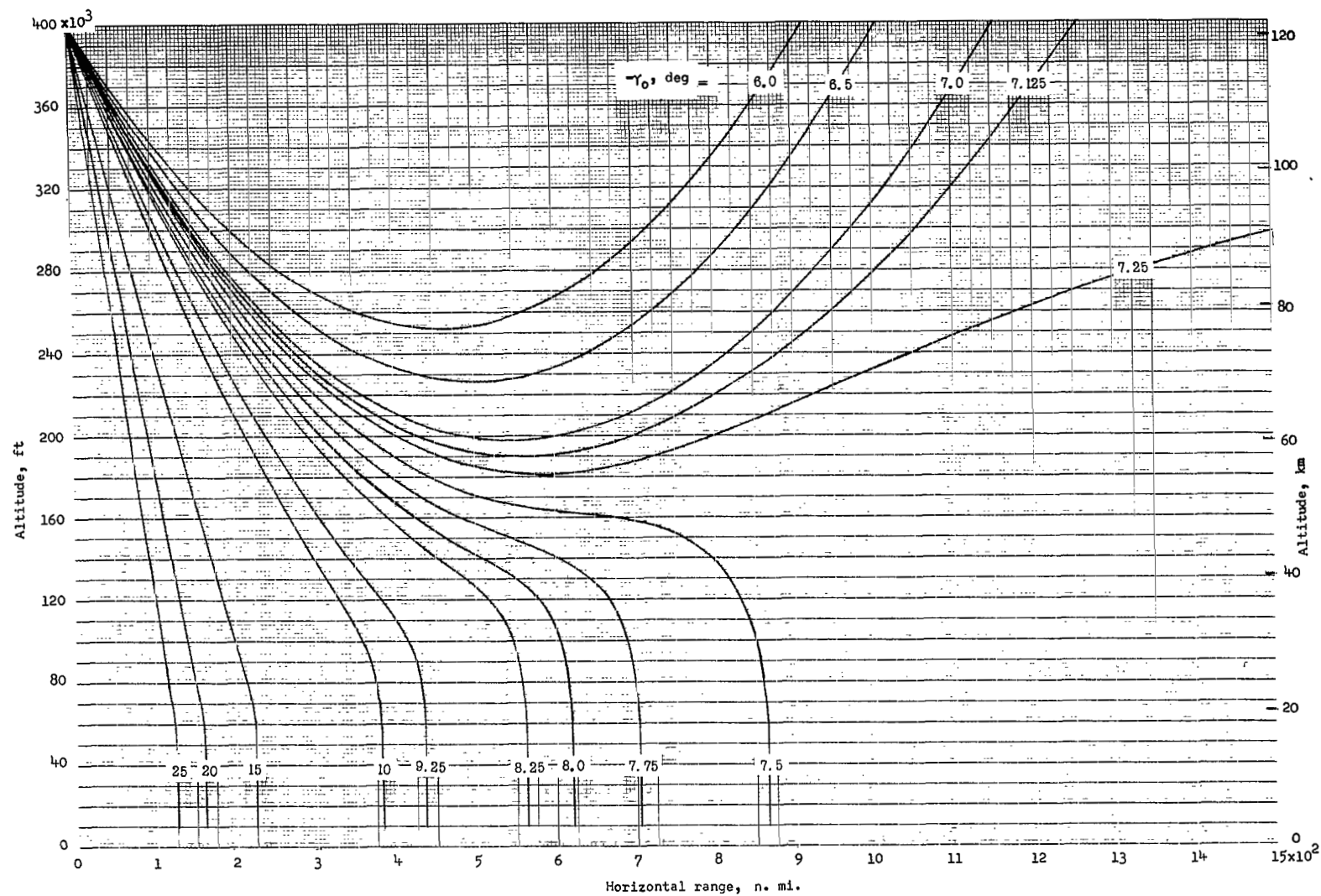
(e) $\frac{W}{C_D A}$ = 60 lbf/ft^2 (2873 N/m^2).

Figure 5.- Continued.
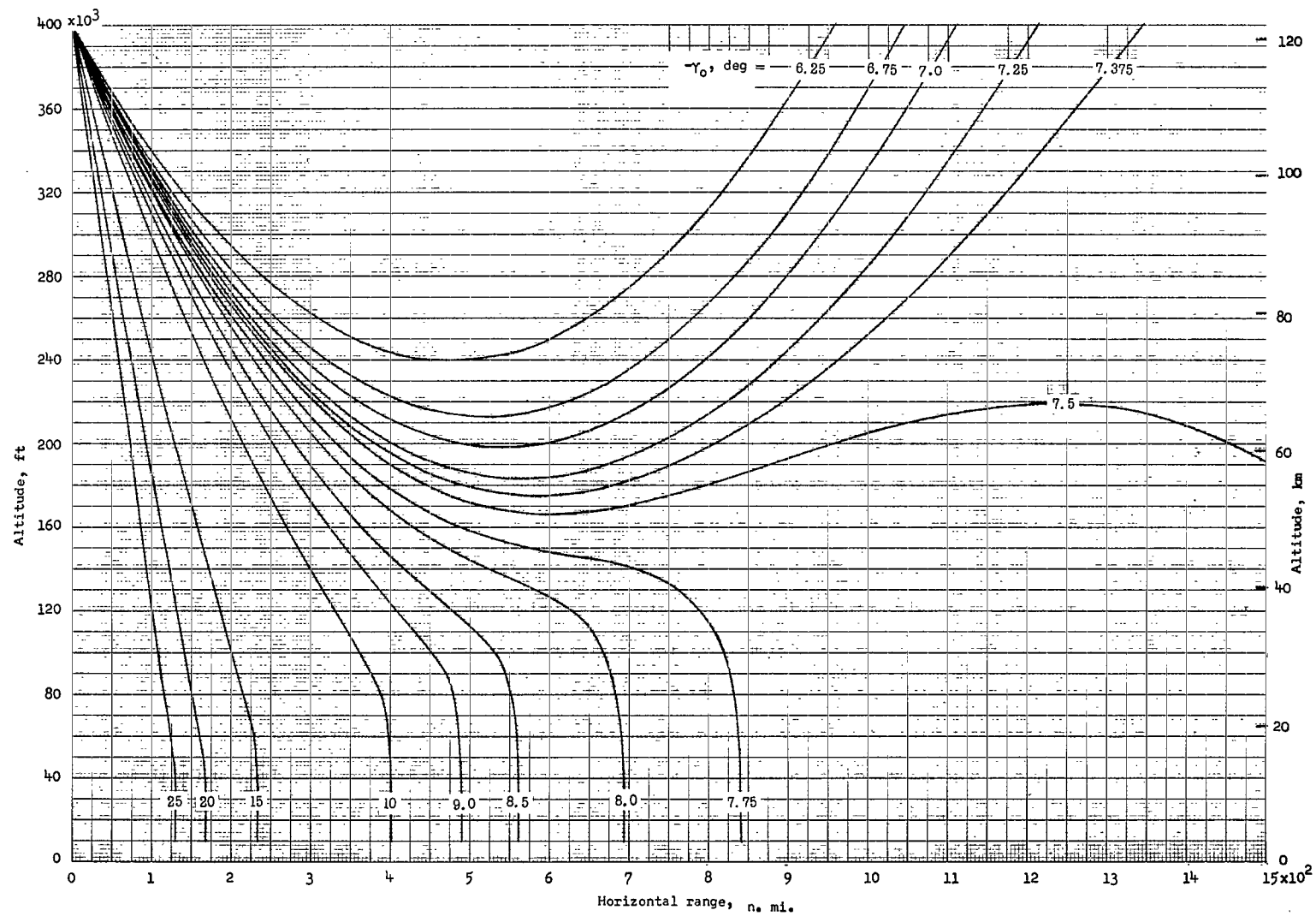
(f) $\frac{W}{C_D A} = 100$ lbf/ft^2 (4788 N/m^2).

Figure 5.- Continued.
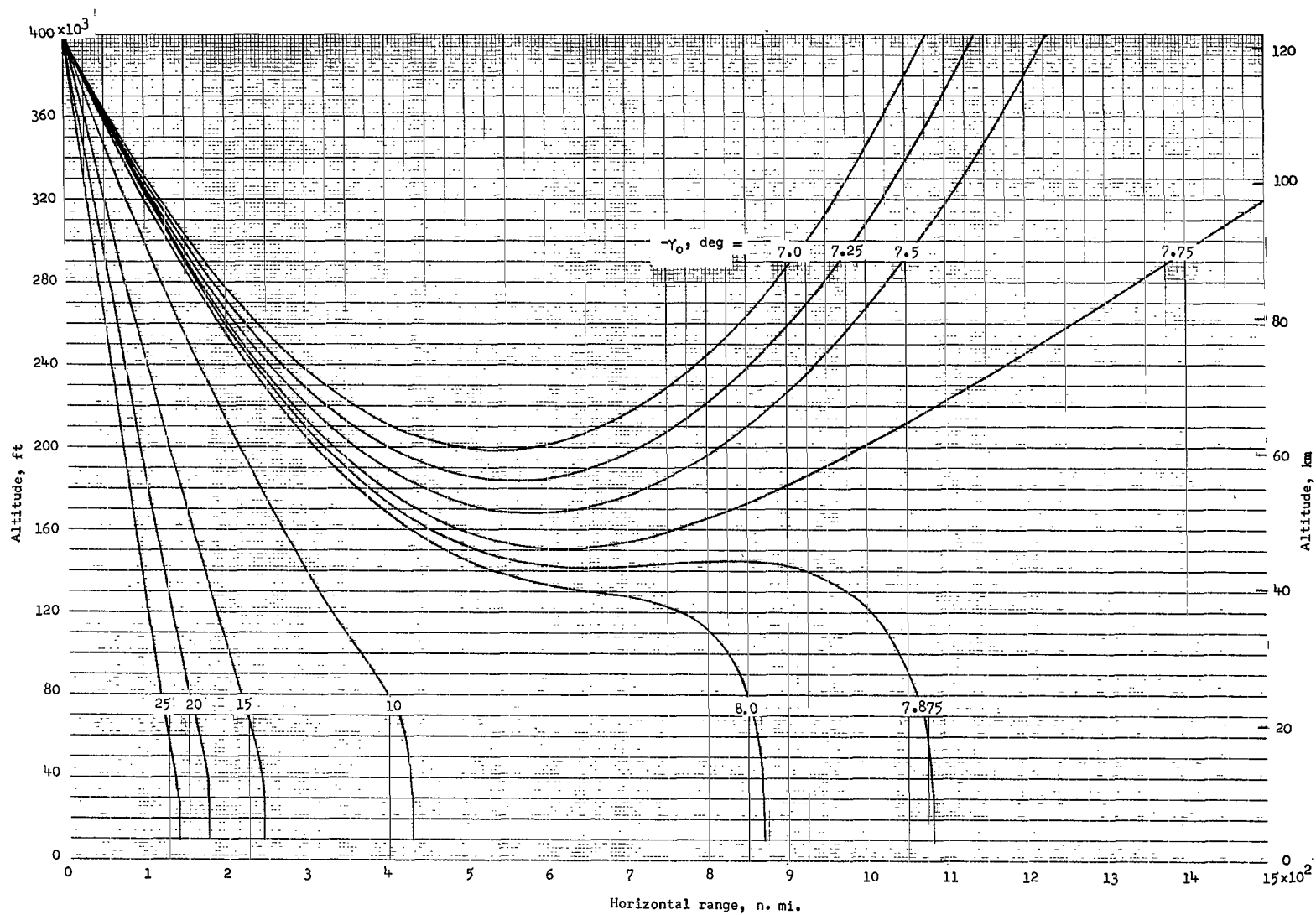
(g) $\dfrac{W}{C_D A}$ = 200 lbf/ft^2 $\left(9576 \text{ N/m}^2\right)$.

Figure 5.- Concluded.
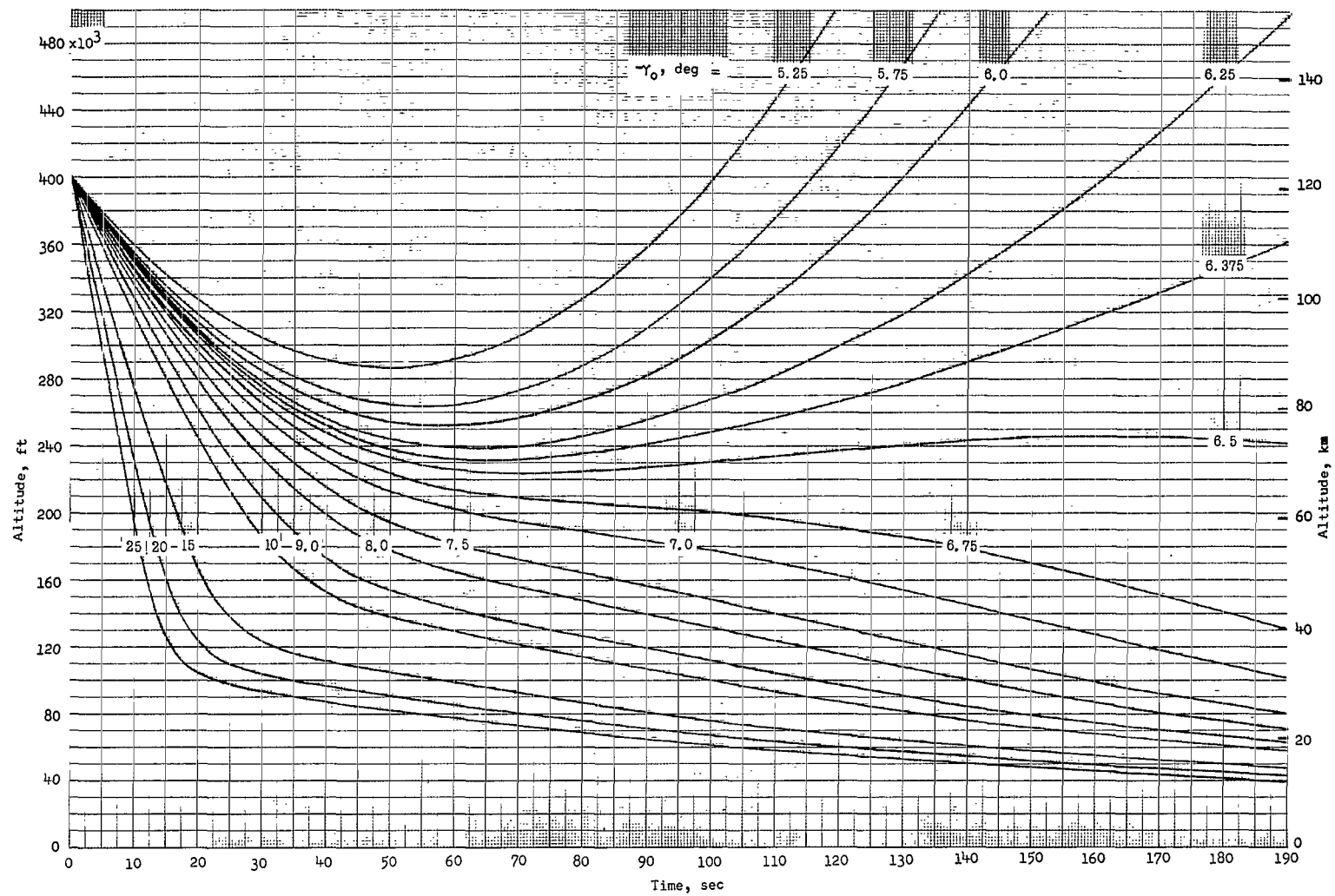
(a) $\frac{W}{C_D A} = 10$ lbf/ft^2 $\left(479 \text{ N/m}^2\right)$.

Figure 6.- Effect of initial reentry angle on the variation of altitude with time for ballistic trajectories. $V_0 = 50\ 000$ ft/sec (15 240 m/sec).
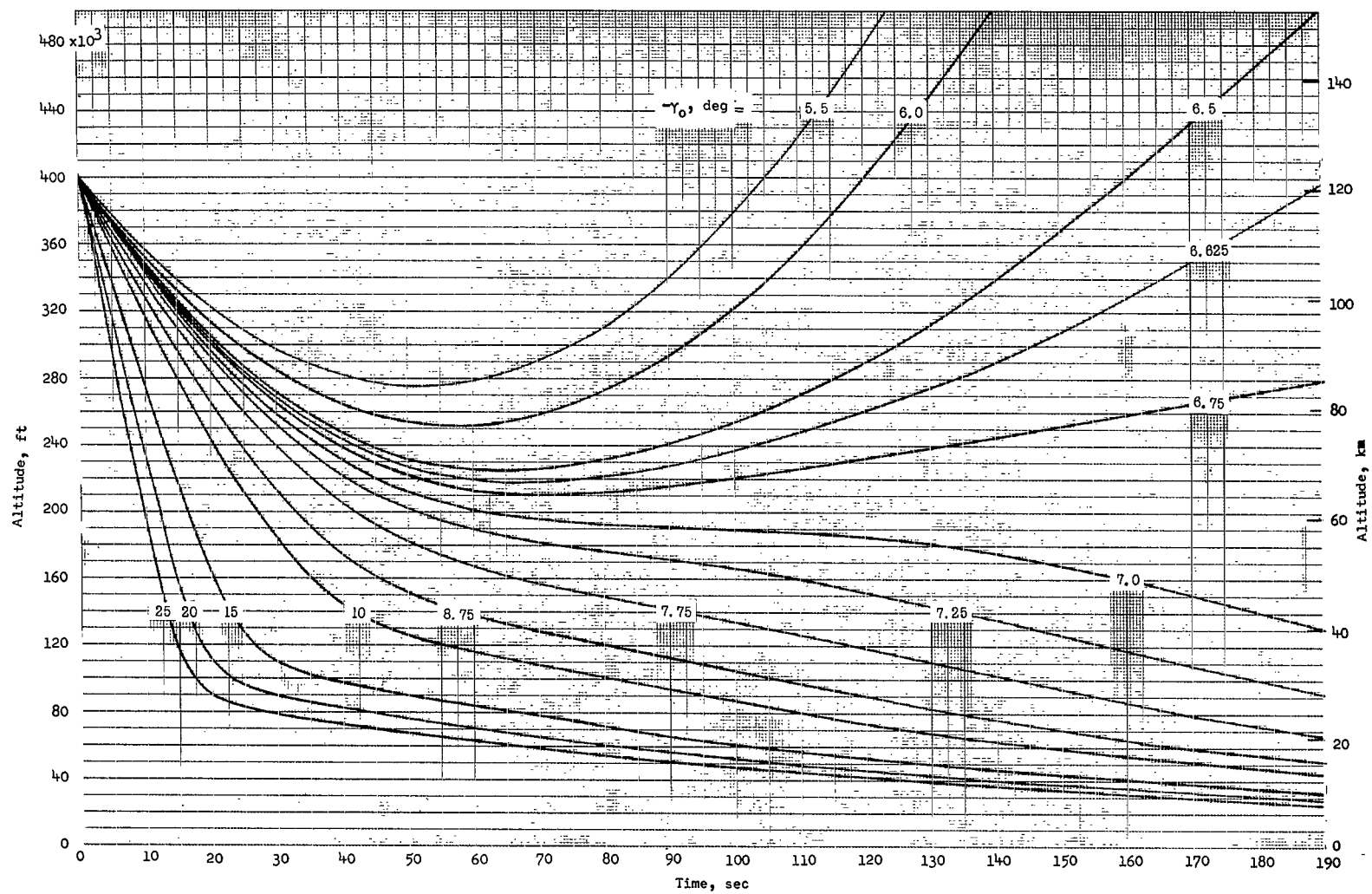
(b) $\frac{W}{C_D A} = 20$ lbf/ft^2 $\left(958 \text{ N/m}^2\right)$.

Figure 6.- Continued.
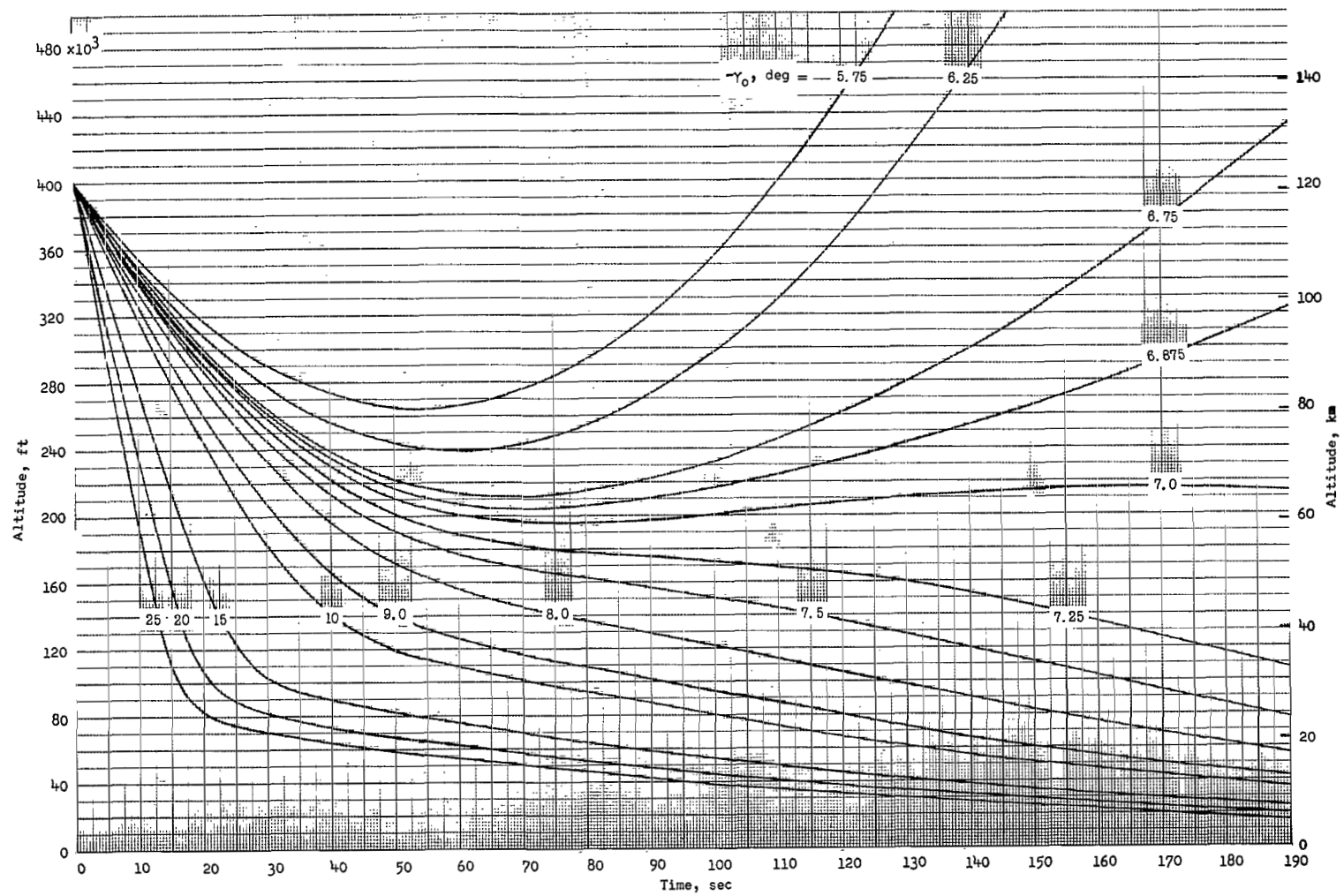
(c) $\frac{W}{C_DA} = 30$ lbf/ft^2 $\left(1436 \text{ N/m}^2\right)$.

Figure 6.- Continued.
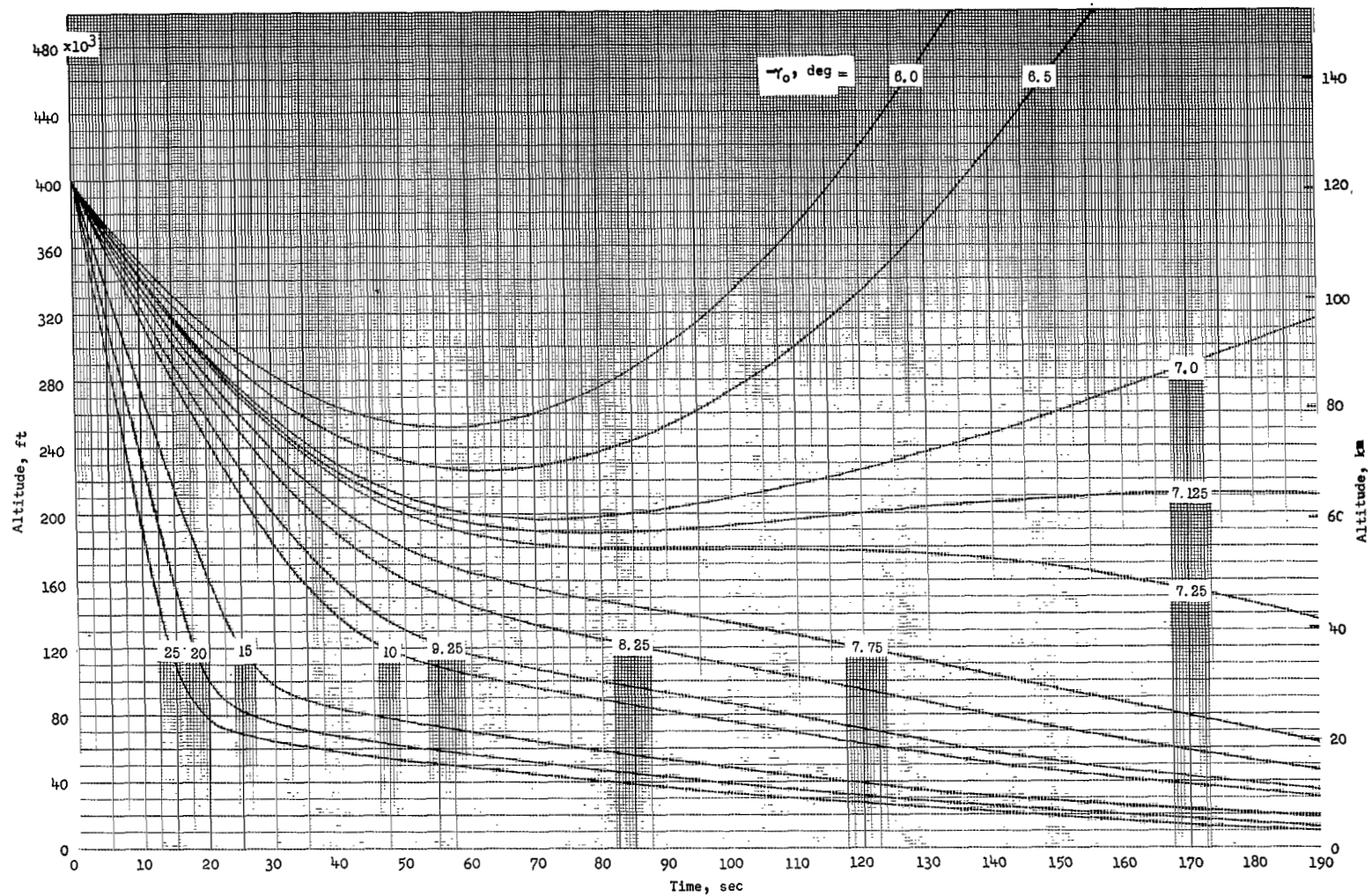
(d) $\dfrac{W}{C_D A}$ = 40 lbf/ft^2 $\left(1915 \text{ N/m}^2\right)$.

Figure 6.- Continued.
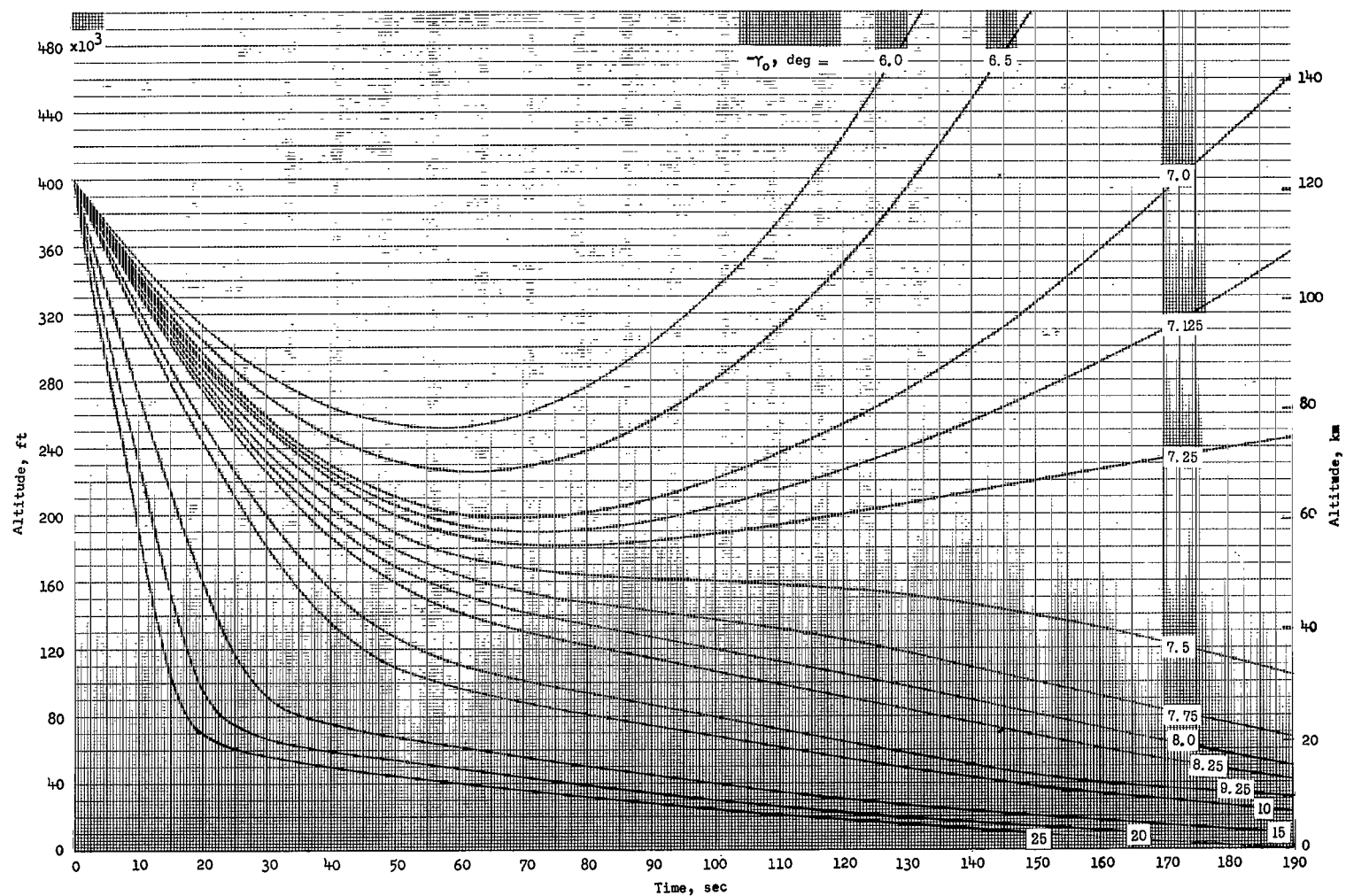
(e) $\frac{W}{C_DA} = 60$ lbf/ft^2 $(2873$ N/m$^2)$.

Figure 6.- Continued.
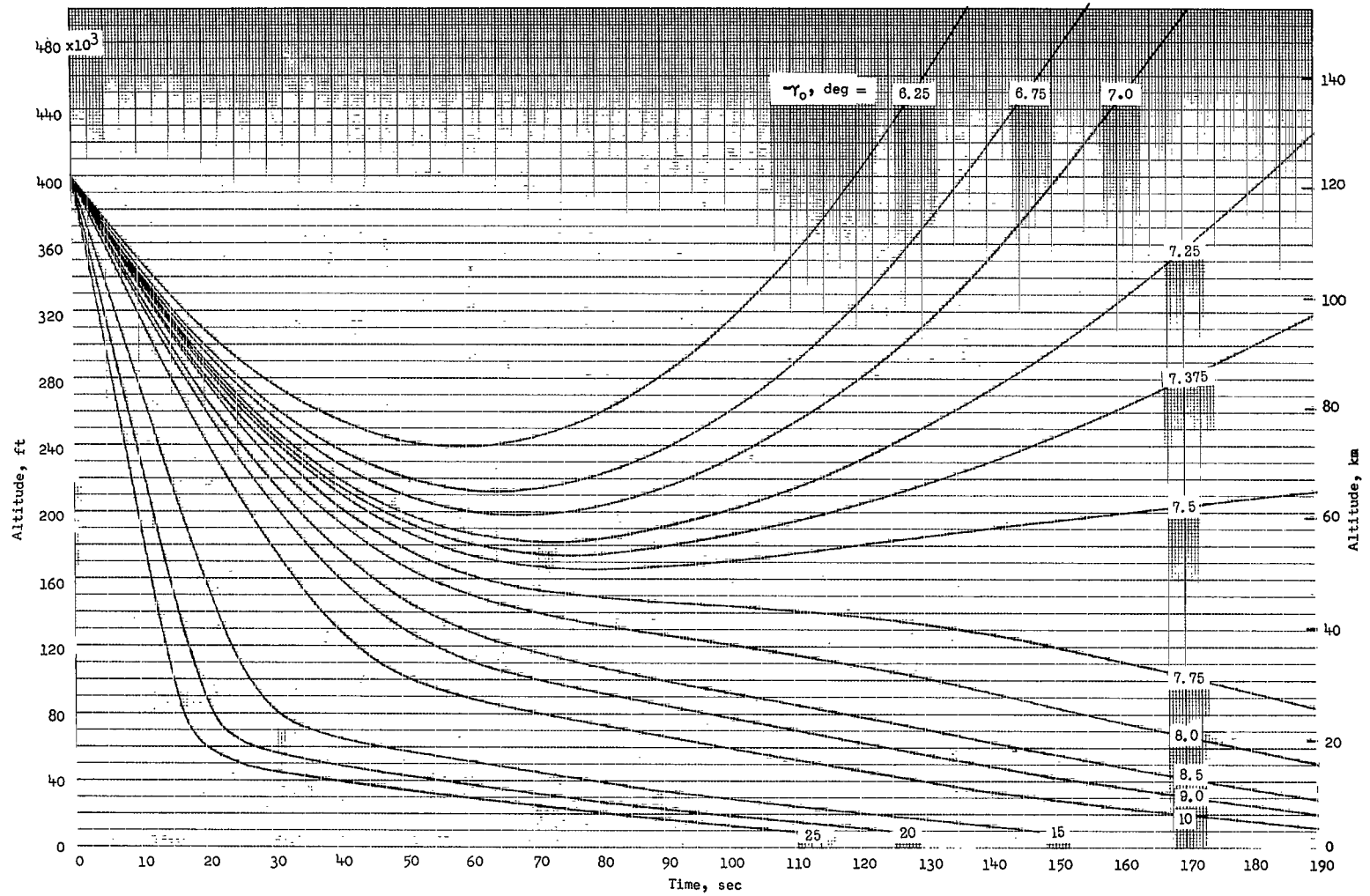
(f) $\frac{W}{C_D A} = 100$ lbf/ft^2 $\left(4788 \text{ N/m}^2\right)$.

Figure 6.- Continued.
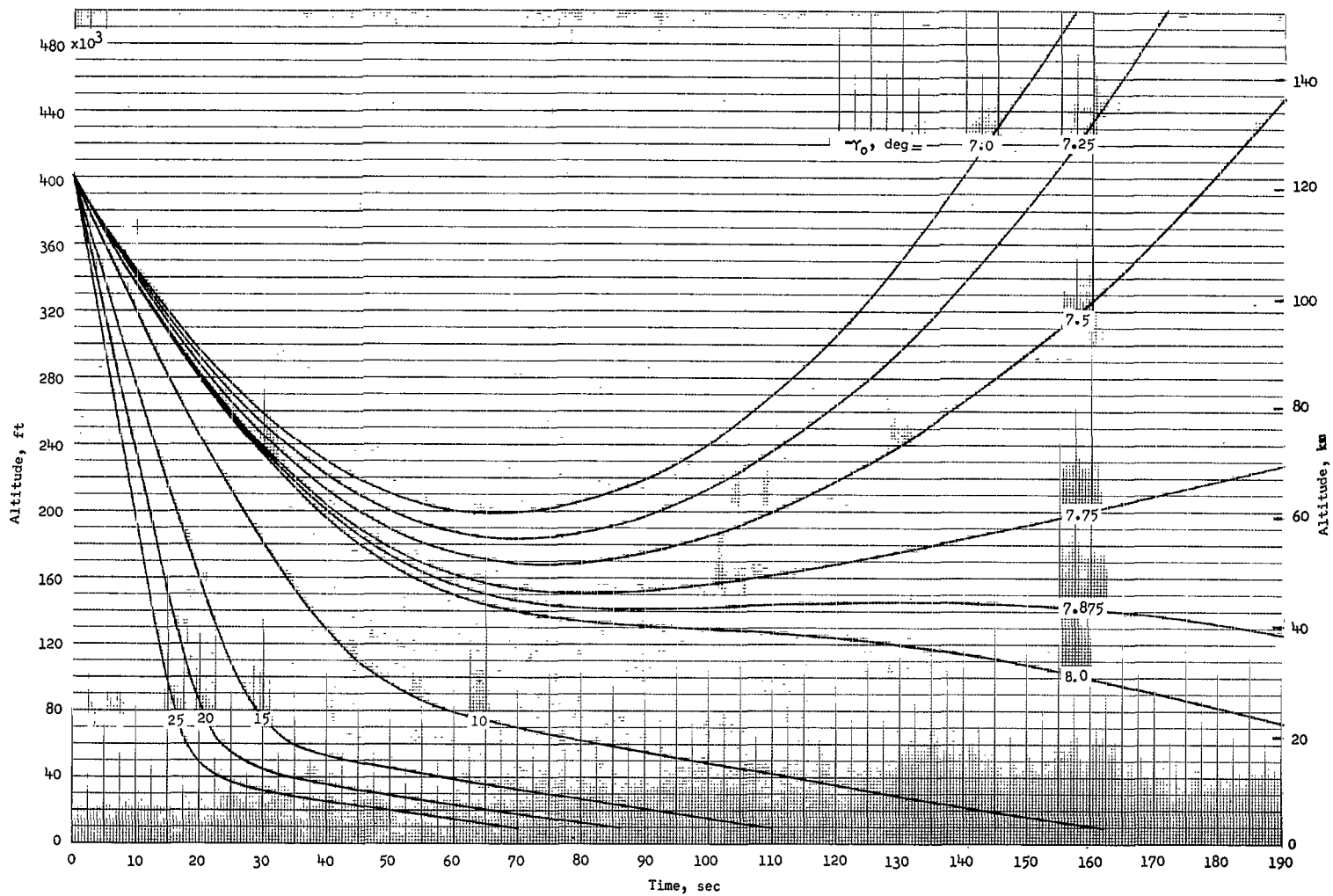
(g) $\frac{W}{C_D A} = 200$ lbf/ft^2 $\left(9576 \text{ N/m}^2\right)$.

Figure 6.- Concluded.
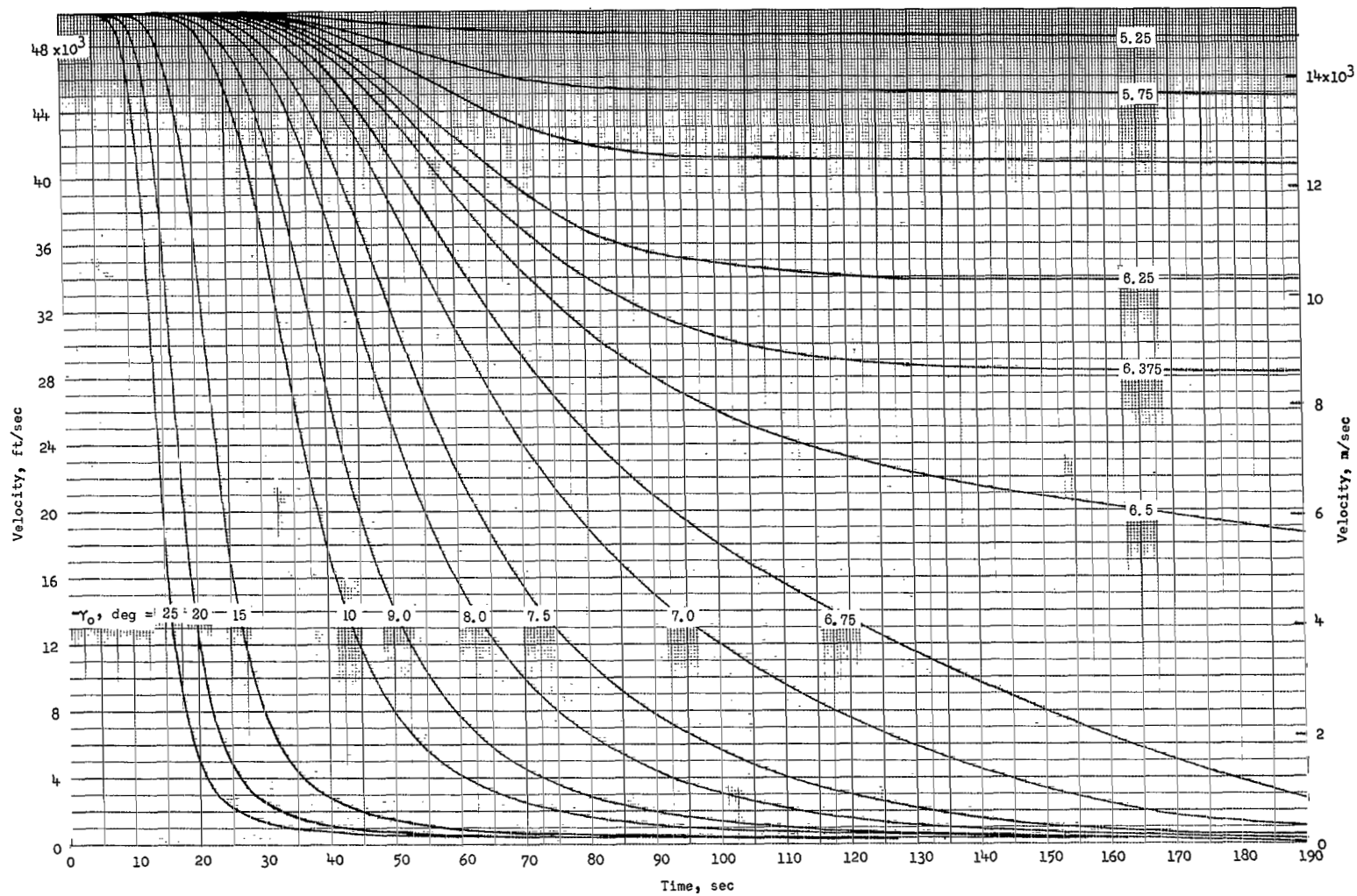
(a) $\frac{W}{C_DA} = 10$ lbf/ft^2 $\left(479 \text{ N/m}^2\right)$.

Figure 7.- Effect of initial reentry angle on the variation of velocity with time for ballistic trajectories. $V_0 = 50\ 000$ ft/sec (15 240 m/sec).
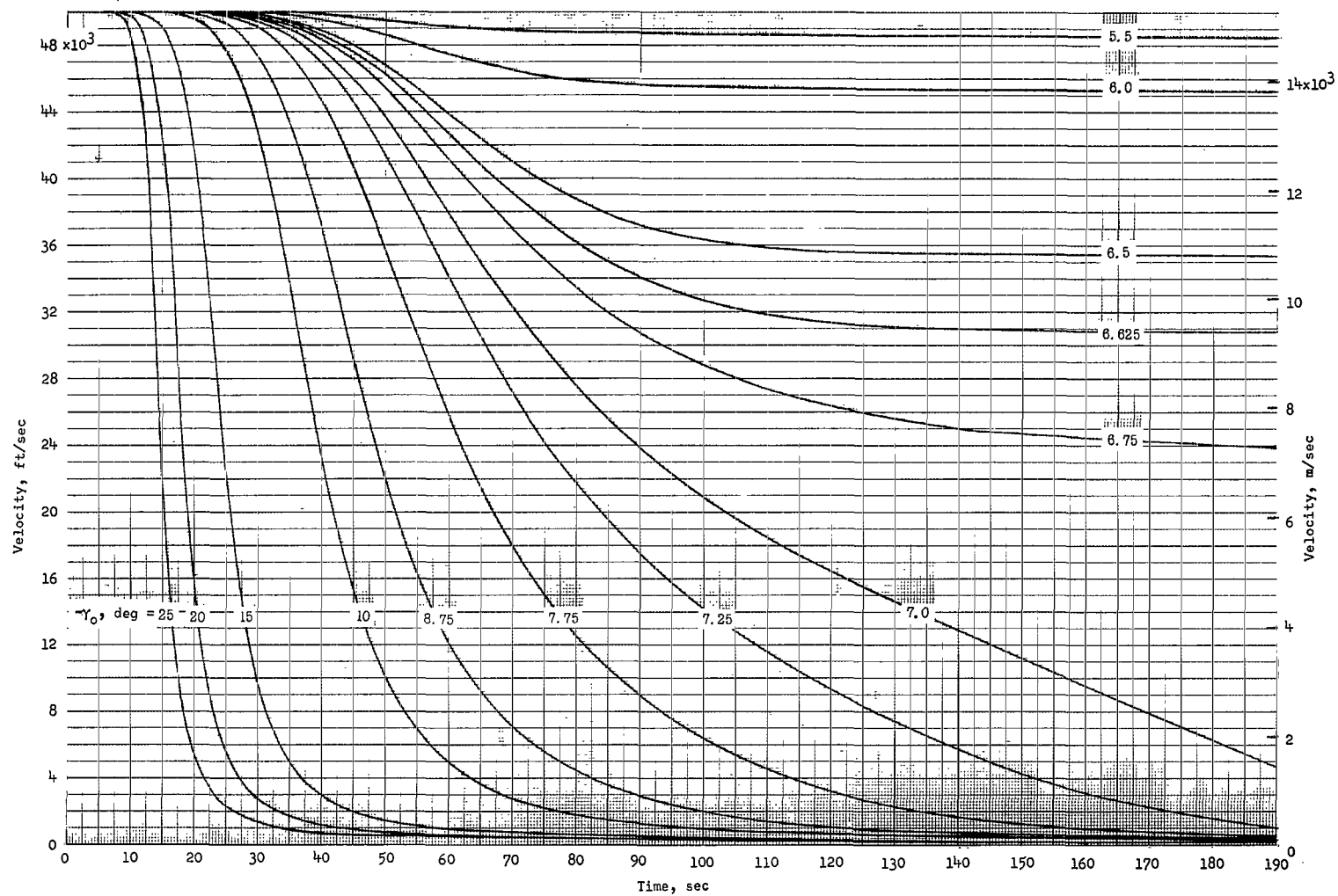
(b) $\frac{W}{C_D A}$ = 20 lbf/ft^2 (958 N/m^2).

Figure 7.- Continued.
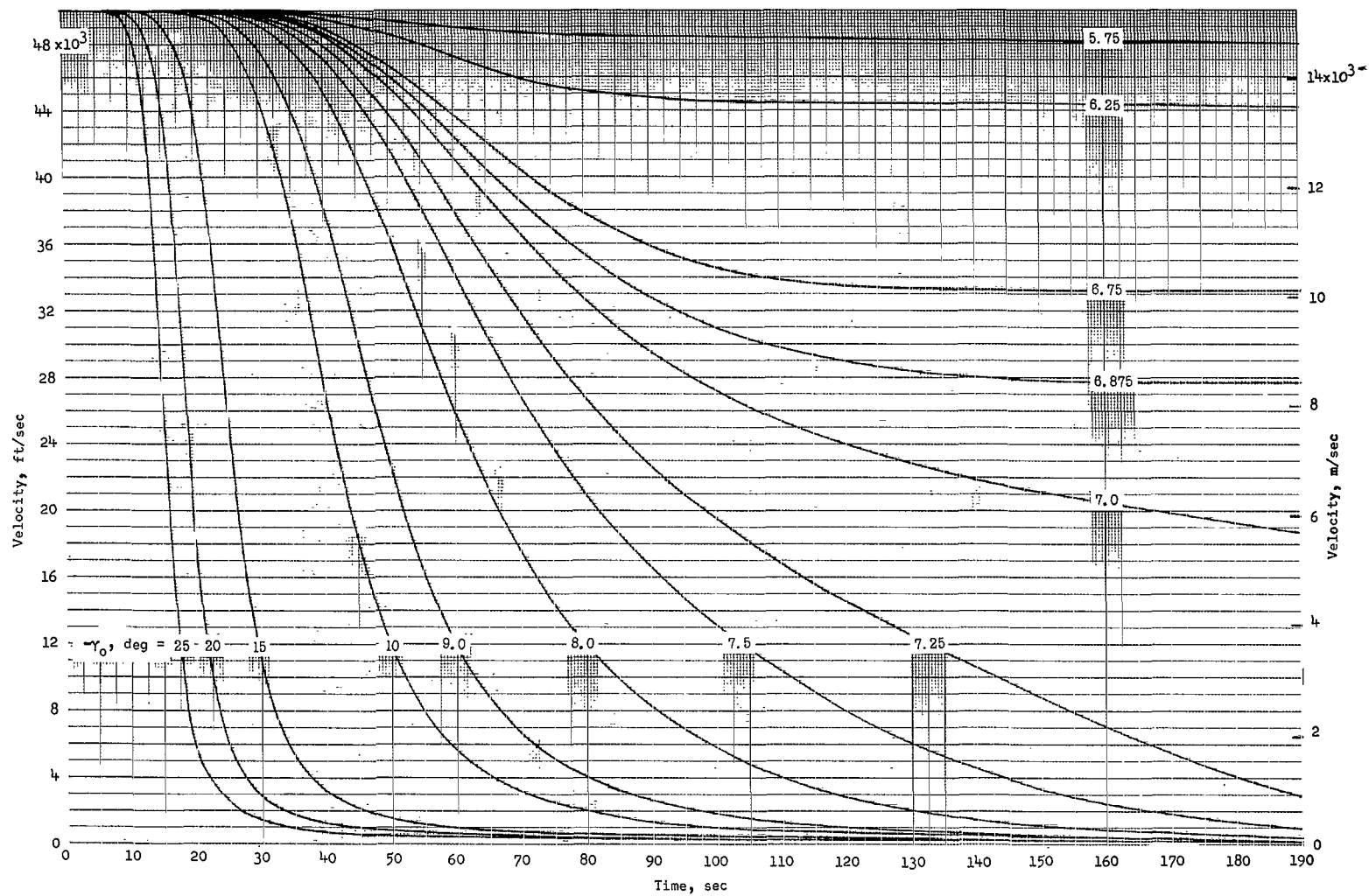
(c) $\frac{W}{C_D A} = 30$ lbf/ft^2 $\left(1436 \text{ N/m}^2\right)$.

Figure 7.- Continued.
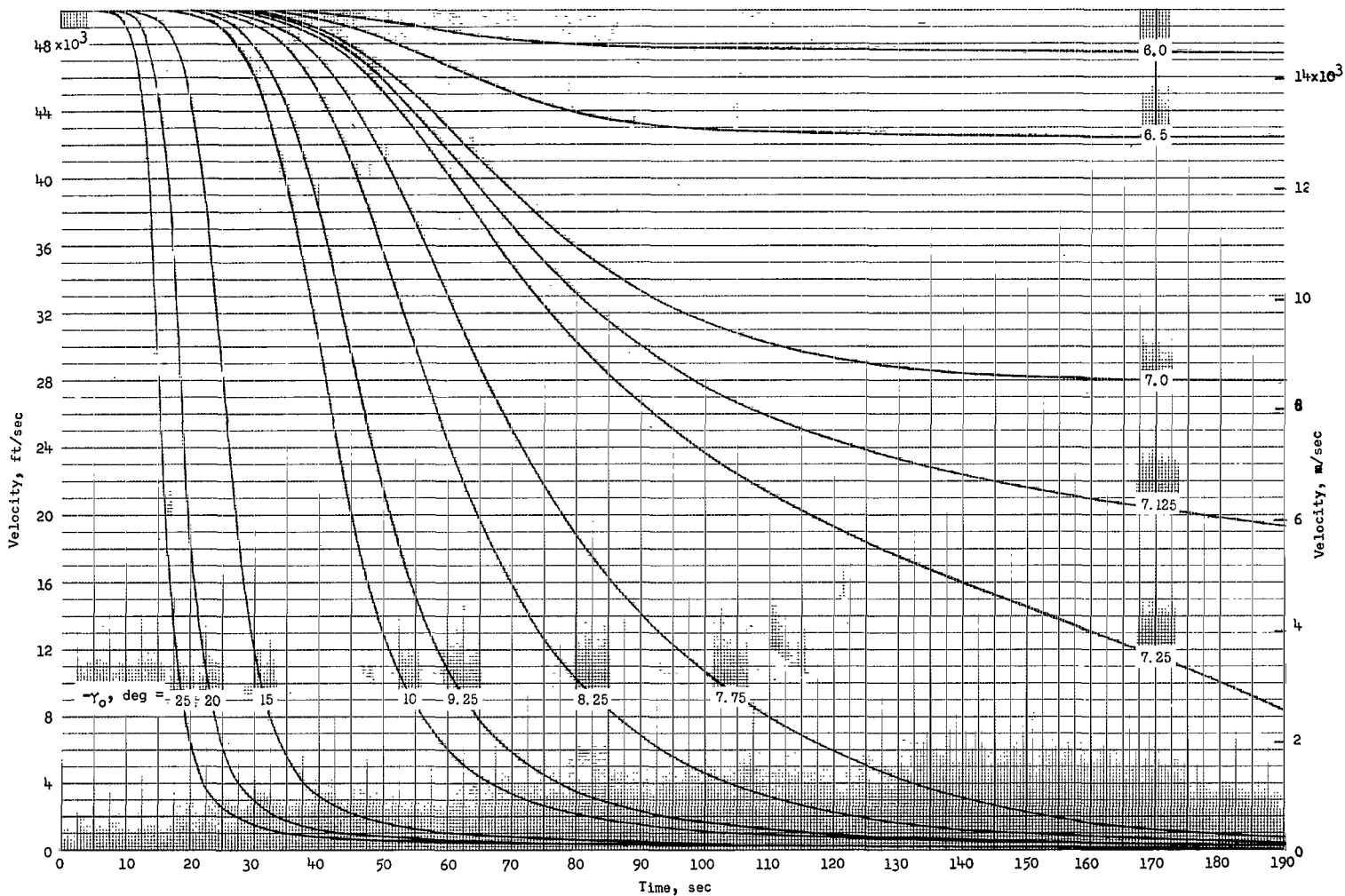
(d) $\frac{W}{C_D A} = 40$ lbf/ft^2 $\left(1915/\text{N m}^2\right)$.

Figure 7.- Continued.
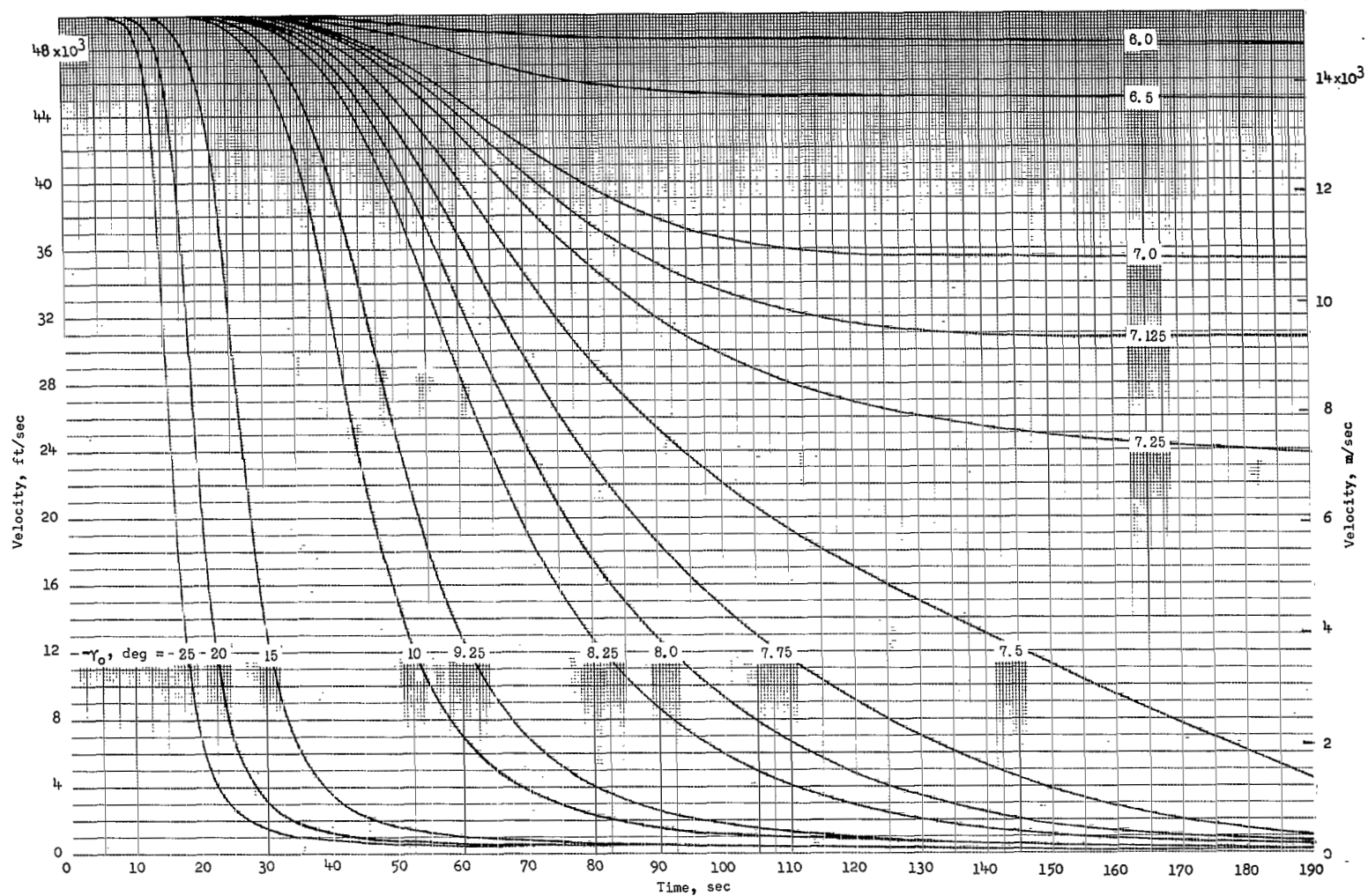
(e) $\dfrac{W}{C_D A}$ = 60 lbf/ft^2 (2873 N/m^2).

Figure 7.- Continued.
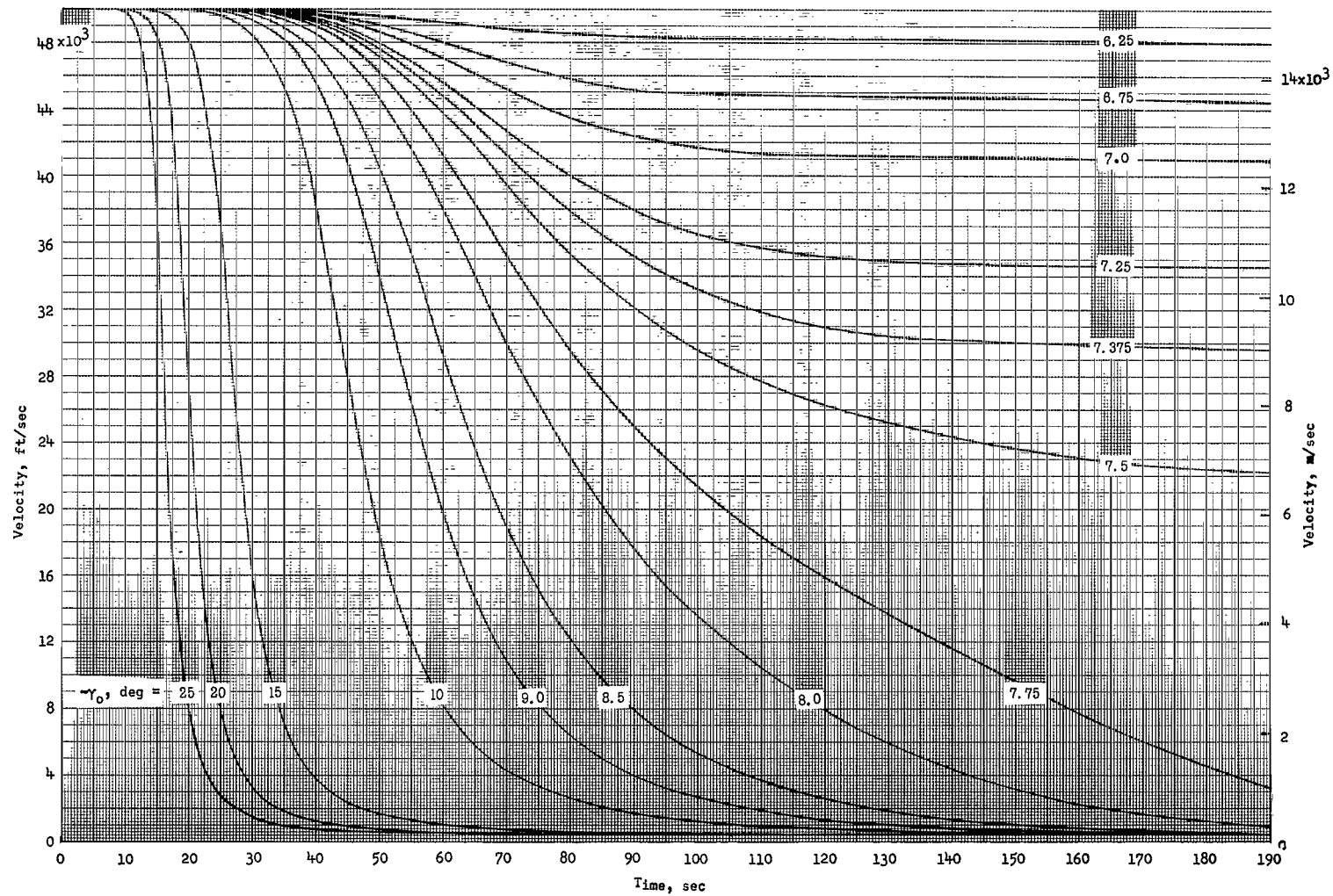
(f) $\frac{W}{C_D A} = 100$ lbf/ft^2 $\left(4788 \ N/m^2\right)$.

Figure 7.- Continued.
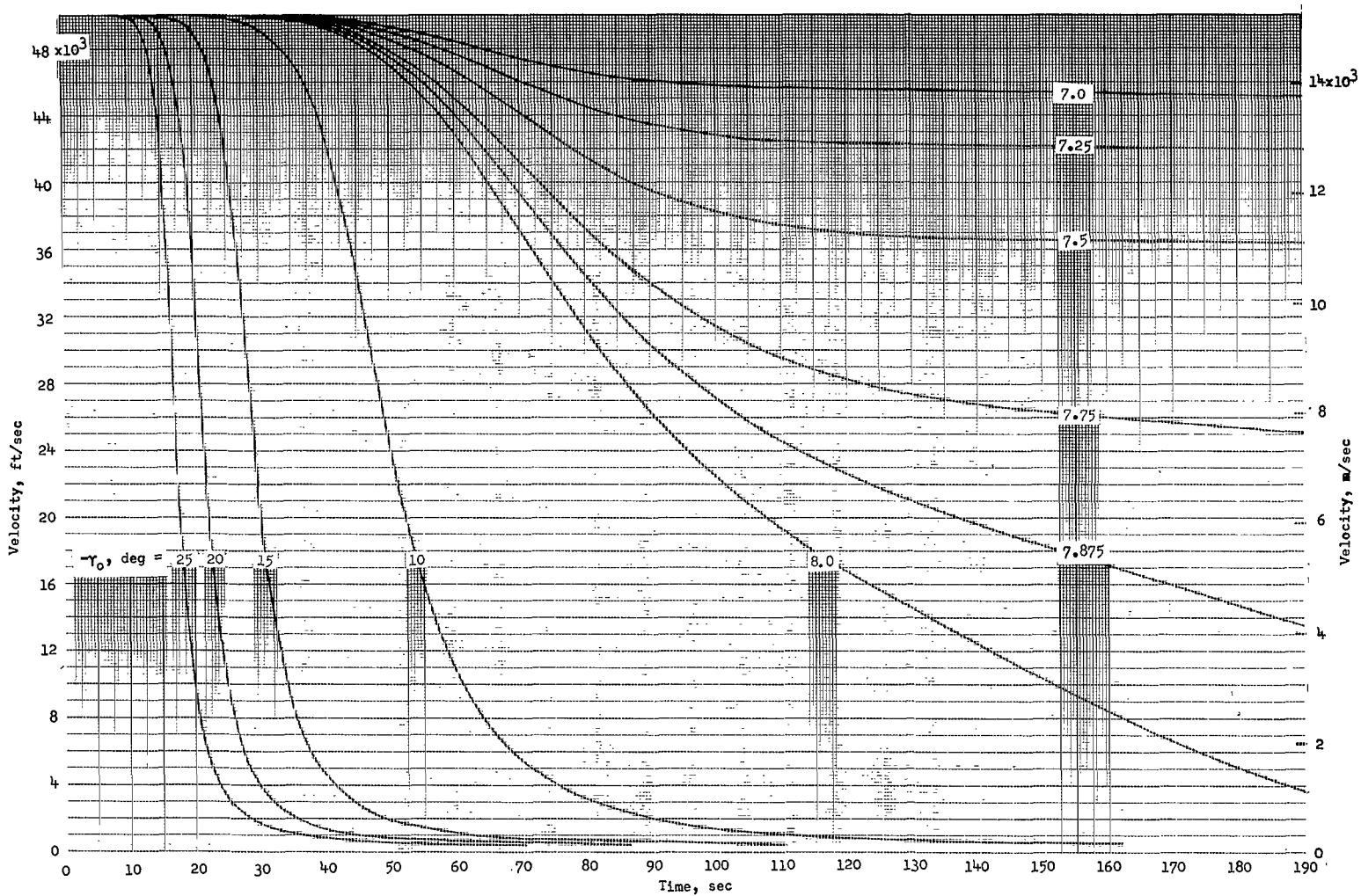
(g) $\frac{W}{C_D A} = 200\ \text{lbf/ft}^2\ \left(9576\ \text{N/m}^2\right).$

Figure 7.- Concluded.
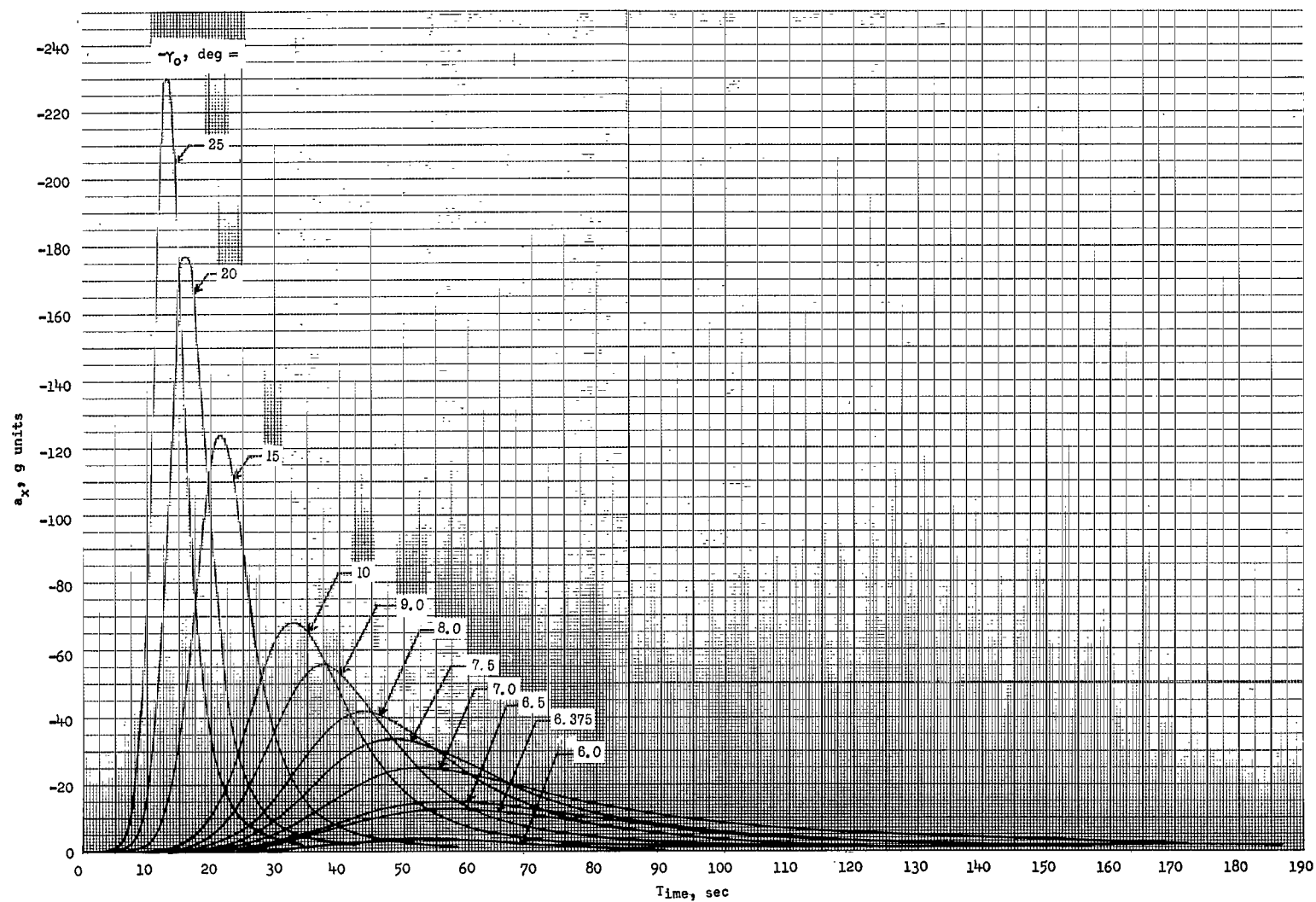
(a) $\frac{W}{C_D A}$ = 10 lbf/ft^2 (479 N/m^2).

Figure 8.- Effect of initial reentry angle on the time history of acceleration along the flight path for ballistic trajectories. V_0 = 50 000 ft/sec (15 240 m/sec).
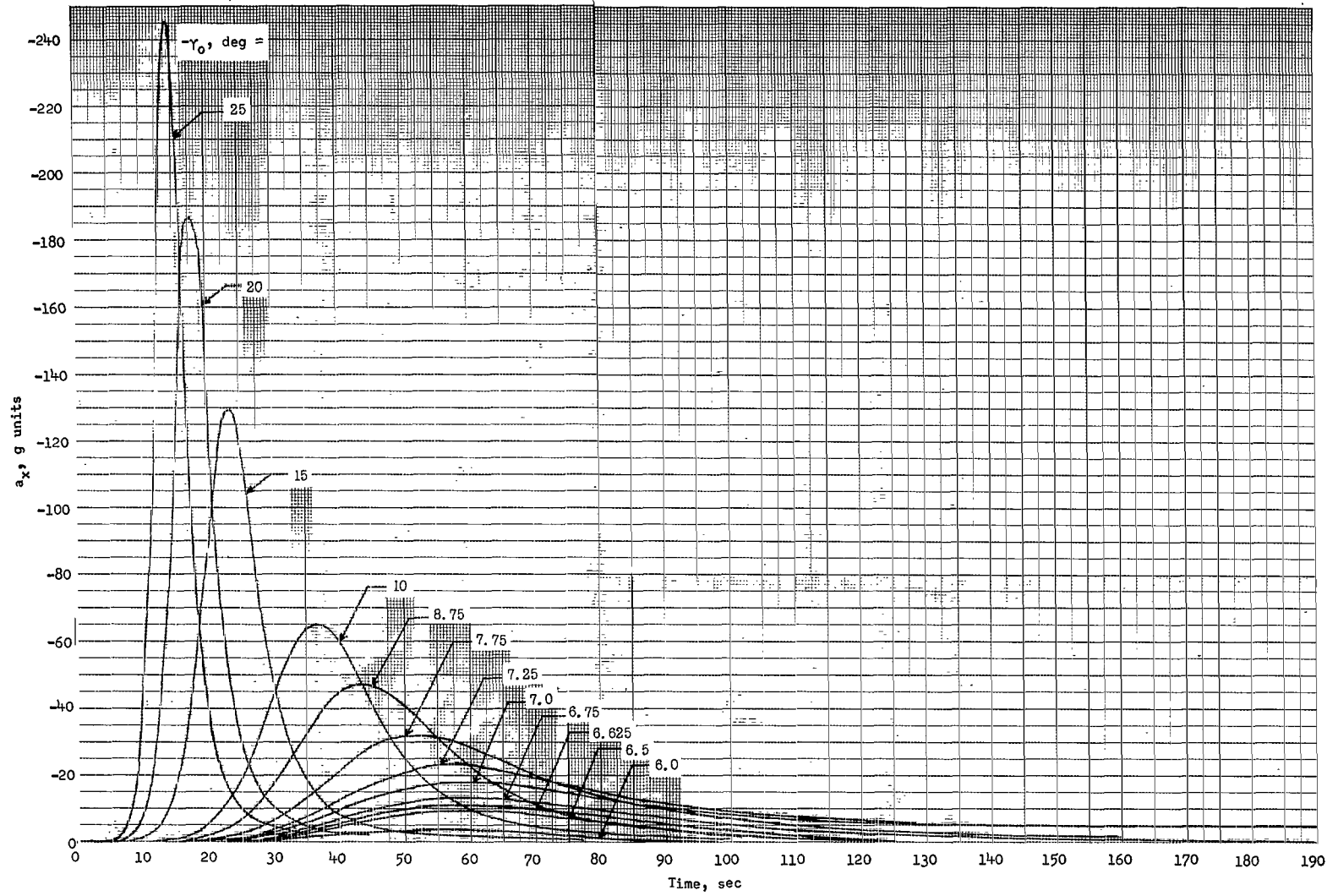
(b) $\frac{W}{C_D A}$ = 20 lbf/ft^2 (958 N/m^2).

Figure 8.- Continued.
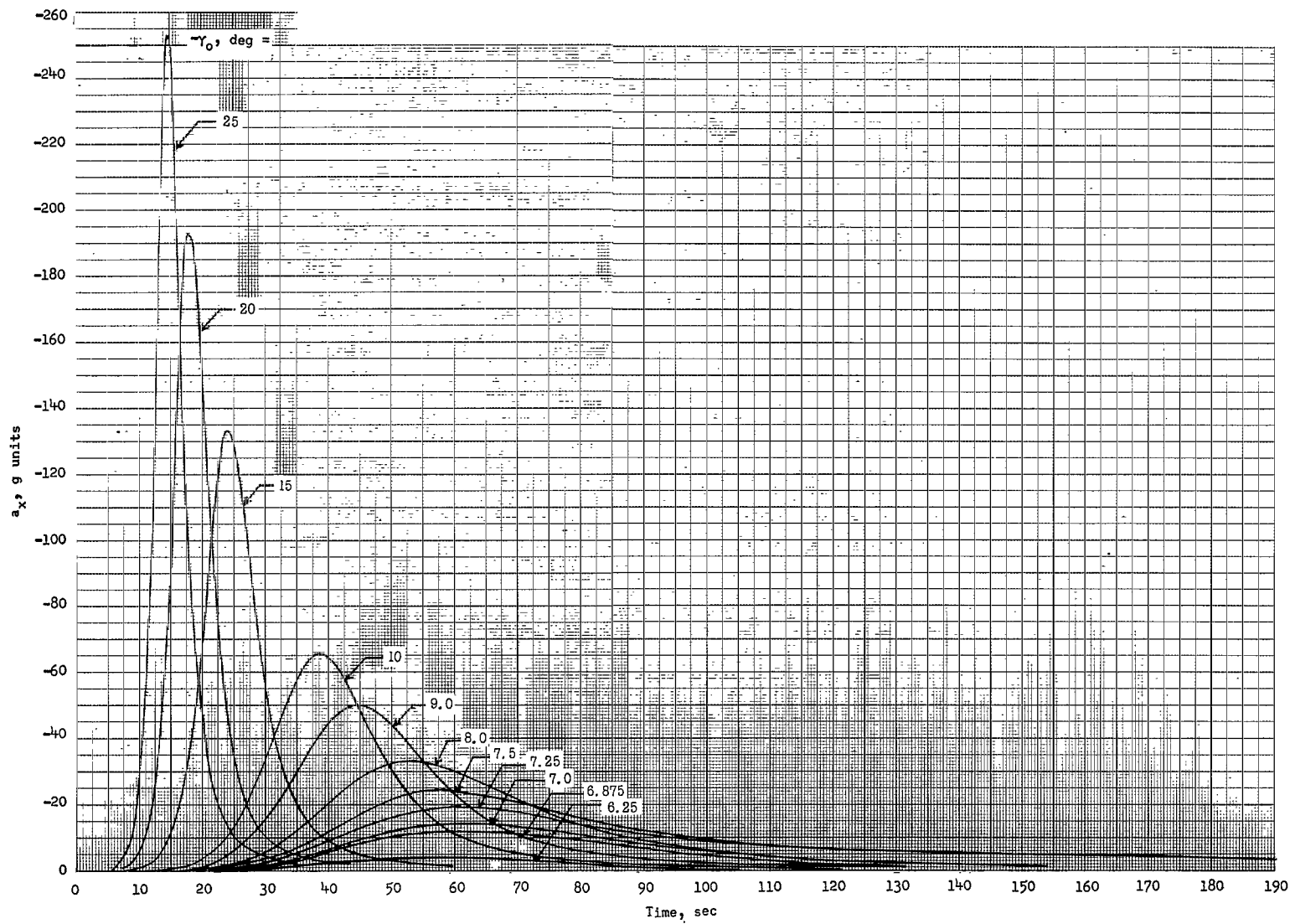
(c) $\frac{W}{C_D A}$ = 30 lbf/ft^2 $\left(1436 \text{ N/m}^2\right)$.

Figure 8.- Continued.
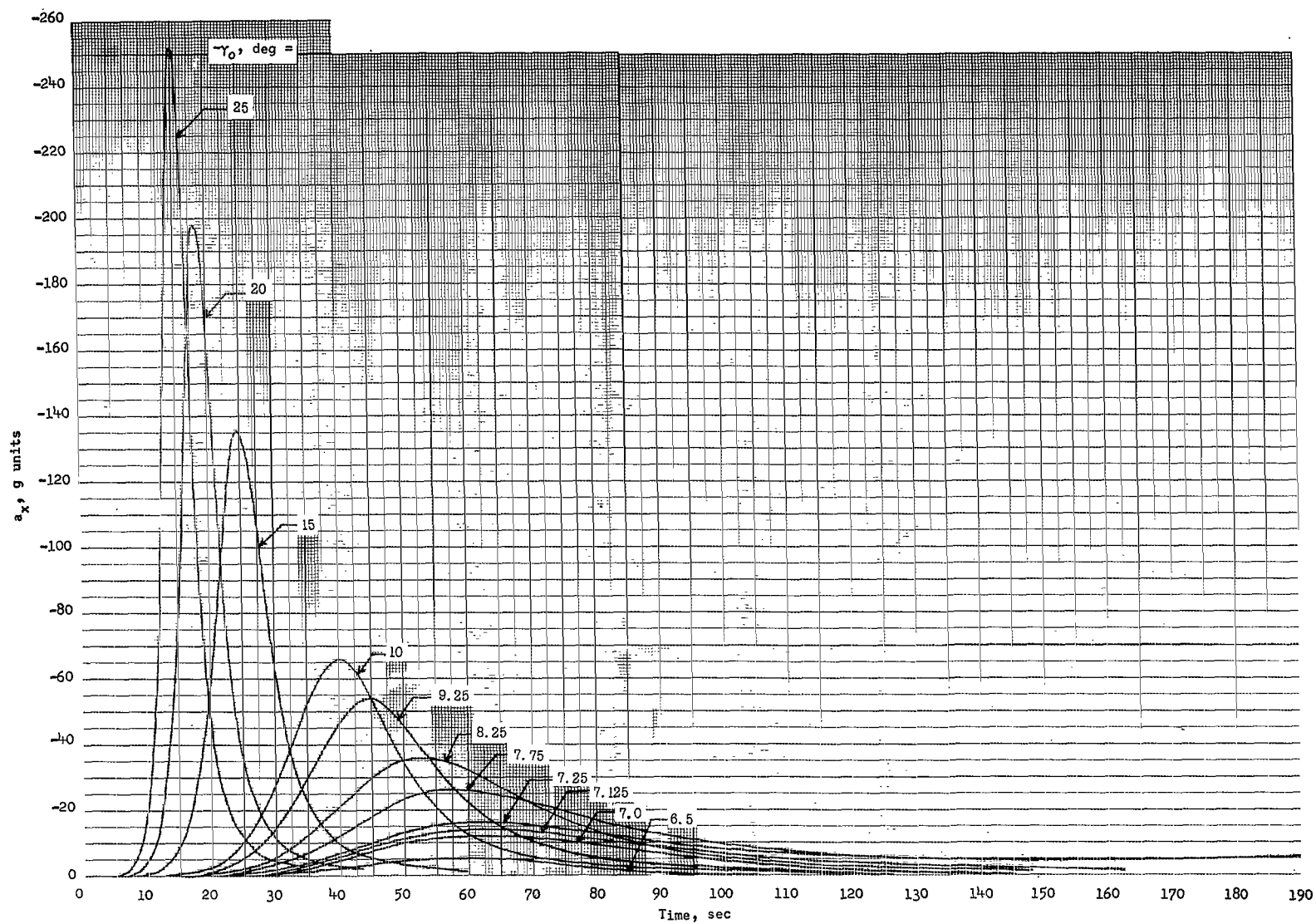
(d) $\frac{W}{C_D A}$ = 40 lbf/ft^2 (1915 N/m^2).

Figure 8.- Continued.
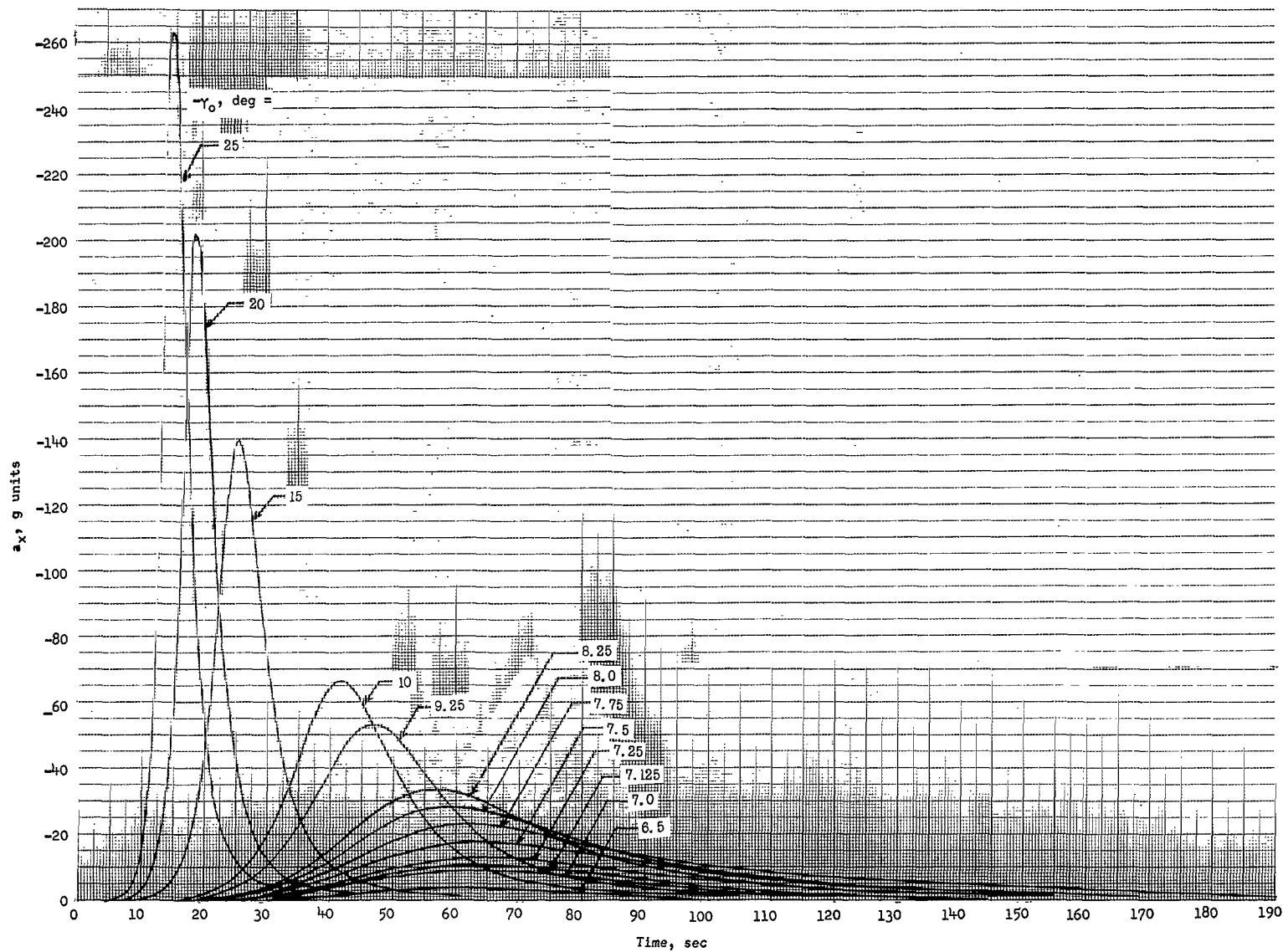
(e) $\frac{W}{C_D A} = 60$ lbf/ft^2 $\left(2873 \text{ N/m}^2\right)$.

Figure 8.- Continued.
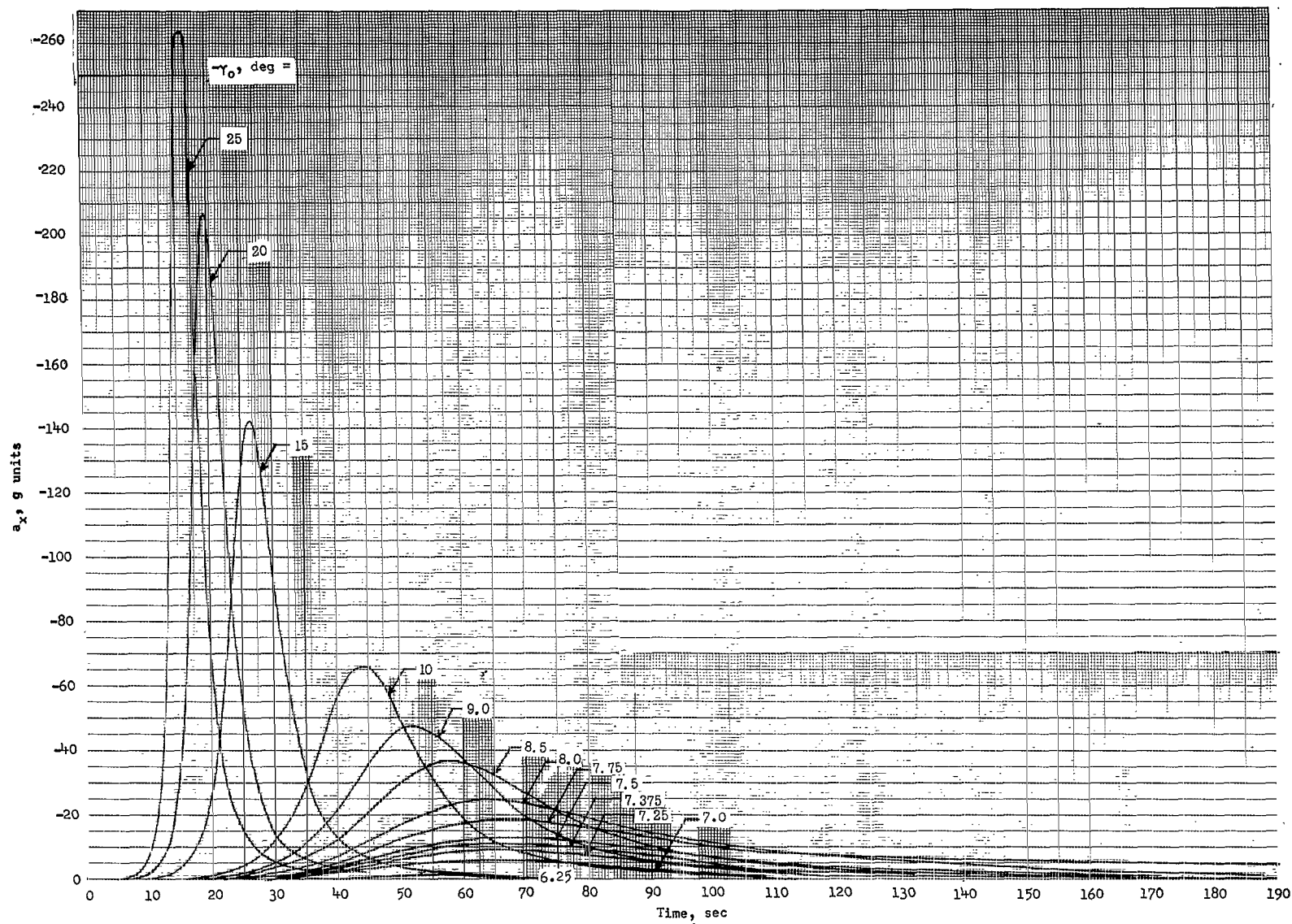
(f) $\frac{W}{C_D A}$ = 100 lbf/ft^2 (4788 N/m^2).

Figure 8.- Continued.
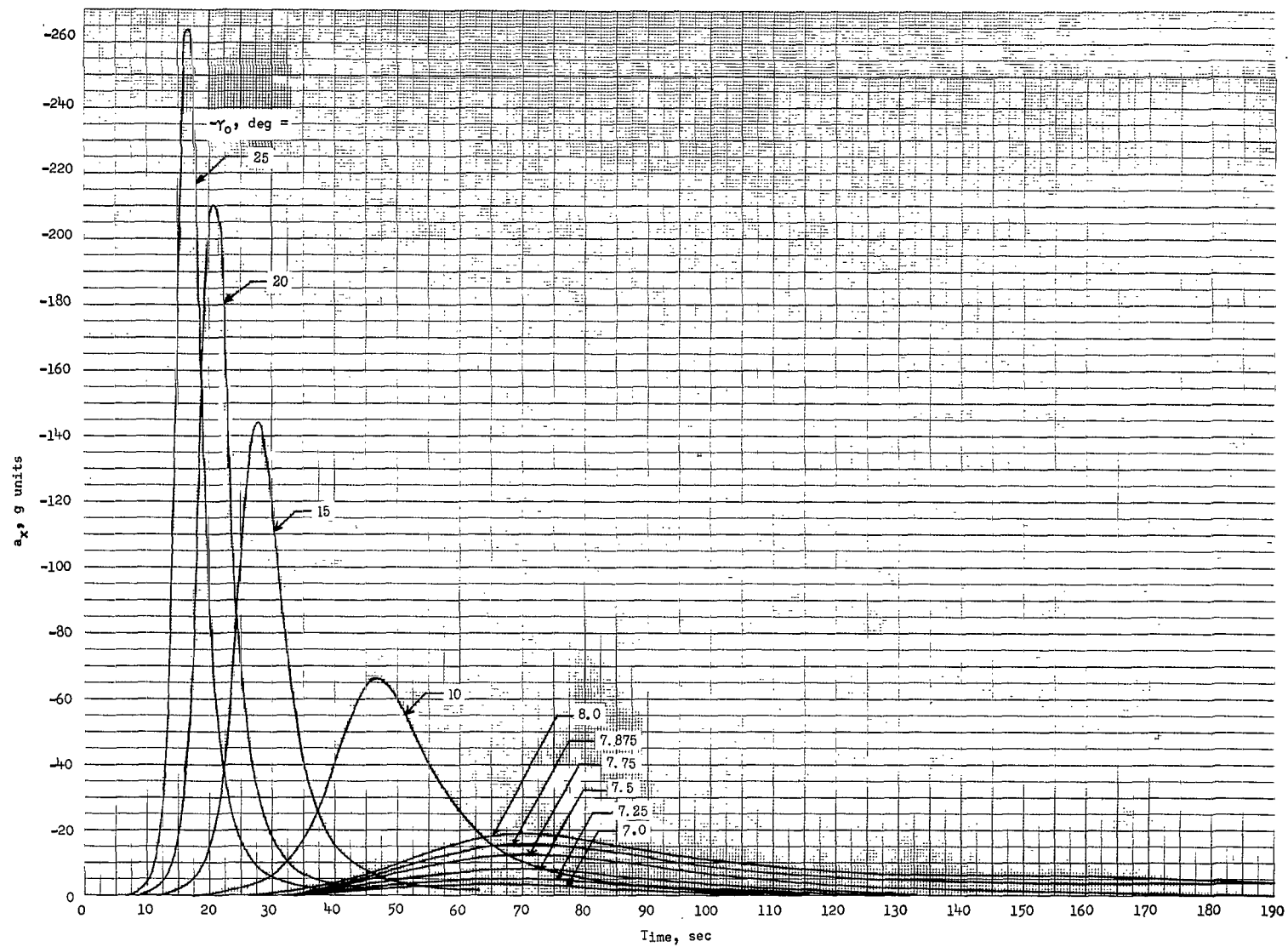
(g) $\frac{W}{C_D A}$ = 200 lbf/ft^2 $\left(9576 \text{ N/m}^2\right)$.

Figure 8.- Concluded.
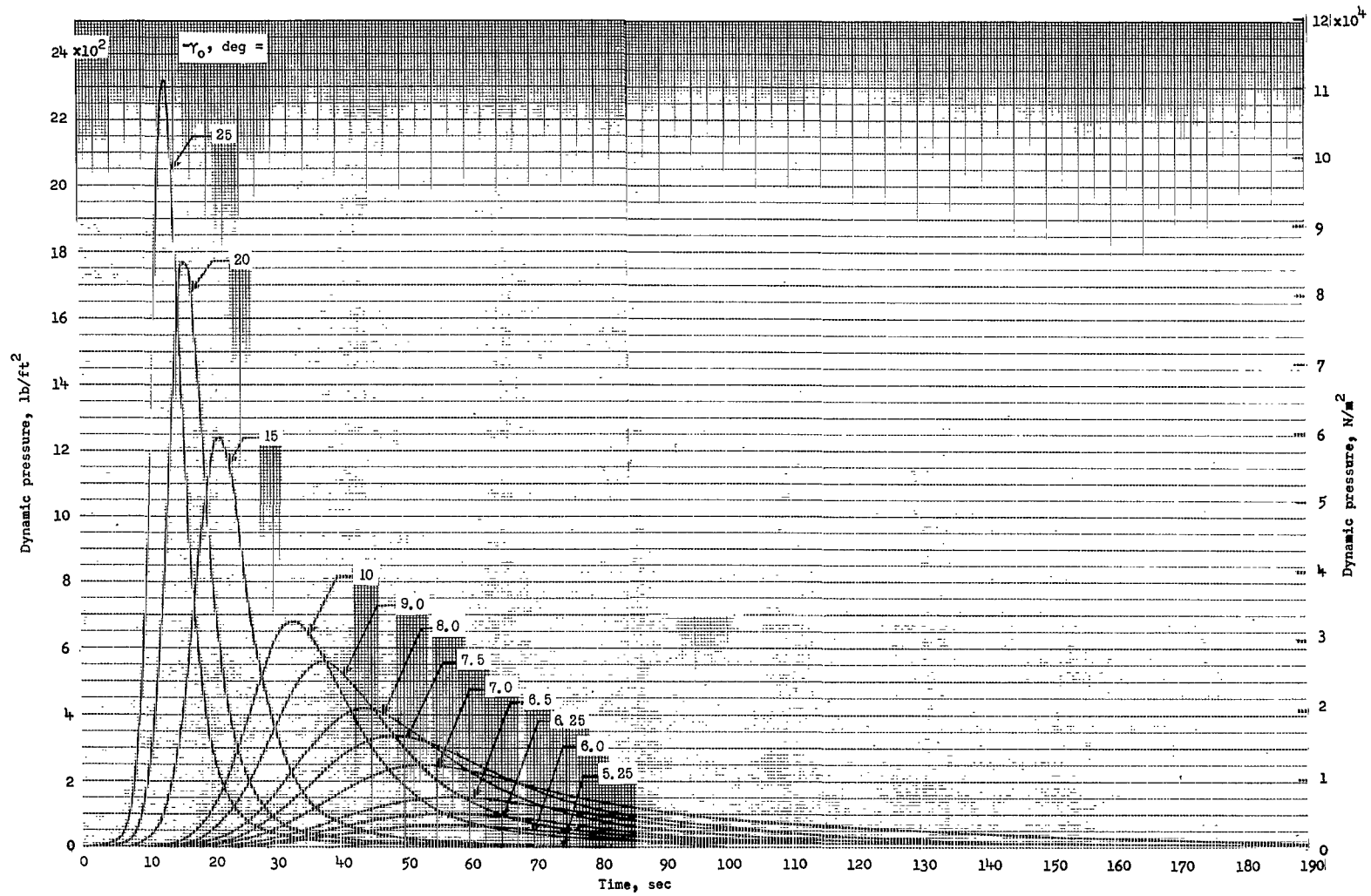
(a) $\dfrac{W}{C_D A} = 10$ lbf/ft^2 $\left(479 \text{ N/m}^2\right)$.

Figure 9.- Effect of initial reentry angle on the time history of dynamic pressure for ballistic trajectories. $V_0 = 50\ 000$ ft/sec (15 240 m/sec).
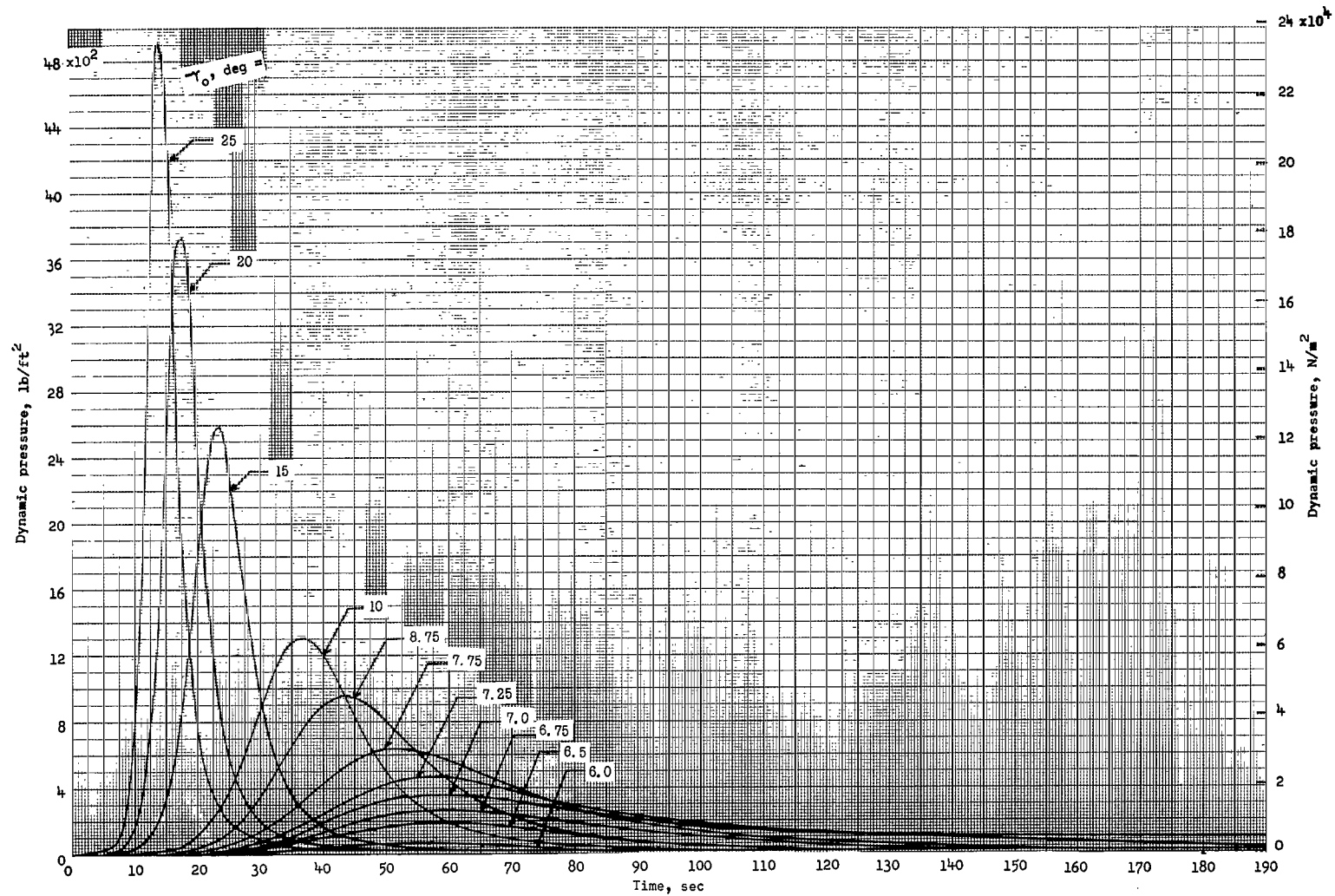
(b) $\frac{W}{C_D A}$ = 20 lbf/ft^2 (958 N/m^2).

Figure 9.- Continued.
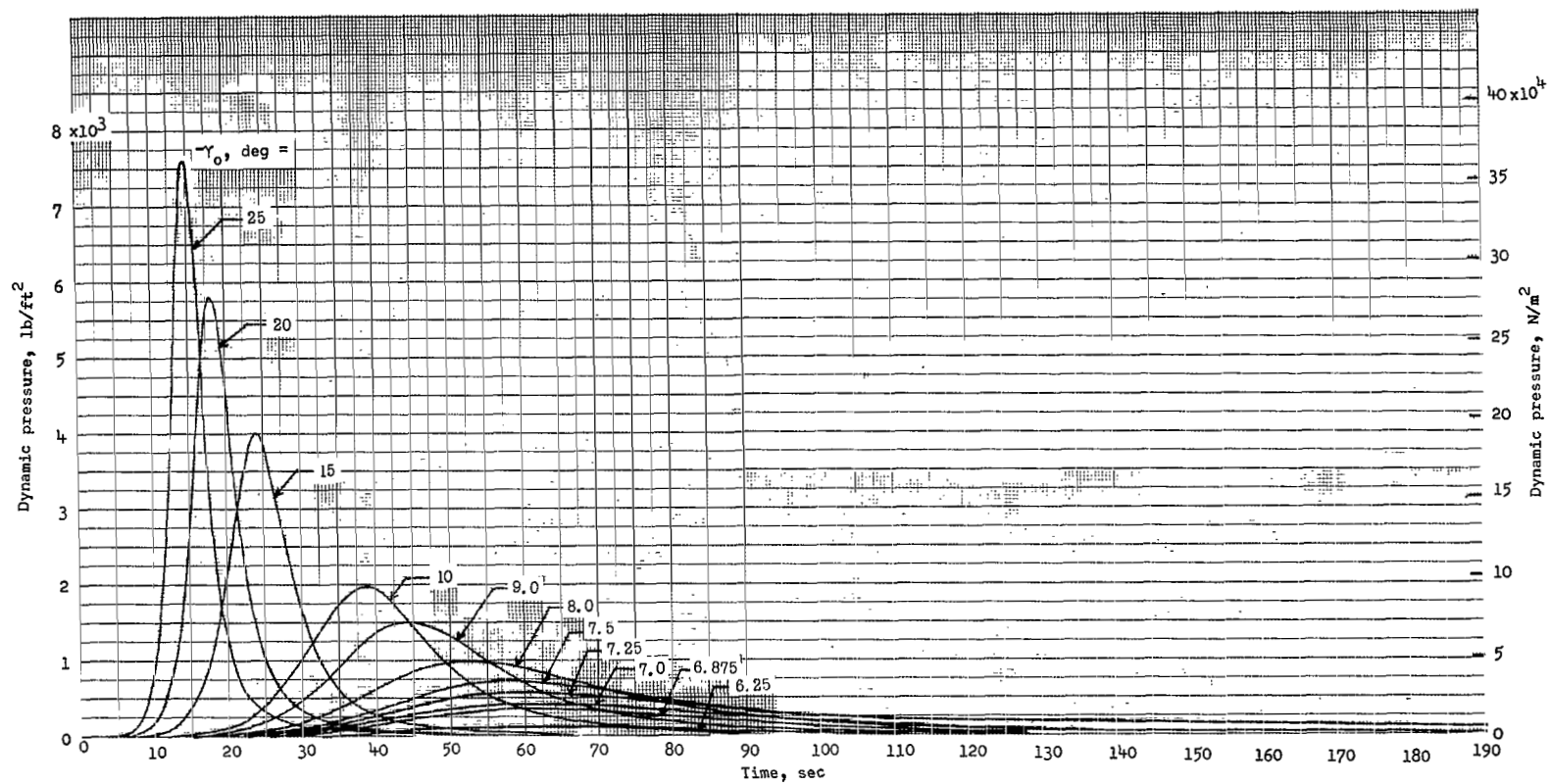
(c) $\frac{W}{C_D A}$ = 30 lbf/ft² $\left(1436 \text{ N/m}^2\right)$.

Figure 9.- Continued.
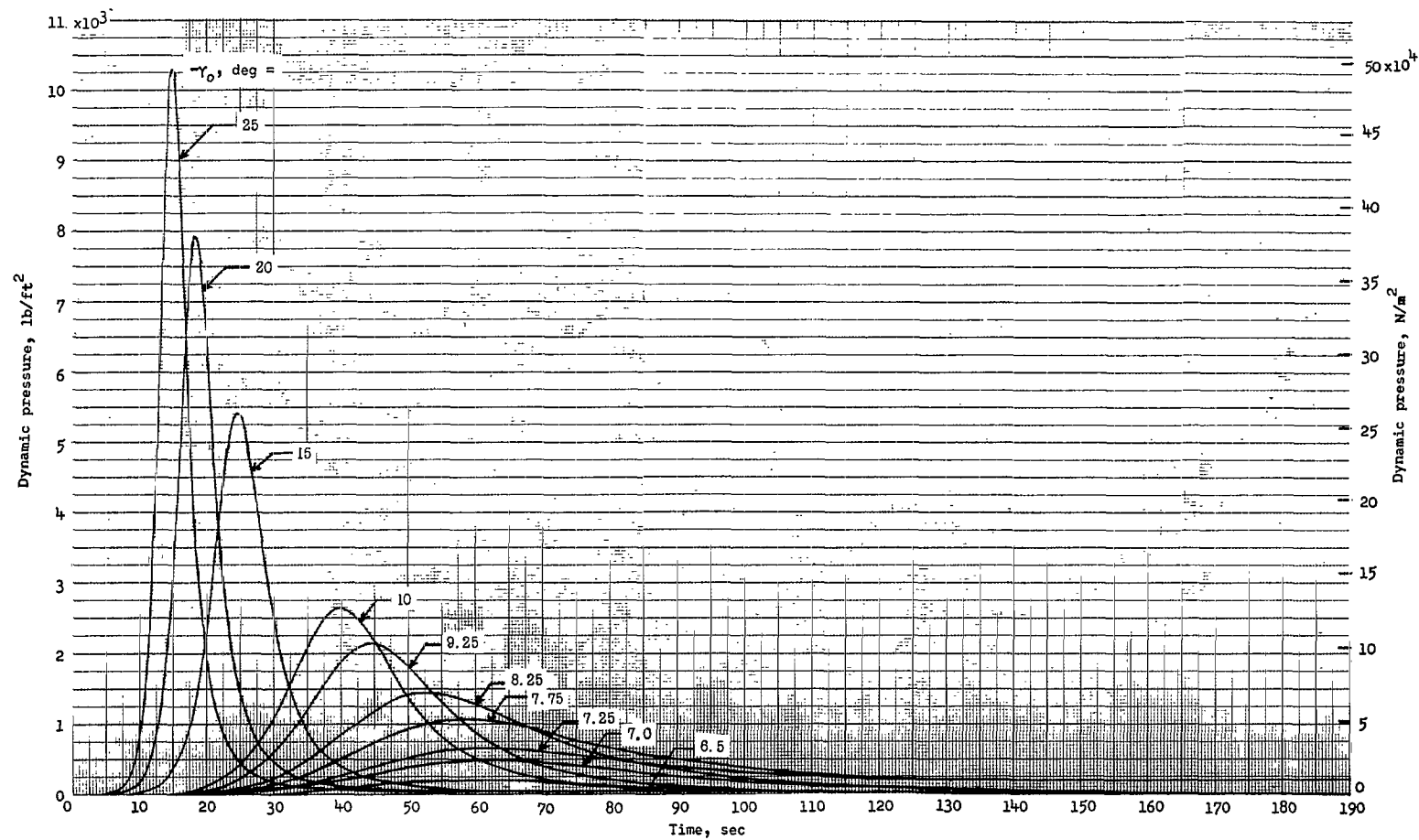
(d) $\frac{W}{C_DA} = 40 \text{ lbf/ft}^2 \left(1915 \text{ N/m}^2\right)$.

Figure 9.- Continued.
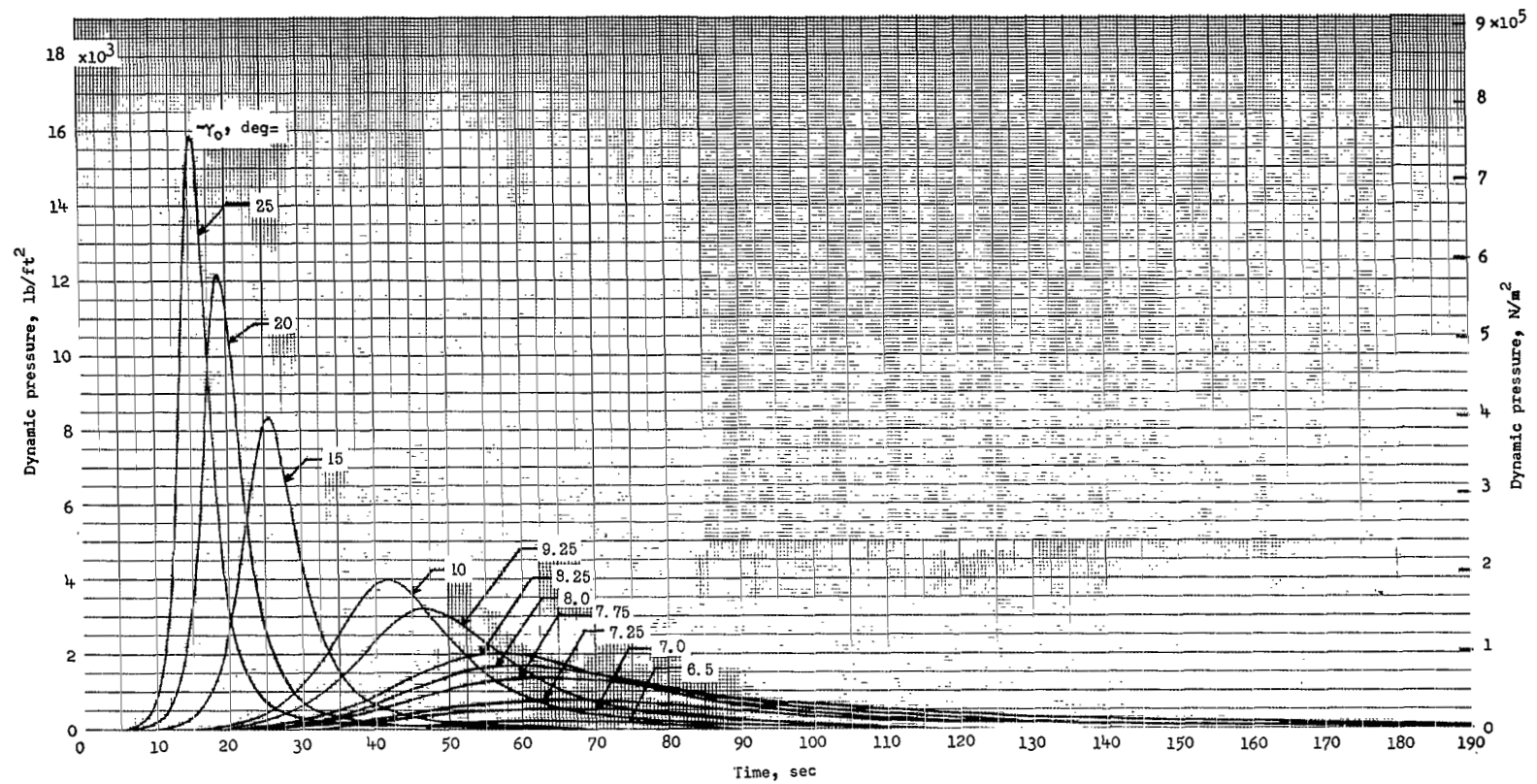
(e) $\dfrac{W}{C_D A} = 60$ lbf/ft^2 (2873 N/m^2).

Figure 9.- Continued.
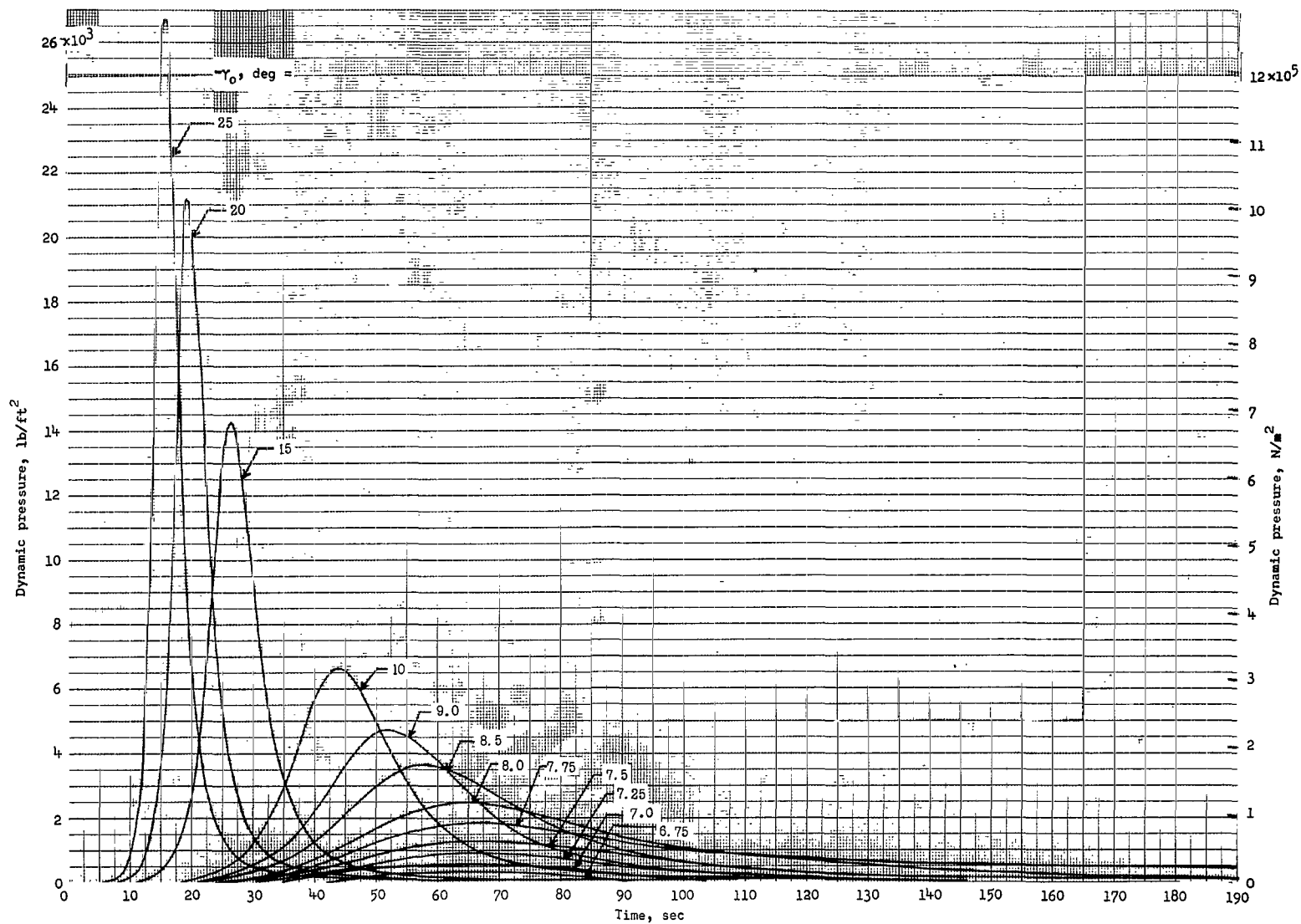
(f) $\frac{W}{C_D A}$ = 100 lbf/ft^2 (4788 N/m^2).

Figure 9.- Continued.
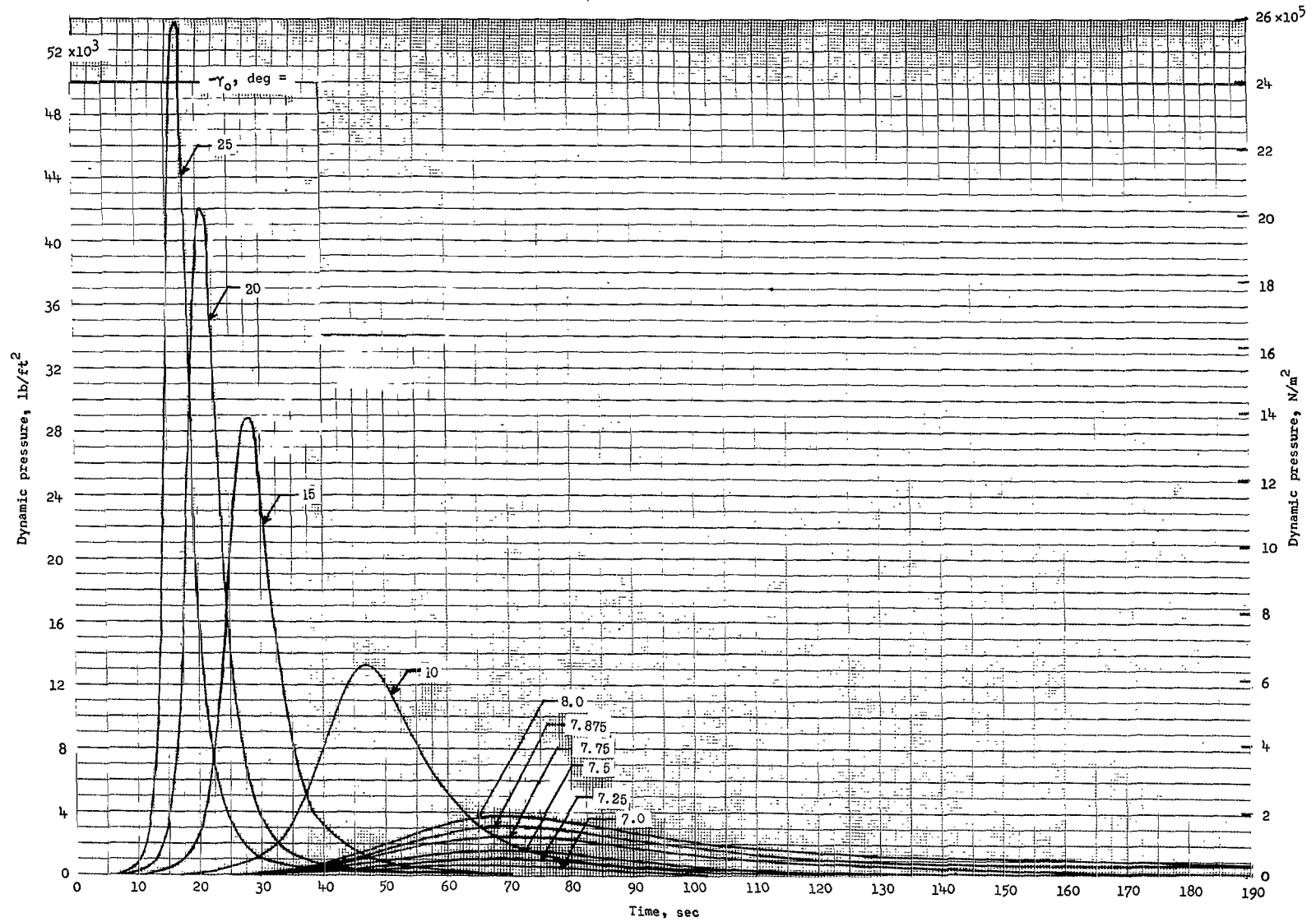
(g) $\frac{W}{C_D A} = 200$ lbf/ft^2 $\left(9576 \text{ N/m}^2\right)$.

Figure 9.- Concluded.

-14

-12

-10

-8

Initial reentry angle, γ_o, deg

-6

-4

-2

0

Direct reentry
trajectories

Skipping
reentry
trajectory

To nearest $1/4°$

To nearest $1/8°$

Skip-out trajectories
(Escape or orbital exit)

0   20   40   60   80   100   120   140   160   180   200

W/C_DA, lbf/ft^2

0   1   2   3   4   5   6   7   8 $9X10^3$

W/C_DA, N/m^2
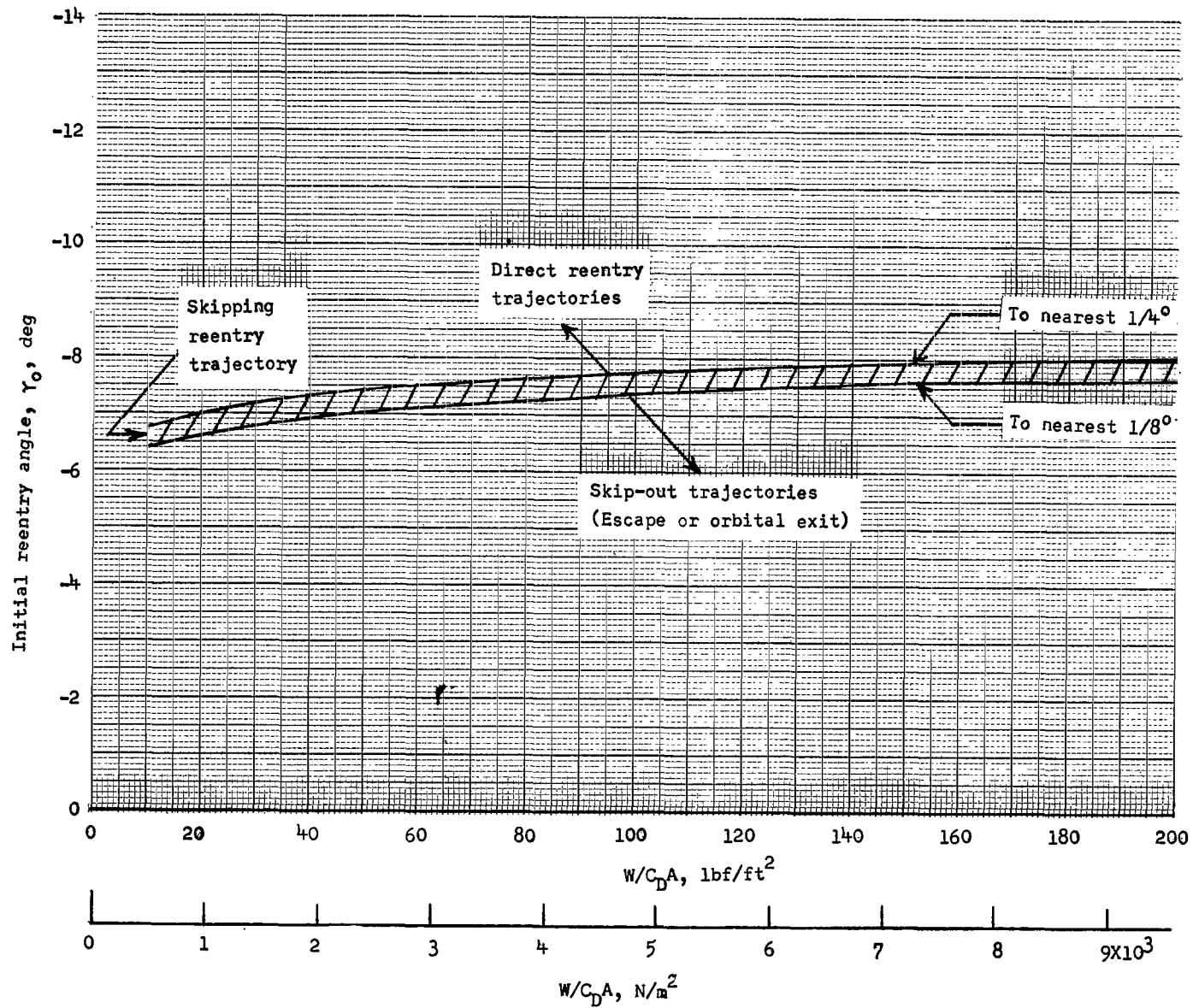
Figure 10.- Boundaries between skip-out, skipping reentry, and direct reentry trajectories.
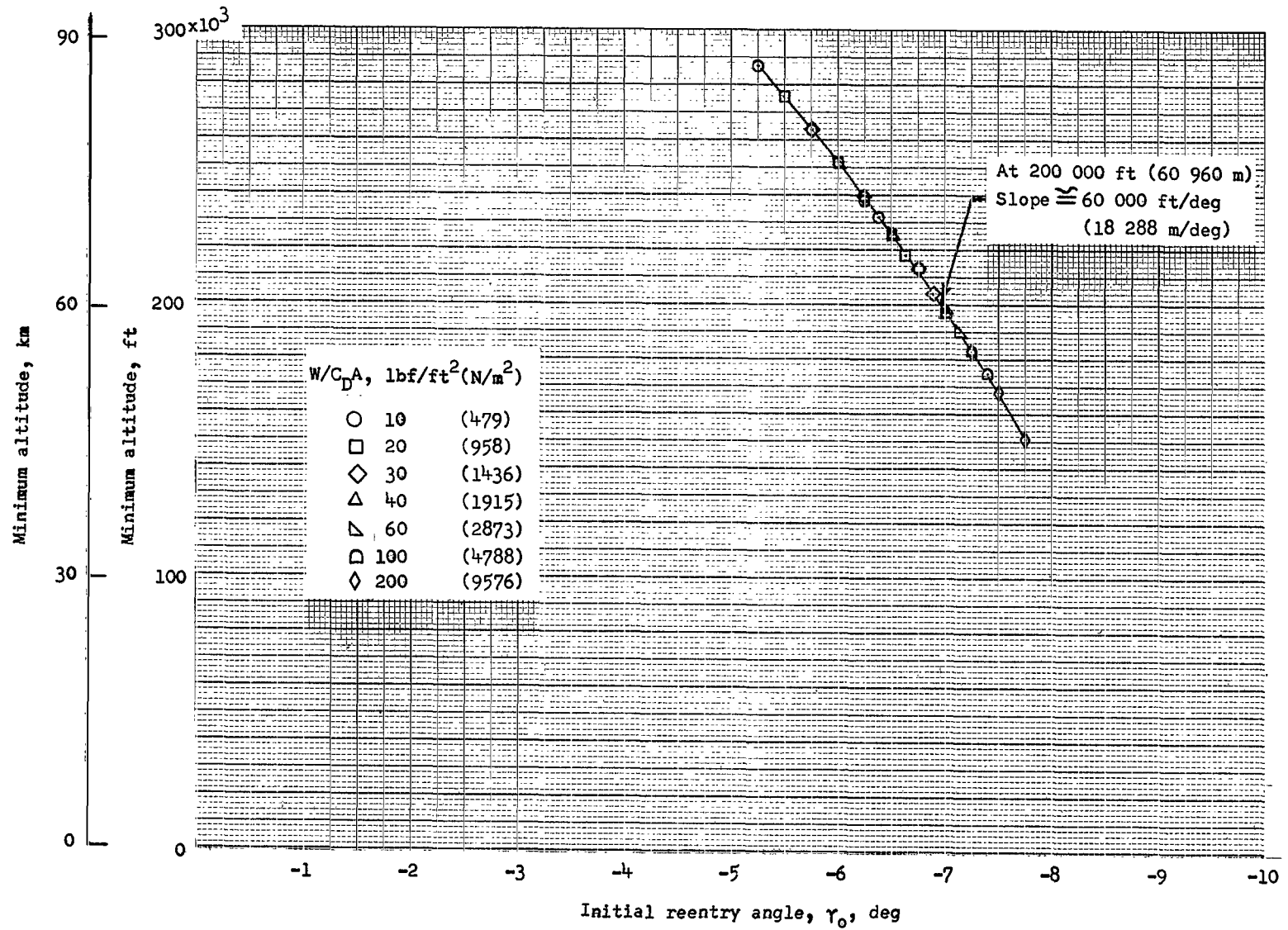
Figure 11.- Minimum altitudes for skip-out trajectories. V_0 = 50 000 ft/sec (15 240 m/sec).
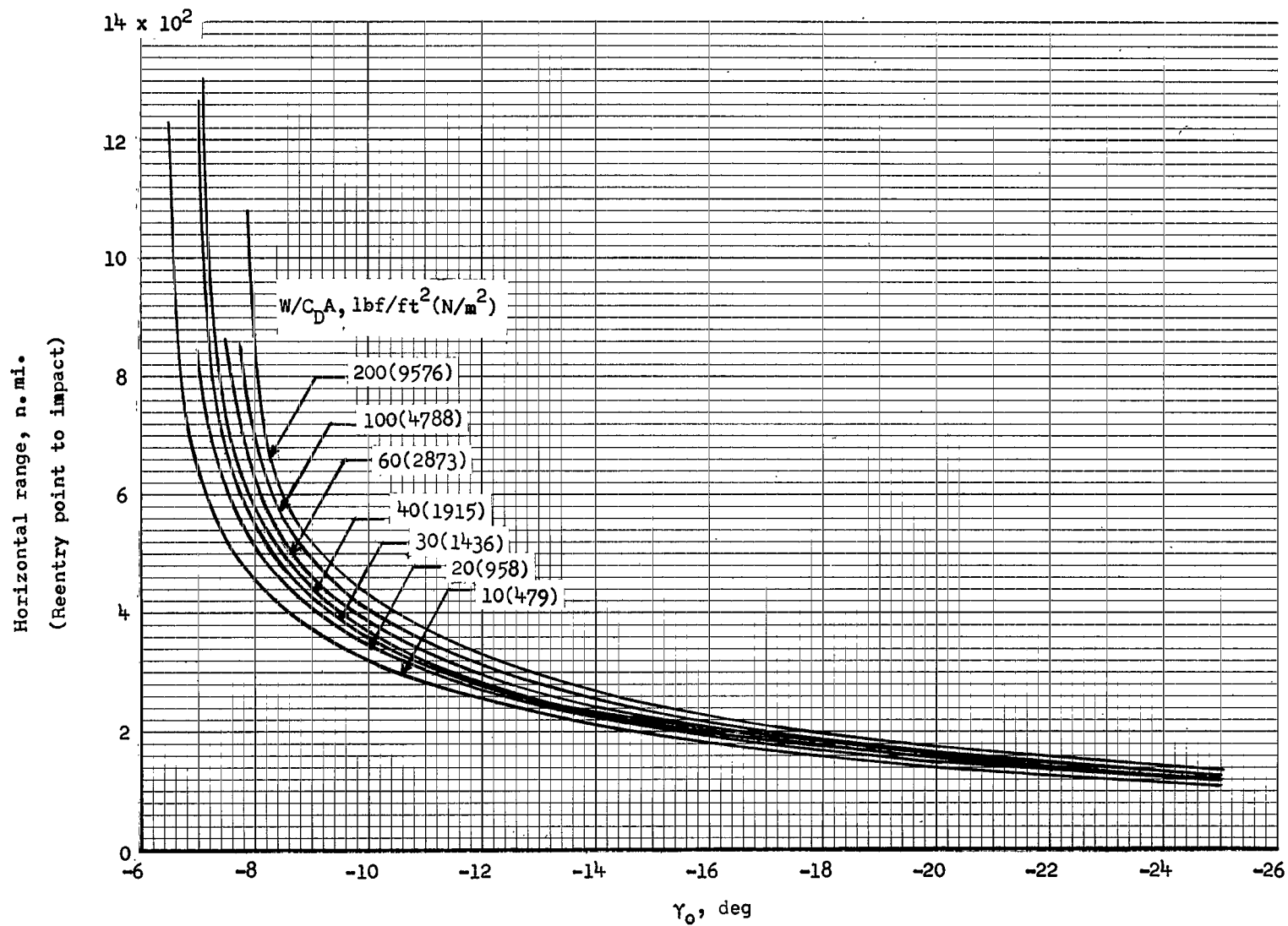
Figure 12.- Horizontal range from reentry point to impact for direct reentry trajectories.
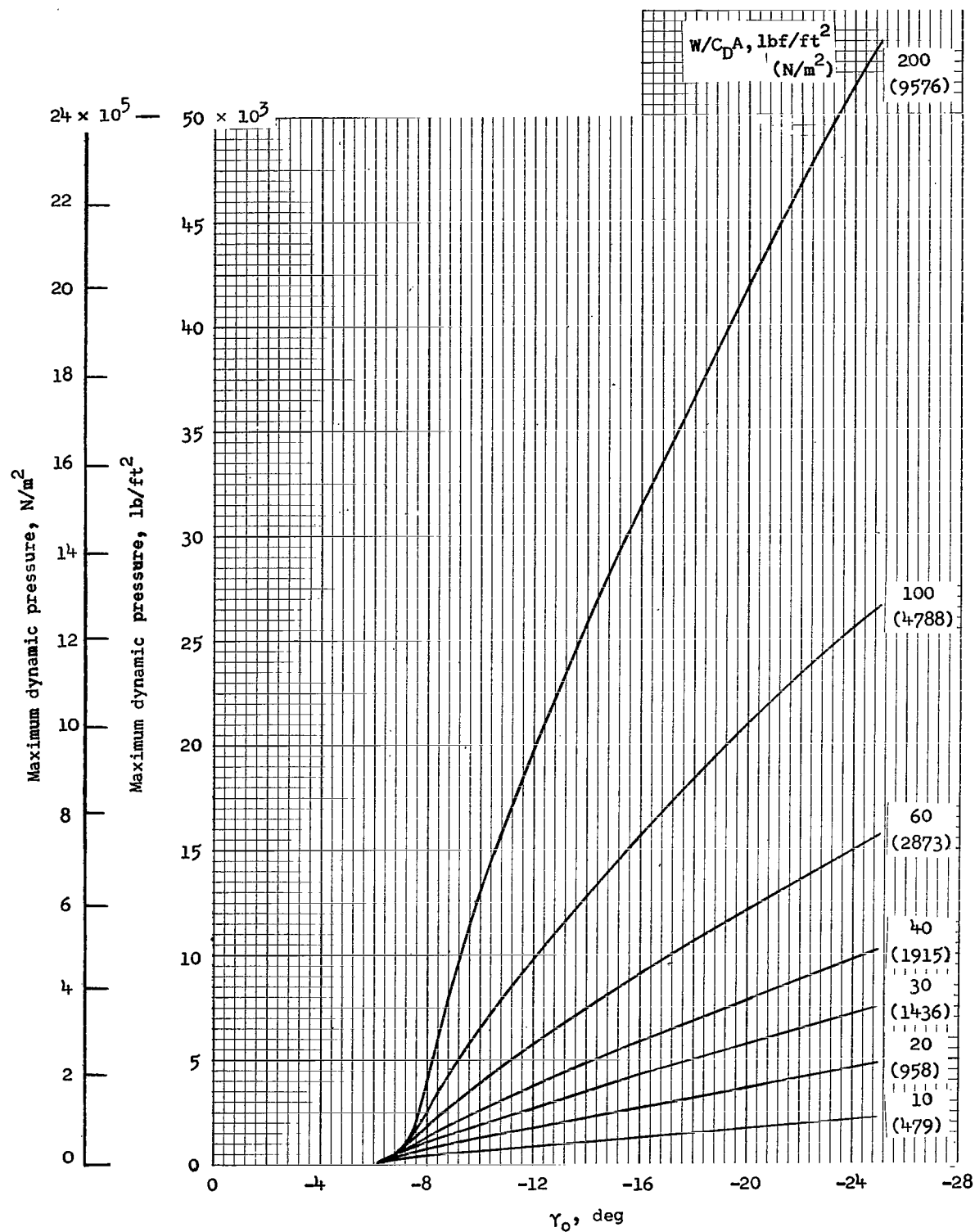
Figure 13.- Maximum dynamic pressure for direct reentry trajectories.
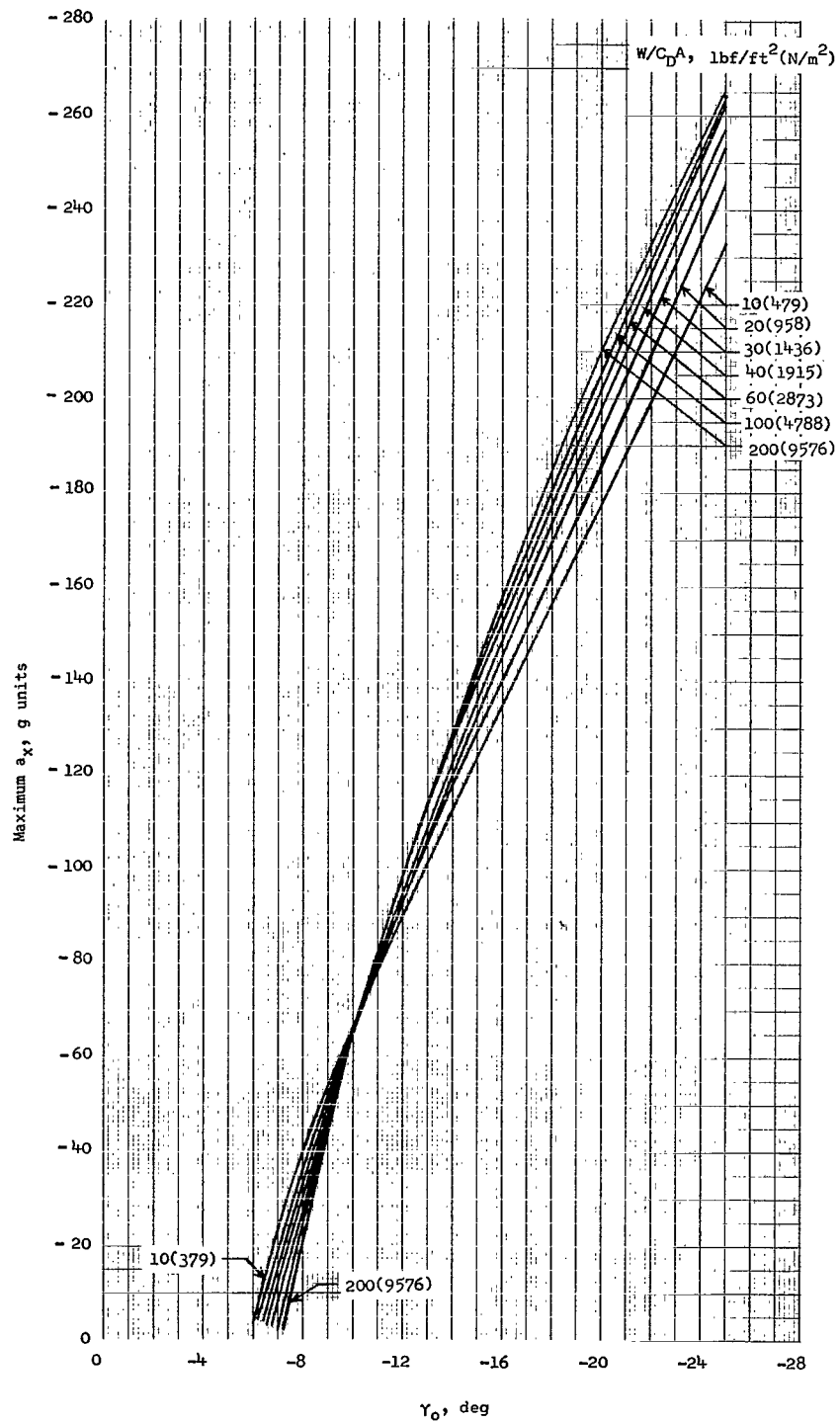
Figure 14.- Maximum acceleration along flight path for direct reentry trajectories.
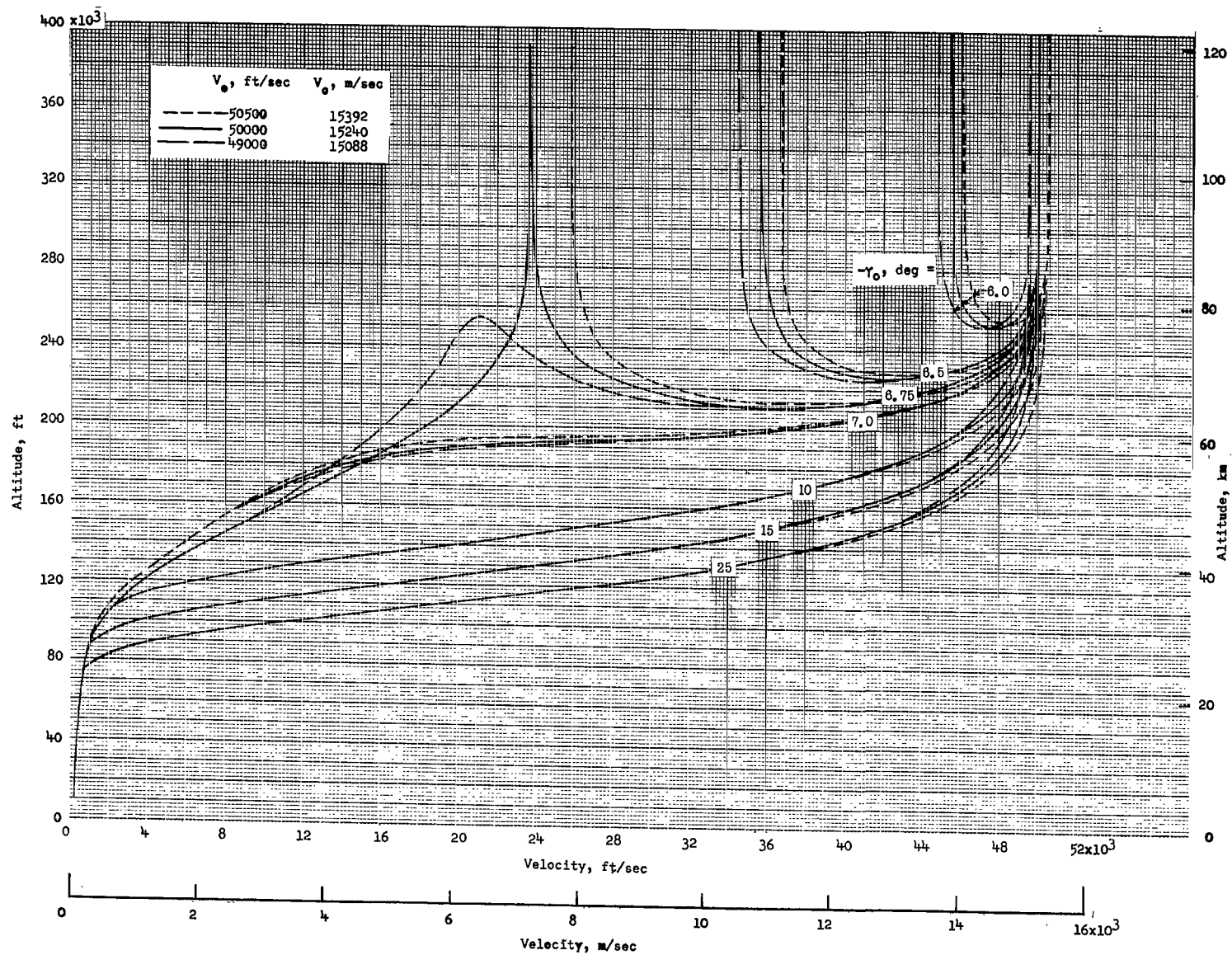
(a) $\frac{W}{C_D A} = 20$ lbf/ft^2 $\left(958 \text{ N/m}^2\right)$.

Figure 15.- Effect of initial-velocity errors on the altitude-velocity profile for various initial reentry angles.
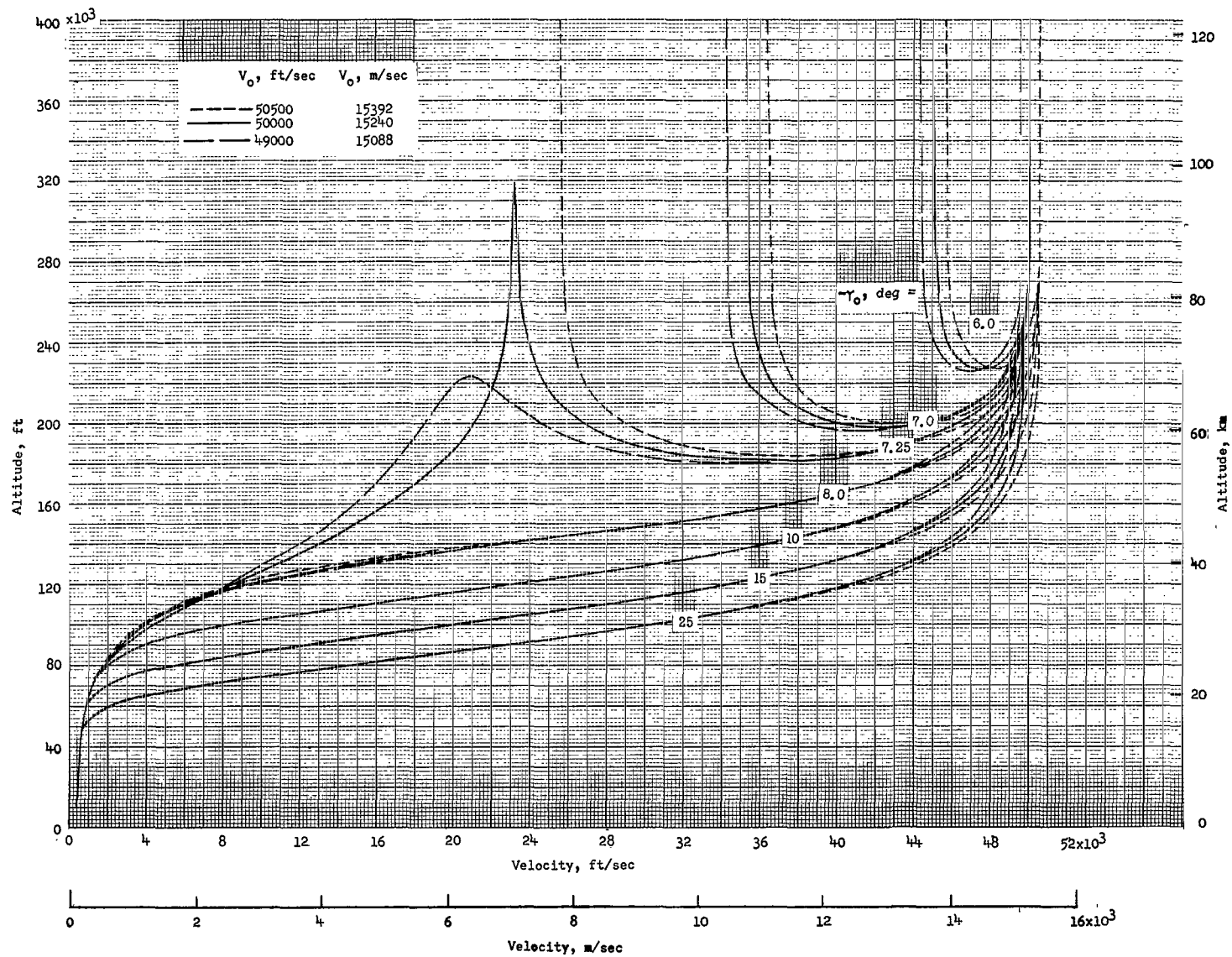
(b) $\frac{W}{C_DA} = 60 \text{ lbf/ft}^2 \left(2873 \text{ N/m}^2\right)$.
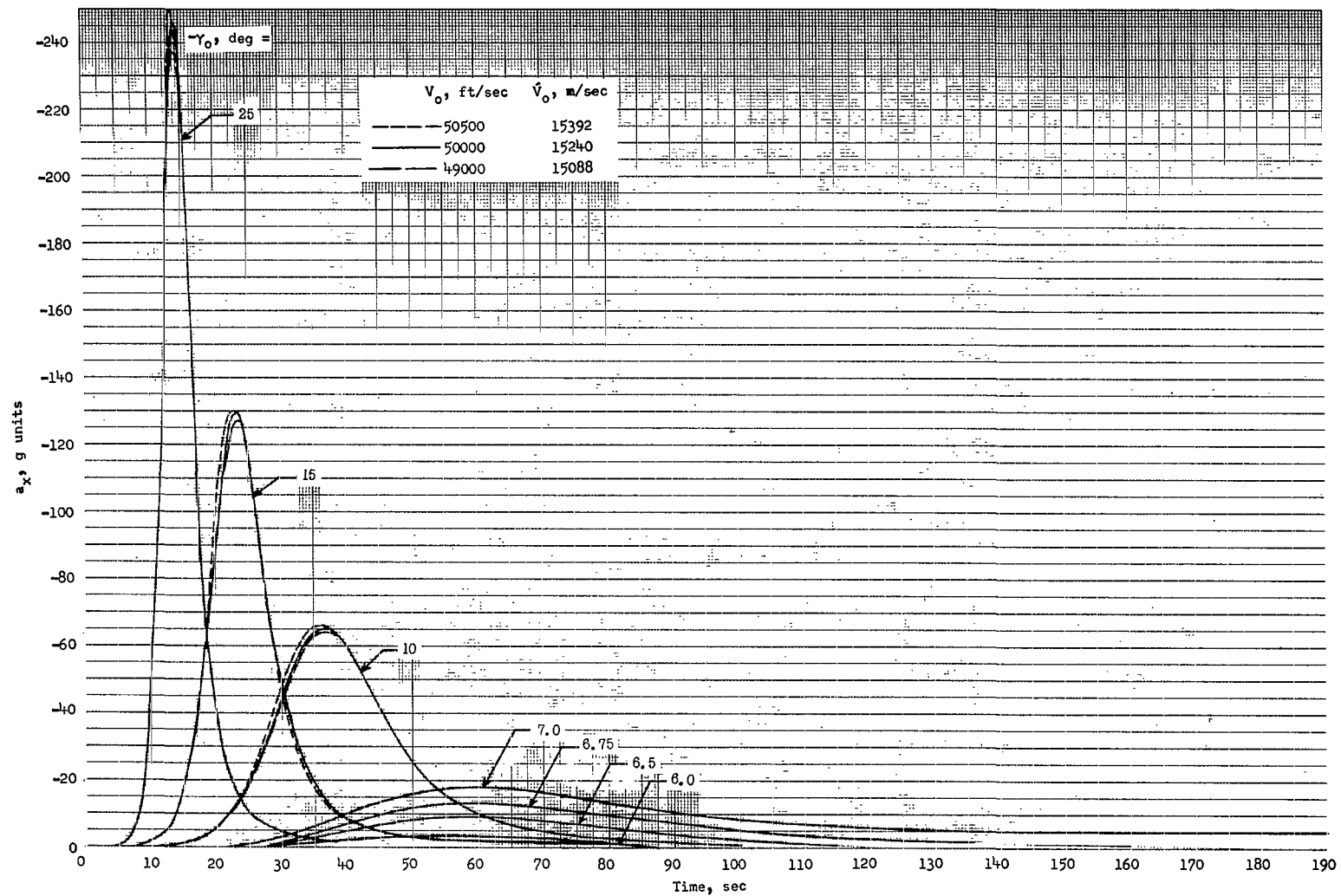
Figure 15.- Concluded.
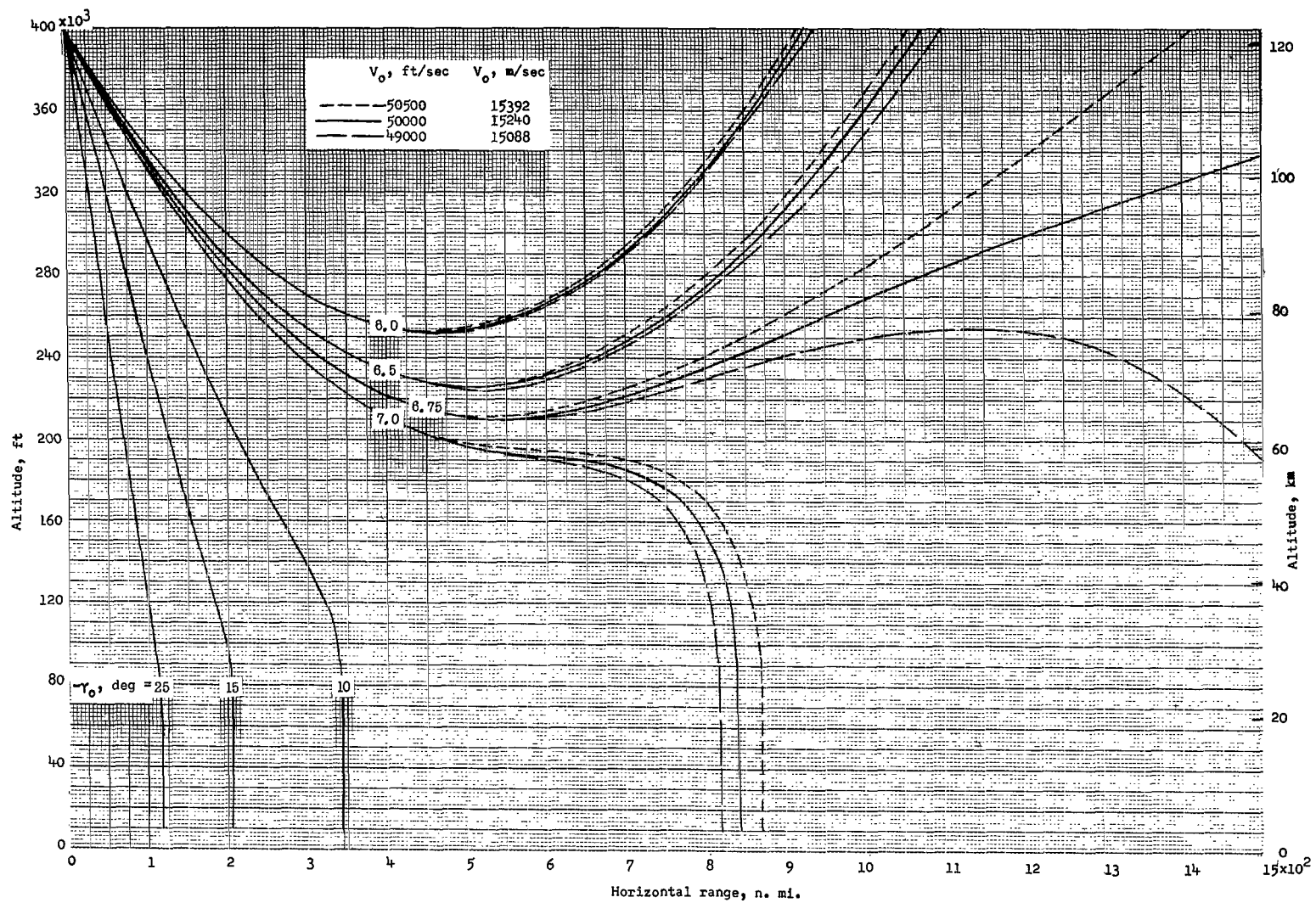
(a) $\dfrac{W}{C_D A}$ = 20 lbf/ft^2 $\left(958 \text{ N/m}^2\right)$.

Figure 16.- Effect of initial-velocity errors on the altitude-range profile for various initial reentry angles.
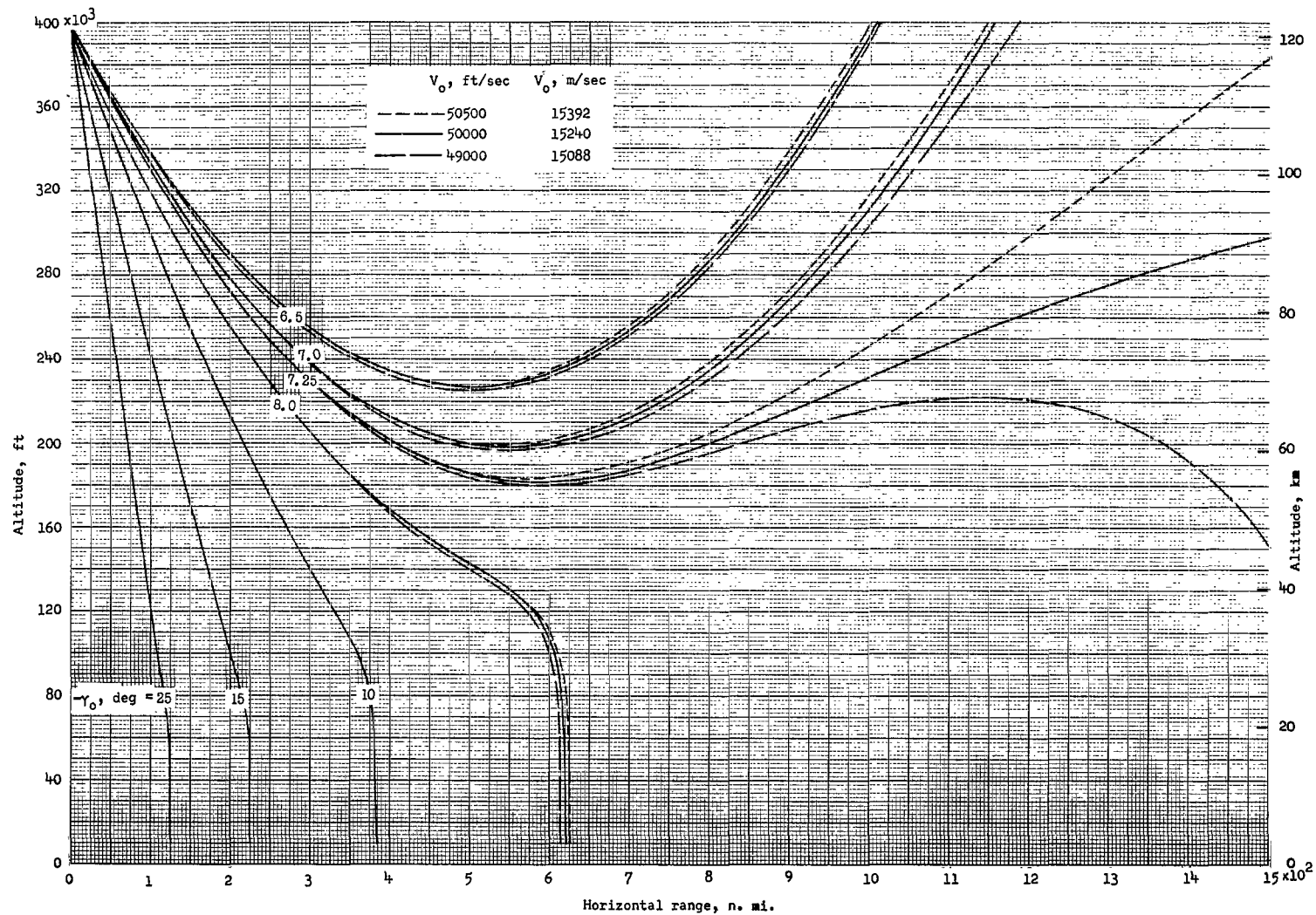
(b) $\dfrac{W}{C_D A} = 60 \text{ lbf/ft}^2 \left(2873 \text{ N/m}^2\right)$.

Figure 16.- Concluded.
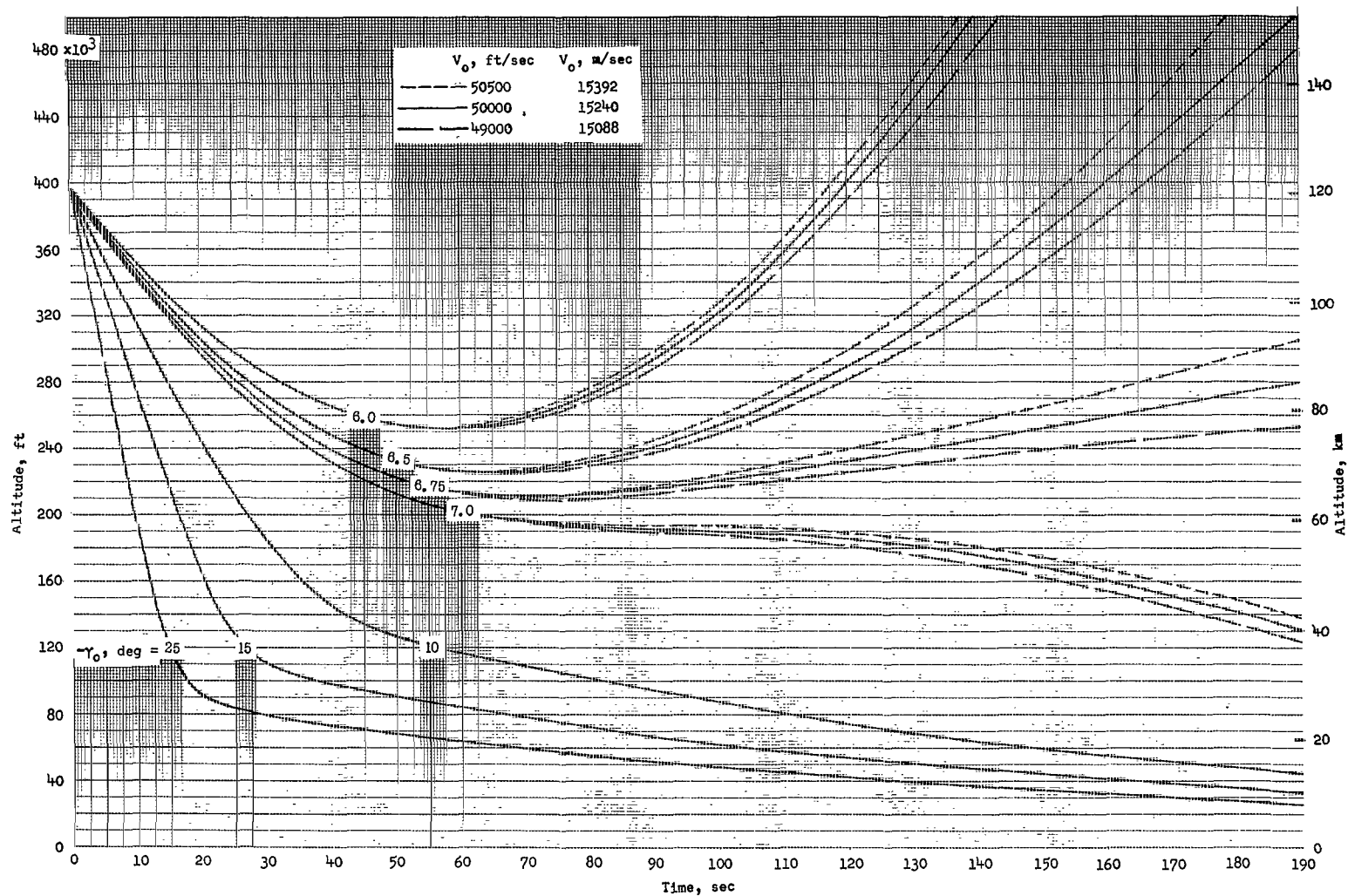
(a) $\frac{W}{C_D A}$ = 20 lbf/ft^2 (958 N/m^2).

Figure 17.- Effect of initial-velocity errors on the variation of altitude with time for various initial reentry angles.
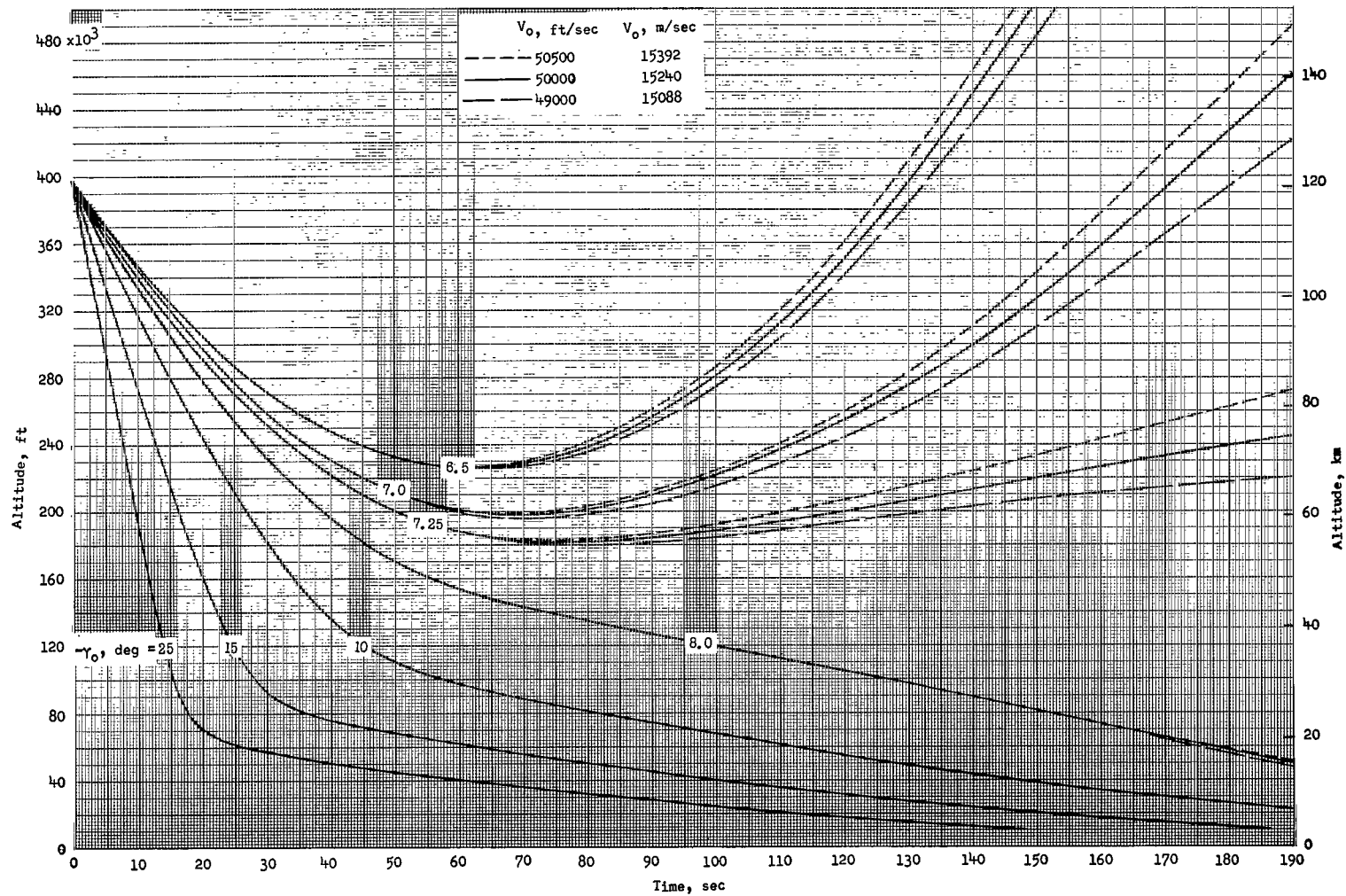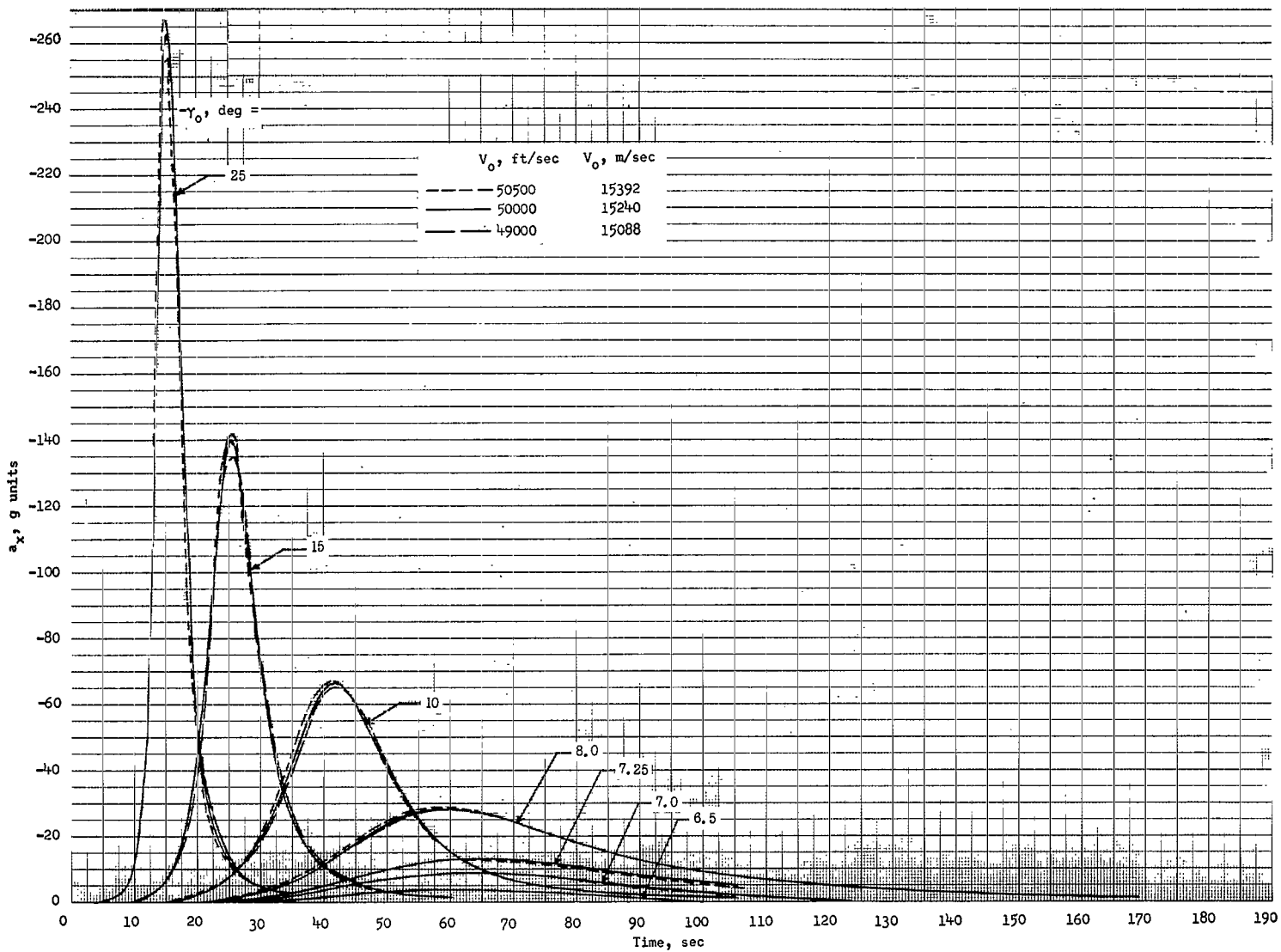
(b) $\frac{W}{C_D A} = 60$ lbf/ft^2 $\left(2873 \text{ N/m}^2\right)$.

Figure 17.- Concluded.
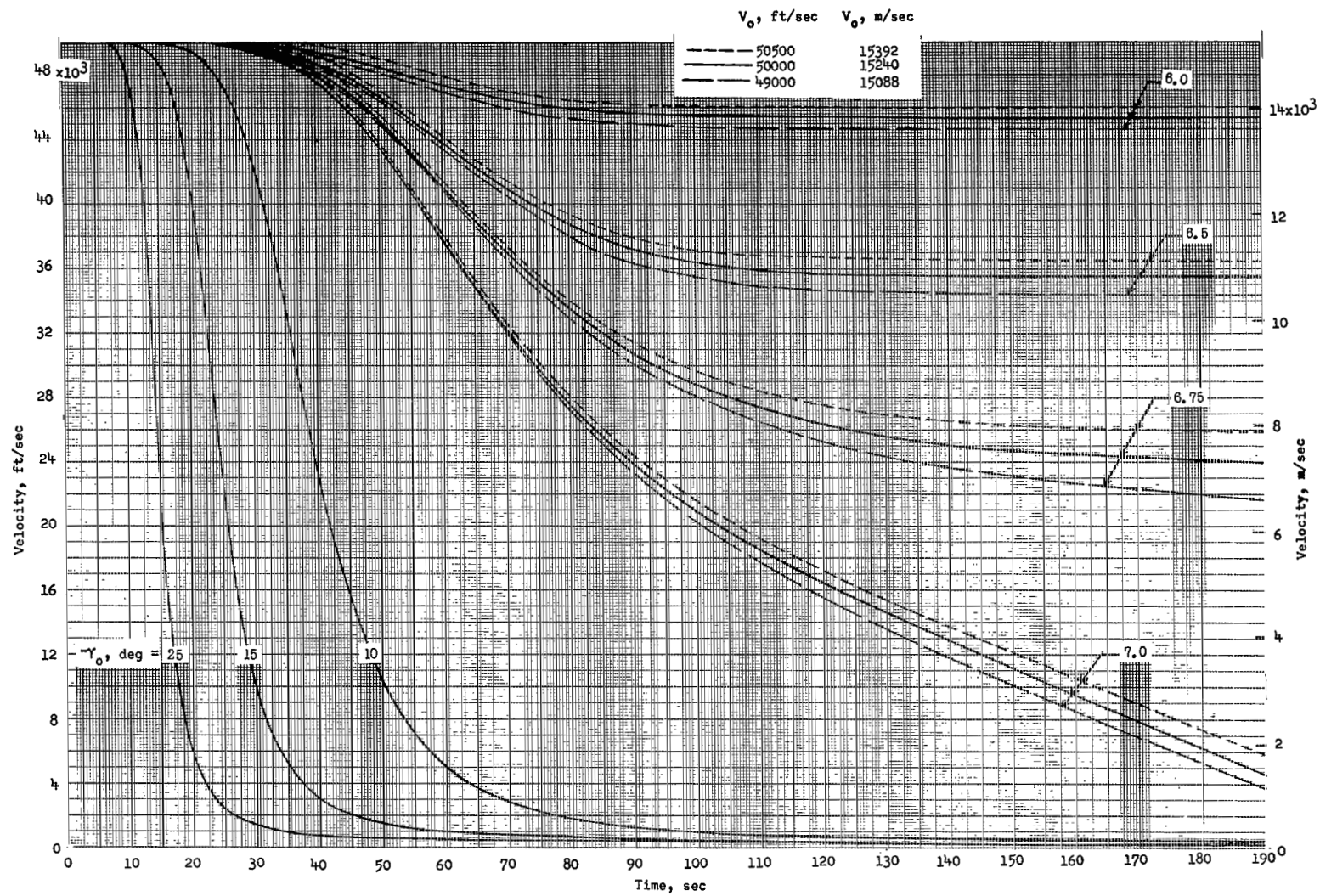
(a) $\frac{W}{C_D A}$ = 20 lbf/ft^2 (958 N/m^2).

Figure 18.- Effect of initial-velocity errors on the variation of velocity with time for various initial reentry angles.
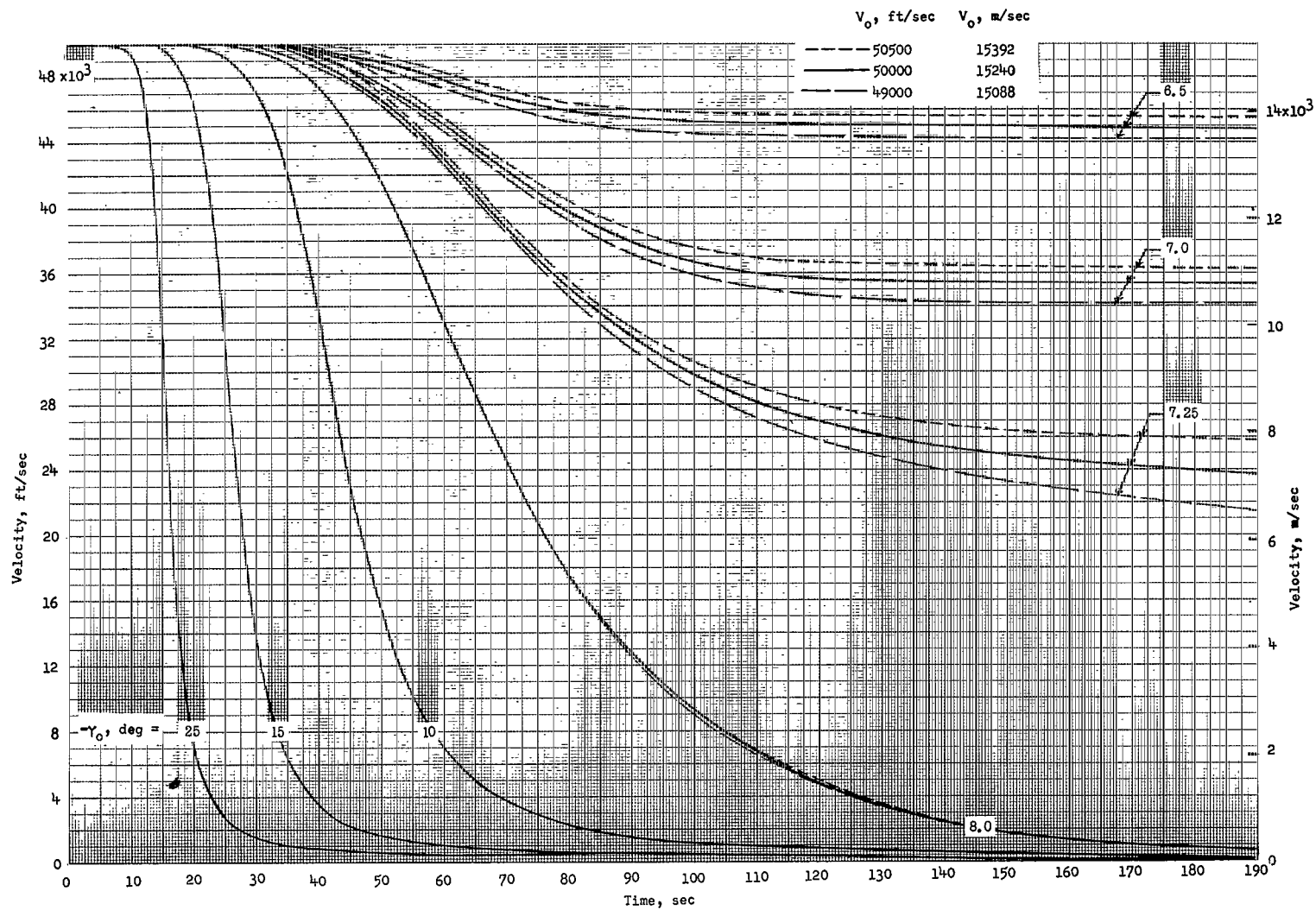
(b) $\dfrac{W}{C_D A} = 60$ lbf/ft^2 $\left(2873 \text{ N/m}^2\right)$.

Figure 18.- Concluded.

(a) $\frac{W}{C_D A}$ = 20 lbf/ft^2 (958 N/m^2).

Figure 19.- Effect of initial-velocity errors on the time history of acceleration along the flight path for various initial reentry angles.
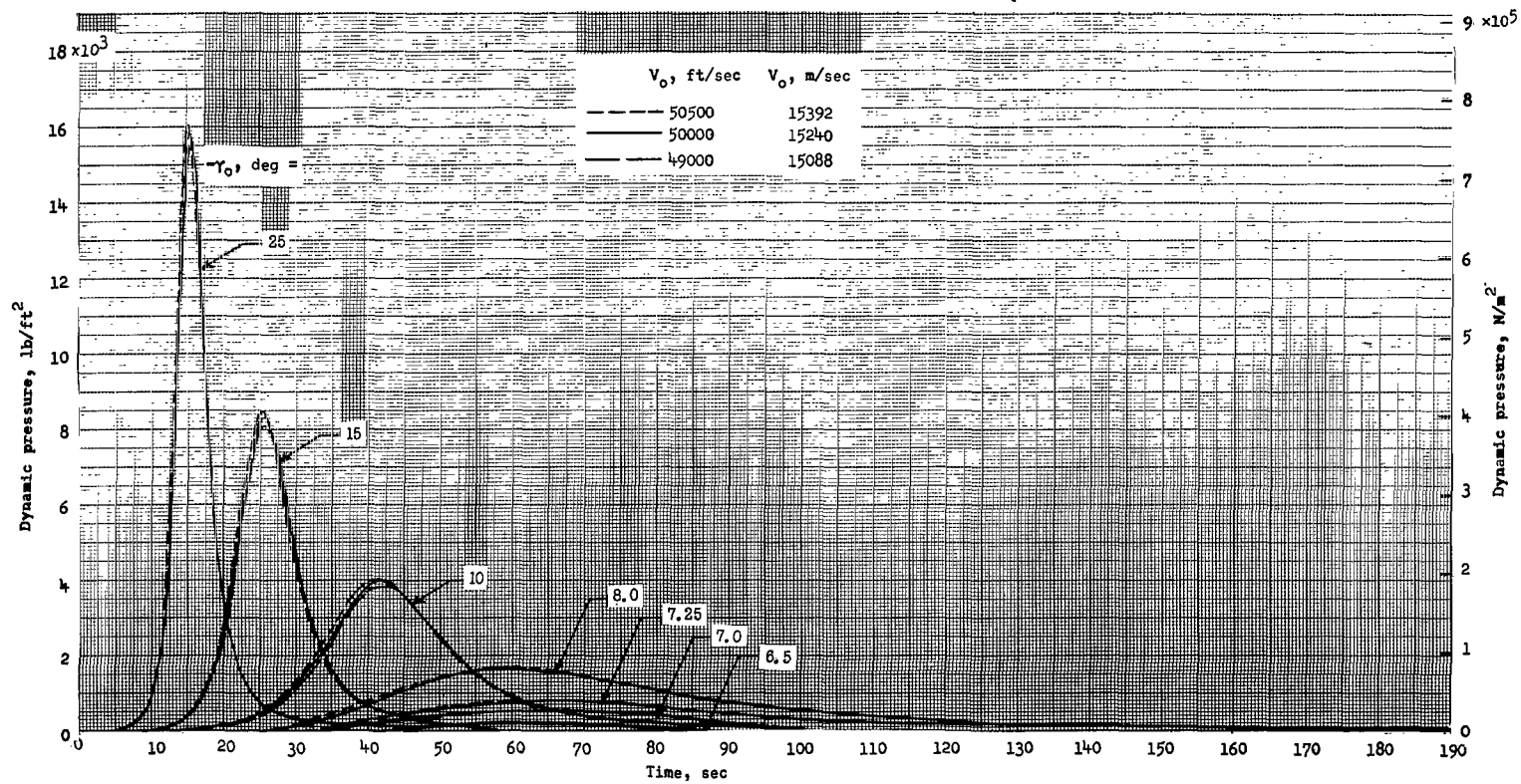
(b) $\frac{W}{C_DA} = 60$ lbf/ft^2 (2873 N/m^2).

Figure 19.- Concluded.
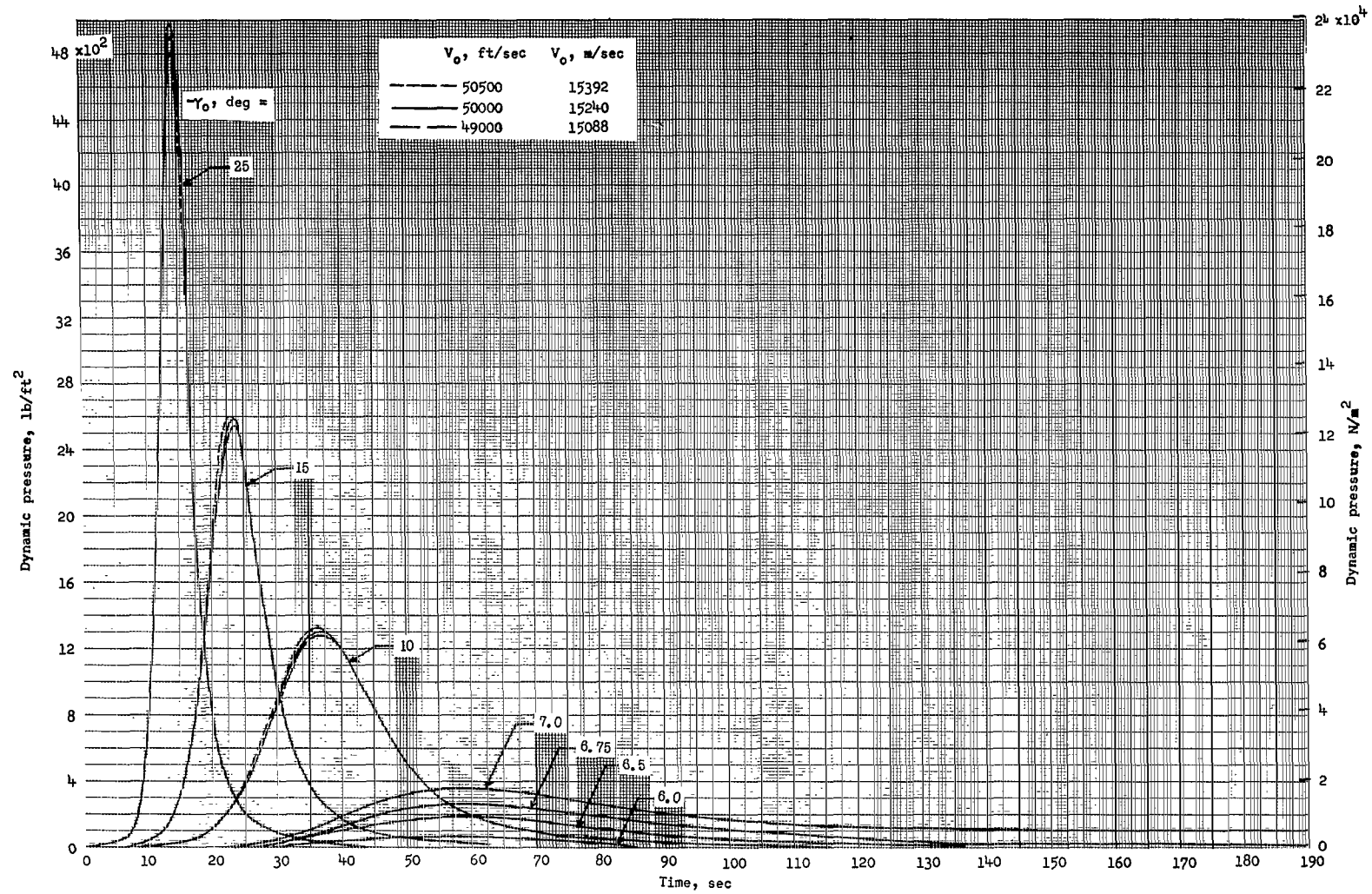
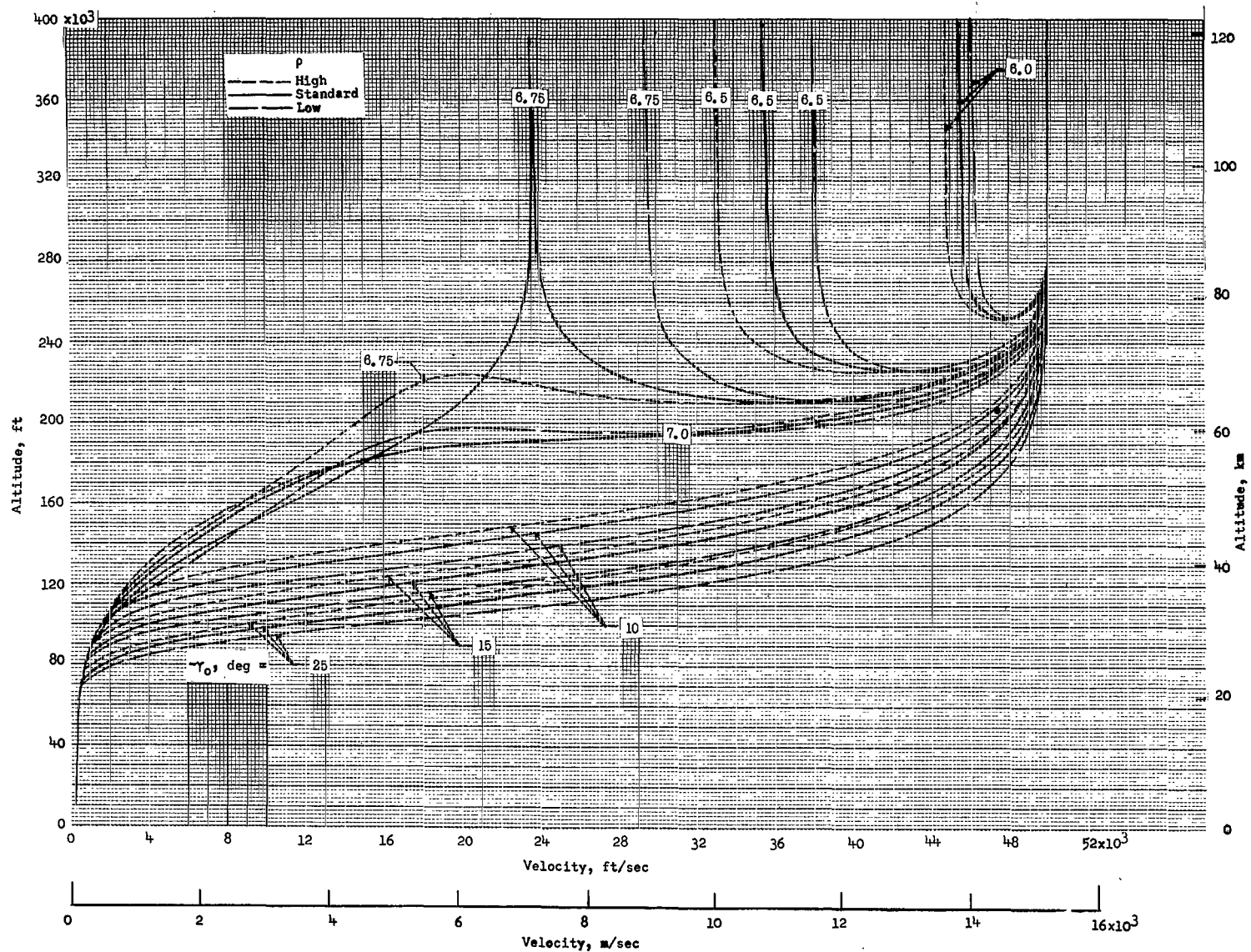(a) $\frac{W}{C_D A} = 20$ lbf/ft^2 $(958$ N/m$^2)$.

Figure 20.- Effect of initial-velocity errors on the time history of dynamic pressure for various initial reentry angles.

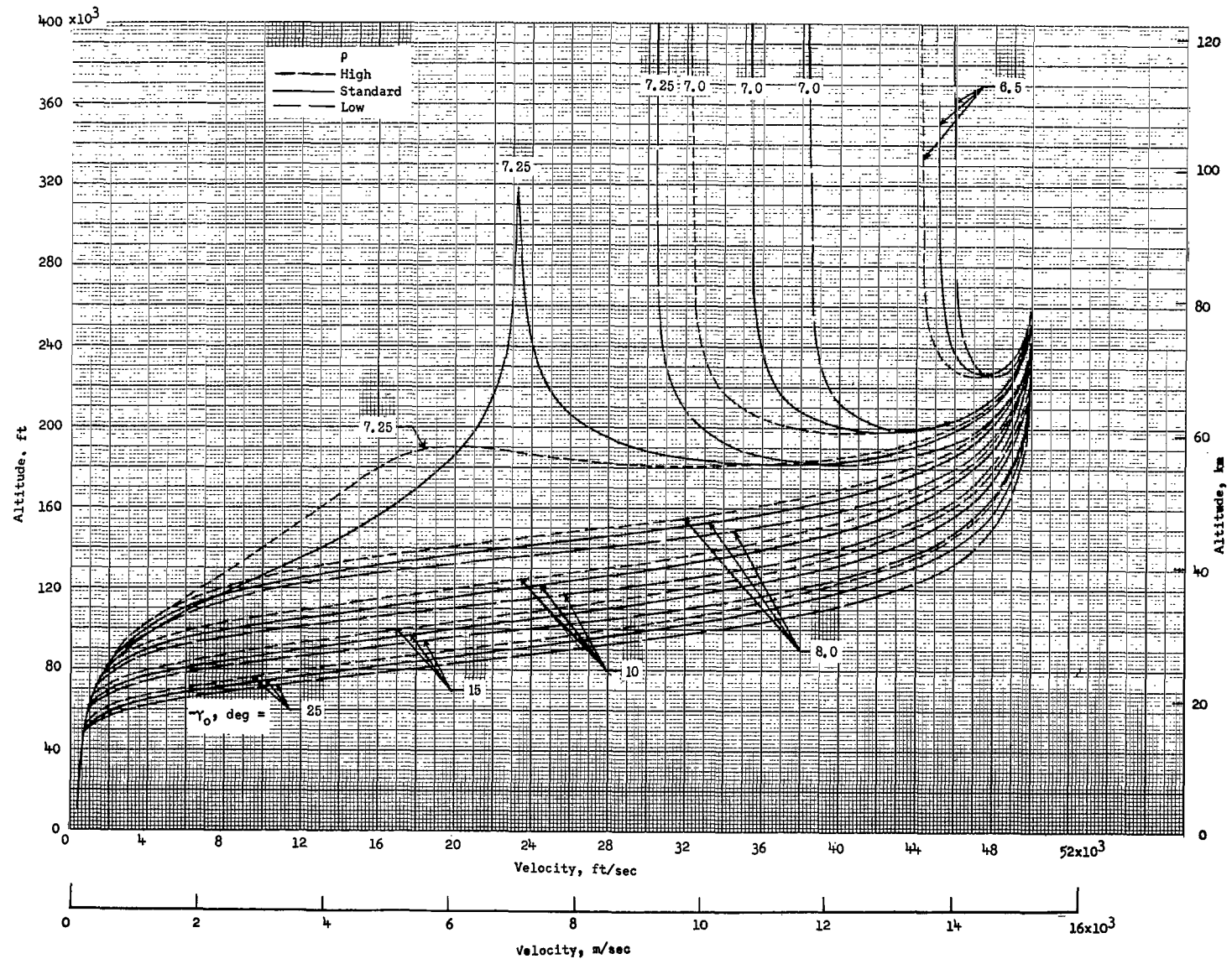(b) $\frac{W}{C_D A}$ = 60 lbf/ft^2 $\left(2873 \text{ N/m}^2\right)$.
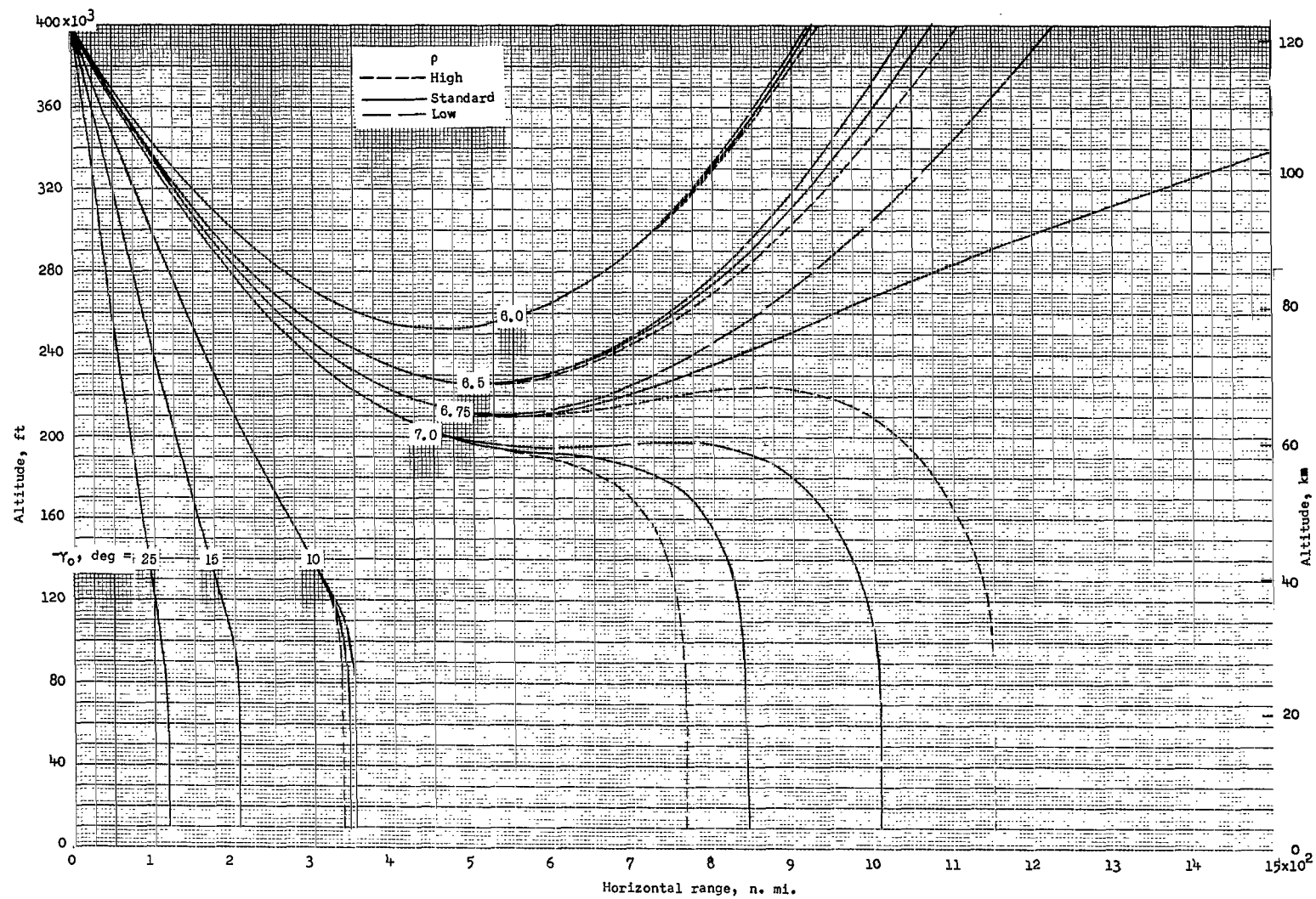
Figure 20.- Concluded.

(a) $\dfrac{W}{C_D A}$ = 20 lbf/ft^2 $\left(958 \text{ N/m}^2\right)$.

Figure 21.- Effect of atmospheric-density perturbations on the altitude-velocity profile for various initial reentry angles. V_0 = 50 000 ft/sec (15 240 m/sec).
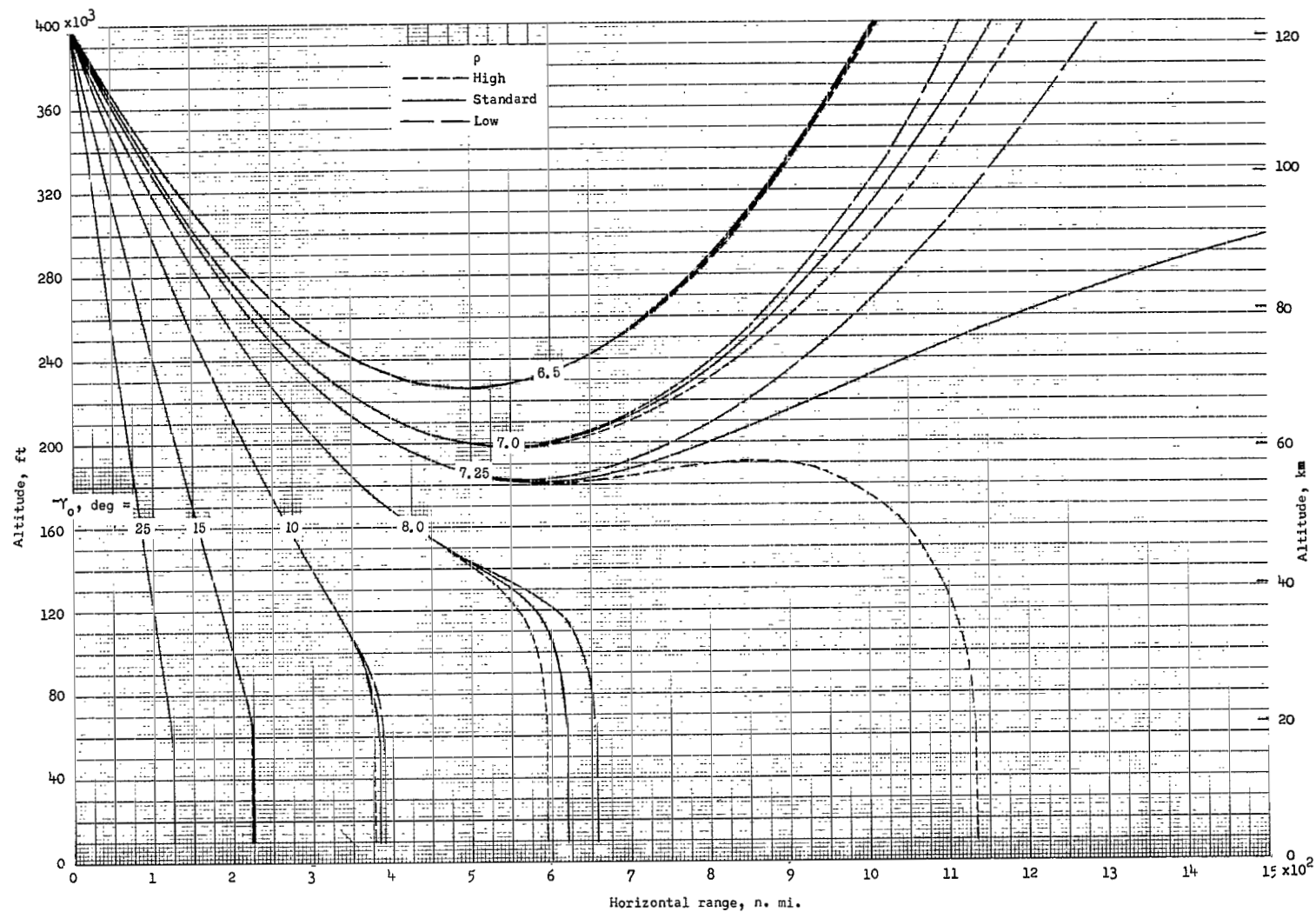
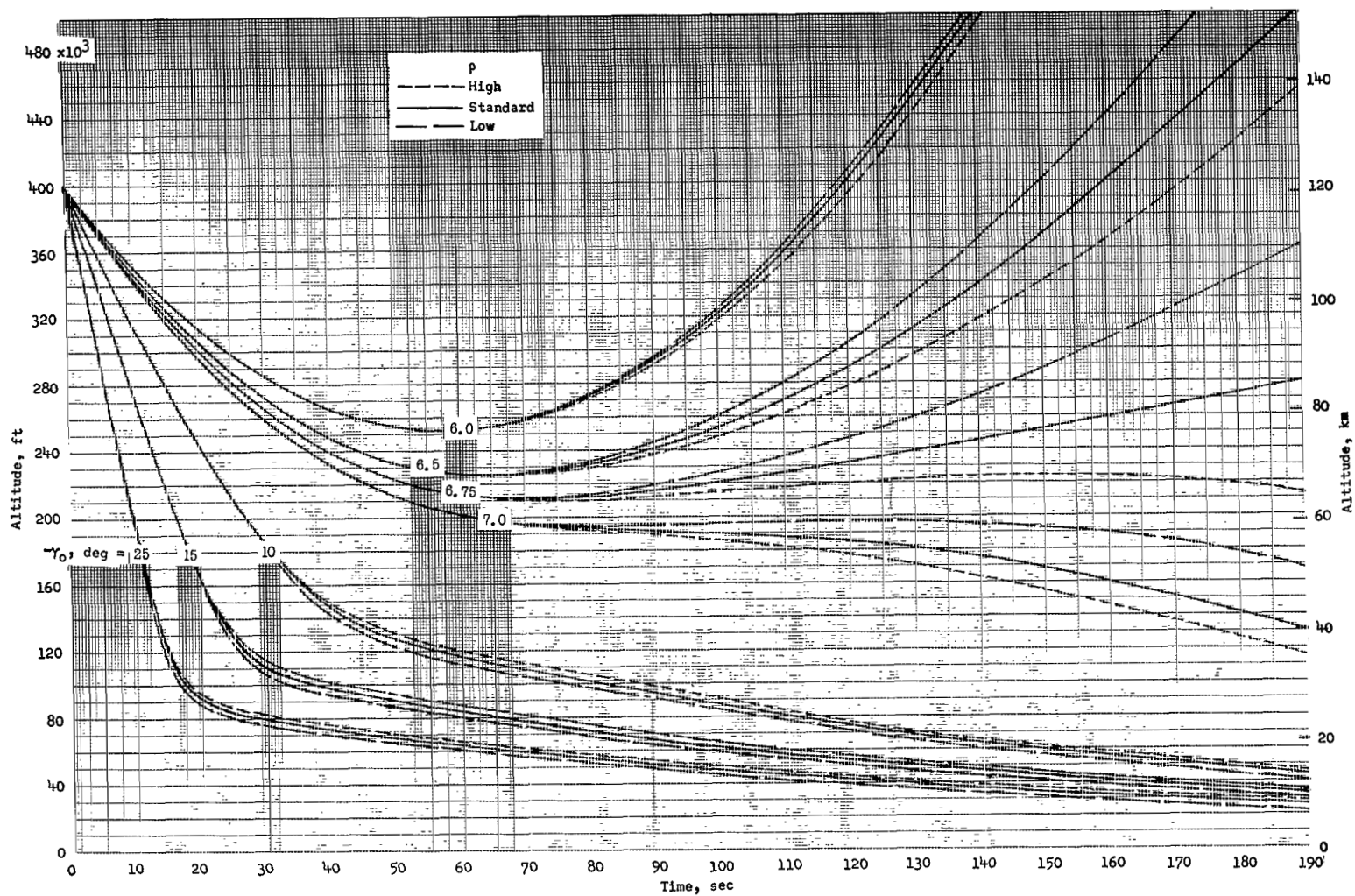(b) $\frac{W}{C_D A}$ = 60 lbf/ft^2 (2873 N/m^2).

Figure 21.- Concluded.

(a) $\dfrac{W}{C_D A} = 20$ lbf/ft^2 $\left(958 \text{ N/m}^2\right)$.

Figure 22.- Effect of atmospheric-density perturbations on the altitude-range profile for various initial reentry angles. $V_0 = 50\,000$ ft/sec (15 240 m/sec).
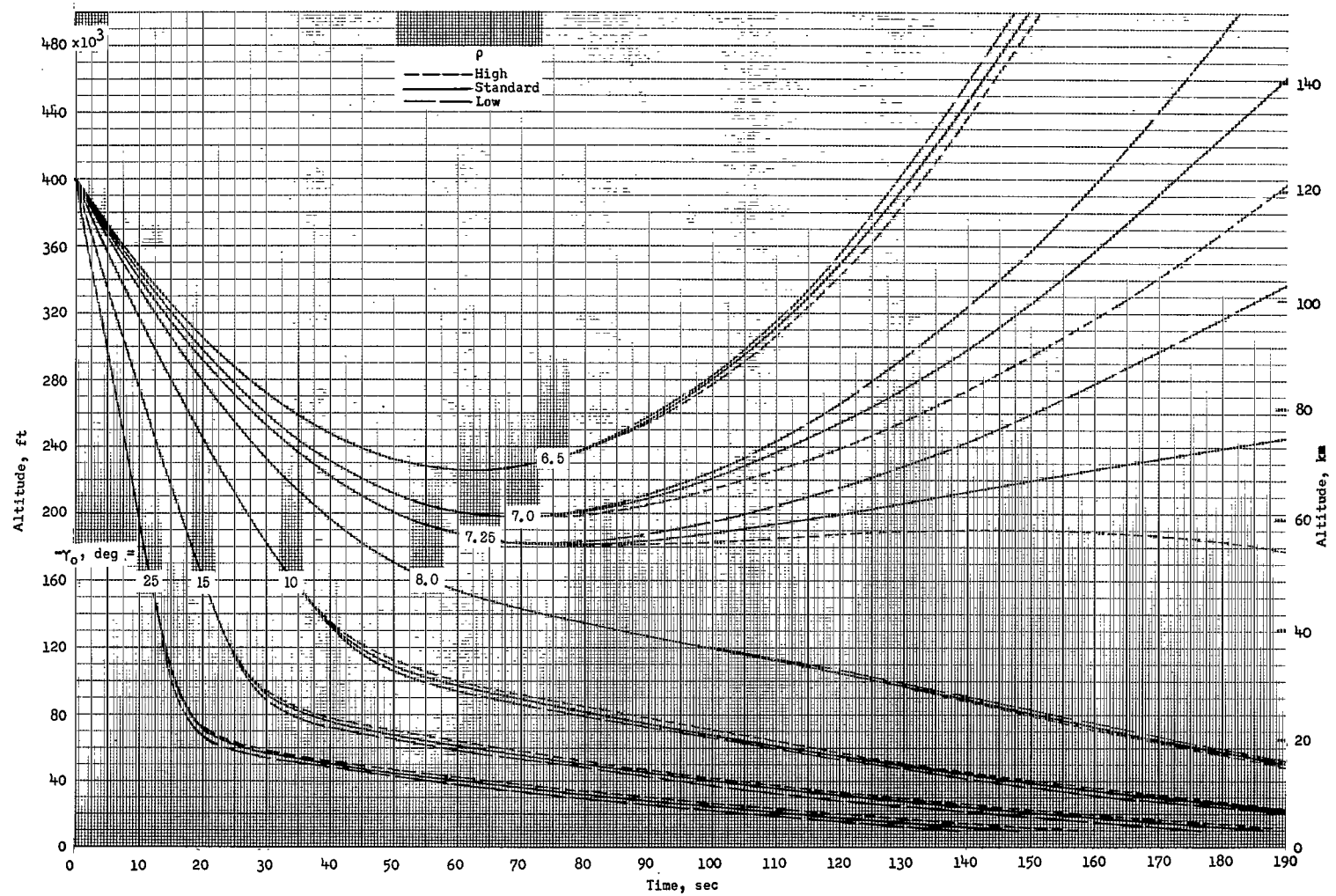
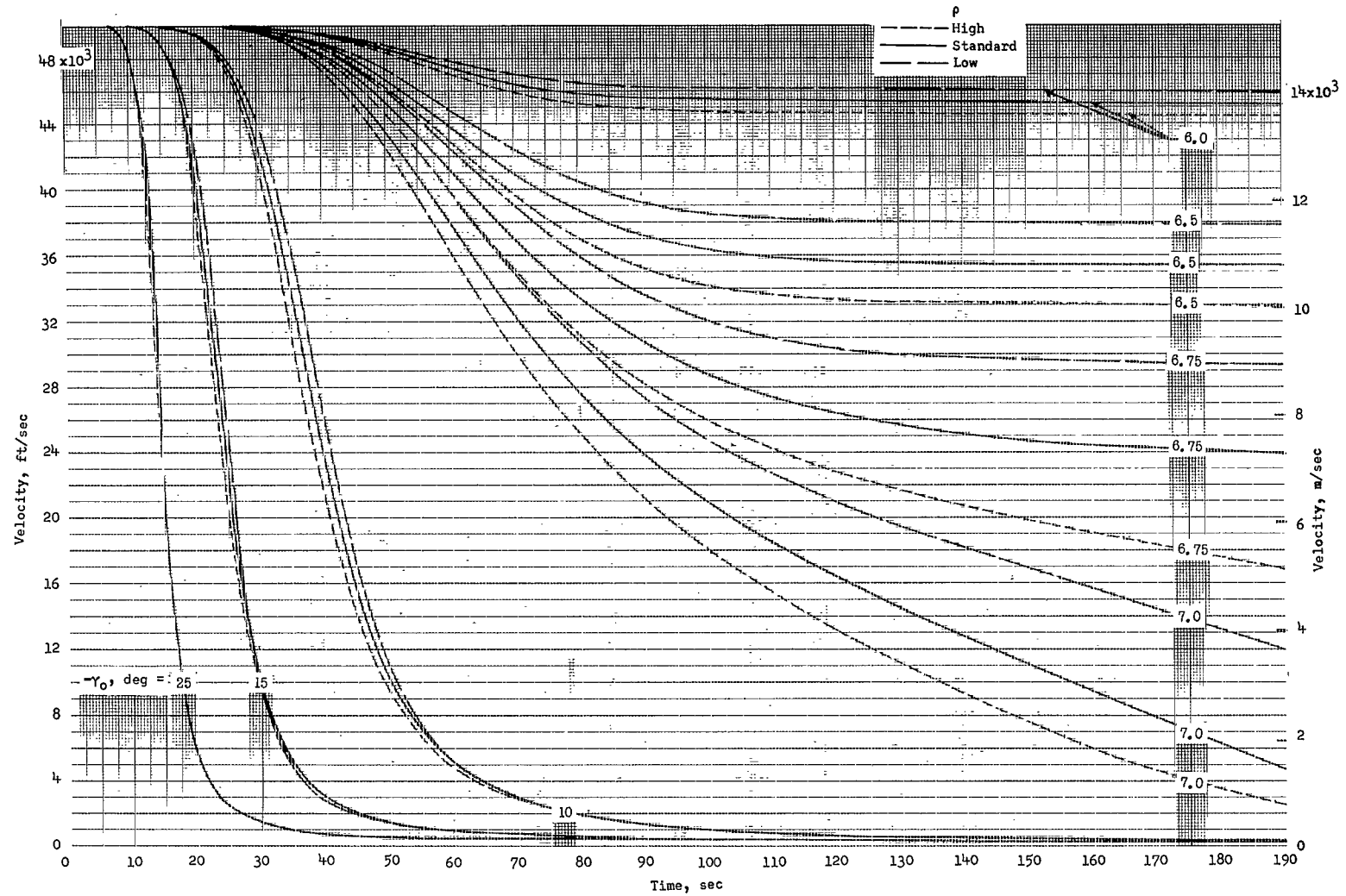(b) $\dfrac{W}{C_D A}$ = 60 lbf/ft^2 (2873 N/m^2).

Figure 22.- Concluded.

(a) $\frac{W}{C_D A}$ = 20 lbf/ft^2 (958 N/m^2).

Figure 23.- Effect of atmospheric-density perturbations on the variation of altitude with time for various initial reentry angles. V_0 = 50 000 ft/sec (15 240 m/sec).

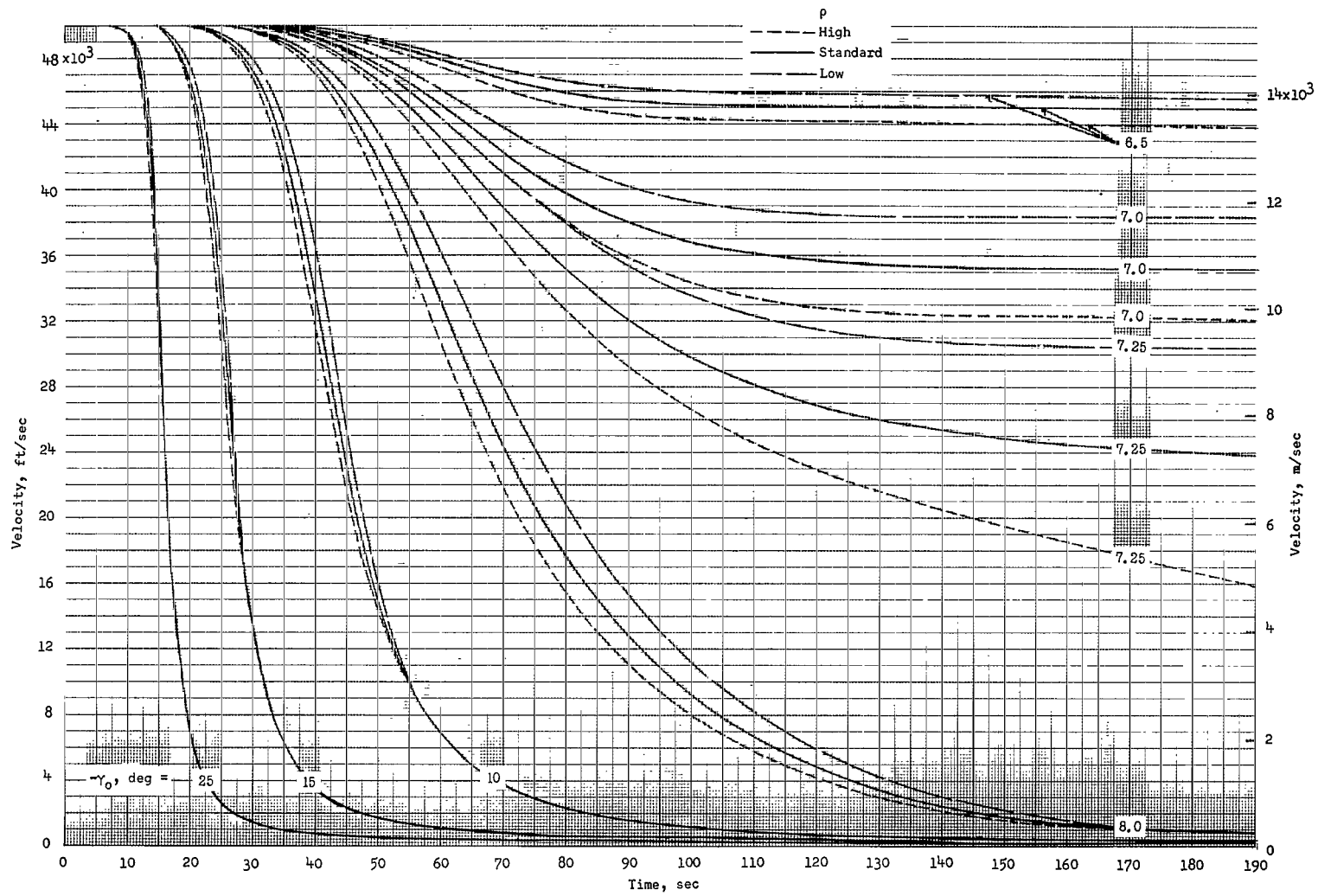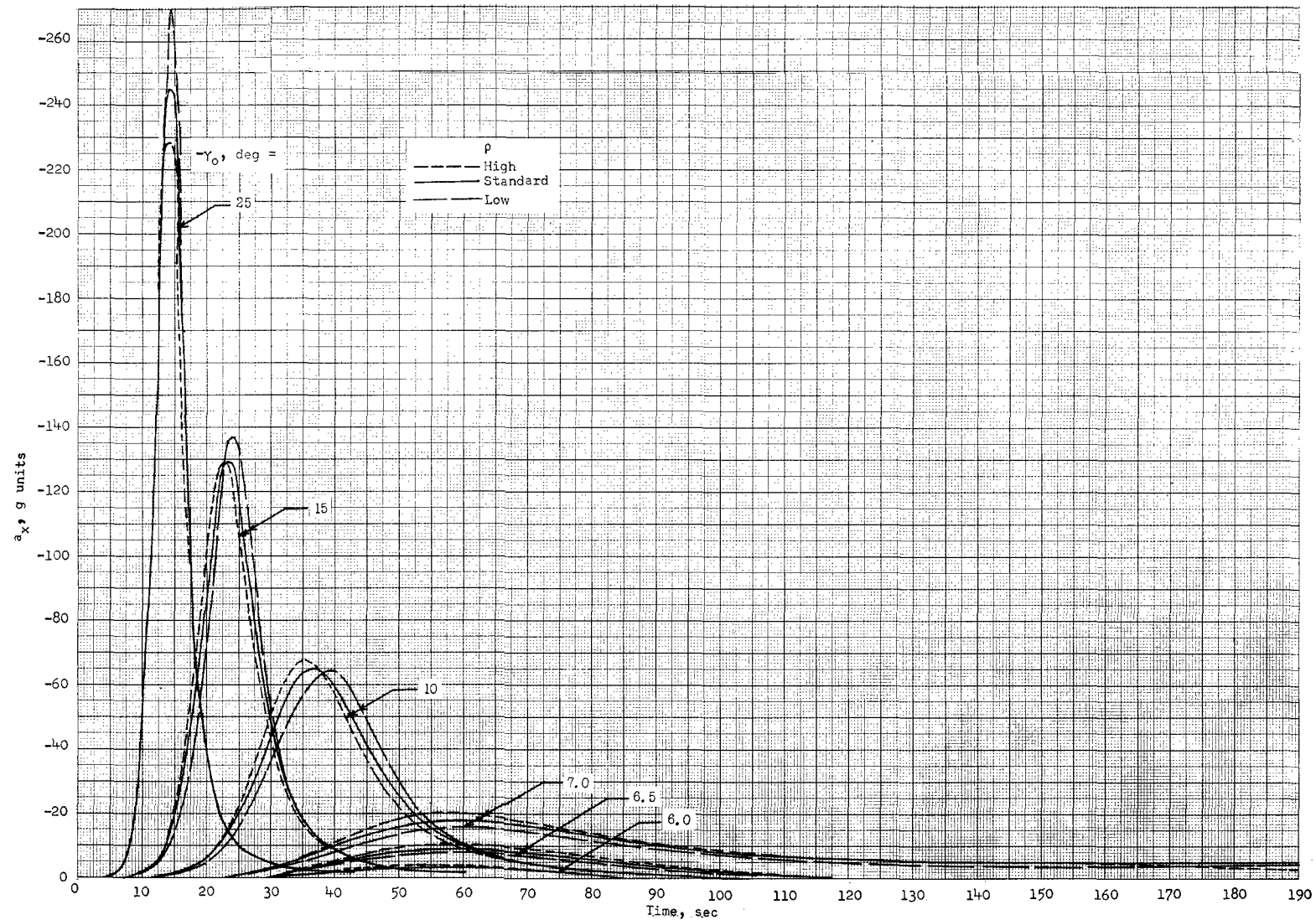(b) $\frac{W}{C_D A}$ = 60 lbf/ft^2 (2873 N/m^2).

Figure 23.- Concluded.

(a) $\frac{W}{C_D A}$ = 20 lbf/ft^2 $\left(958 \text{ N/m}^2\right)$.

Figure 24.- Effect of atmospheric-density perturbations on the variation of velocity with time for various initial reentry angles. V_0 = 50 000 ft/sec (15 240 m/sec).
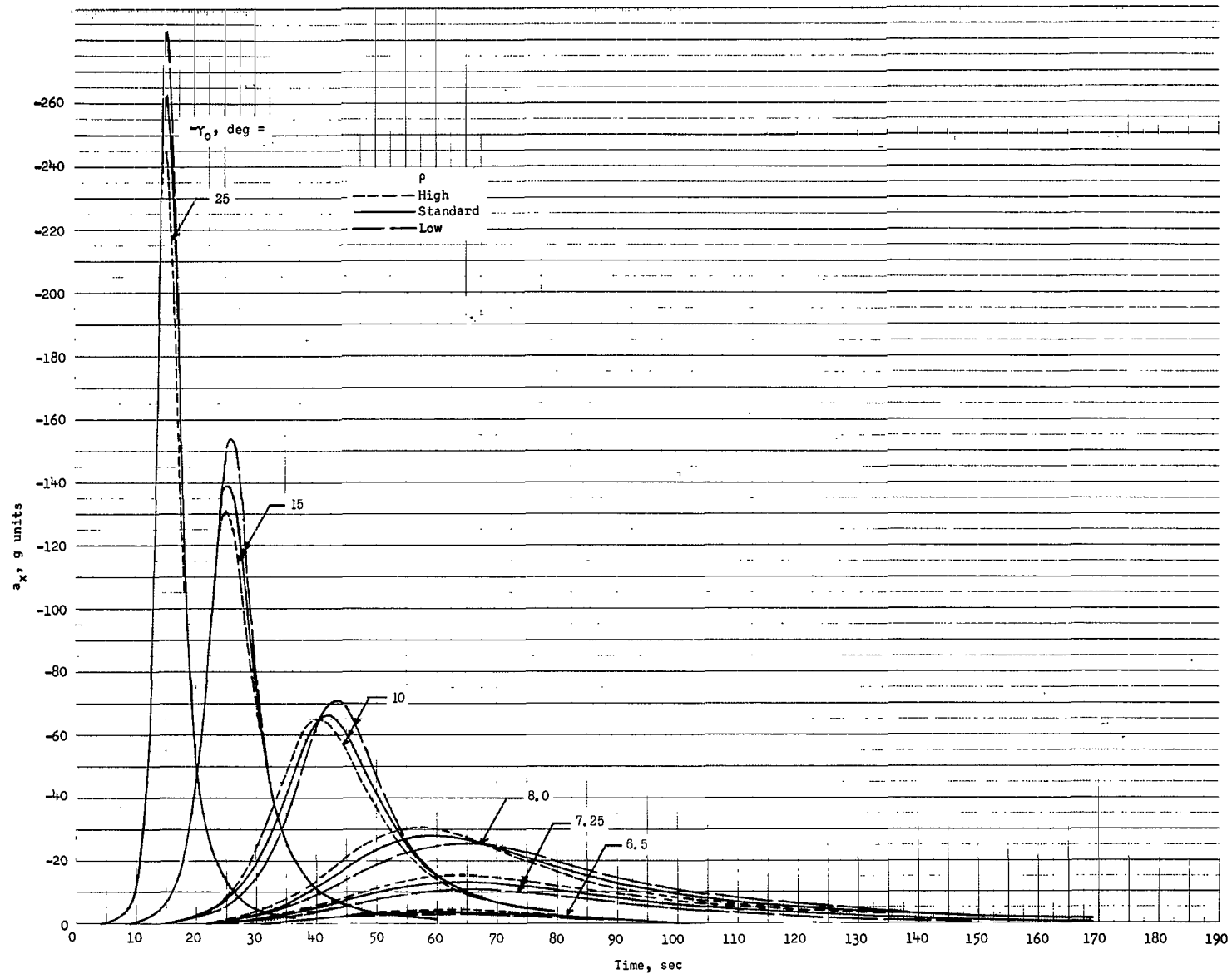
(b) $\frac{W}{C_D A} = 60 \ \text{lbf/ft}^2 \ \left(2873 \ \text{N/m}^2\right)$.

Figure 24.- Concluded.

(a) $\dfrac{W}{C_D A}$ = 20 lbf/ft^2 $\left(958 \text{ N/m}^2\right)$.

Figure 25.- Effect of atmospheric-density perturbations on the time history of acceleration along the flight path for various initial reentry angles. V_0 = 50 000 ft/sec (15 240 m/sec).

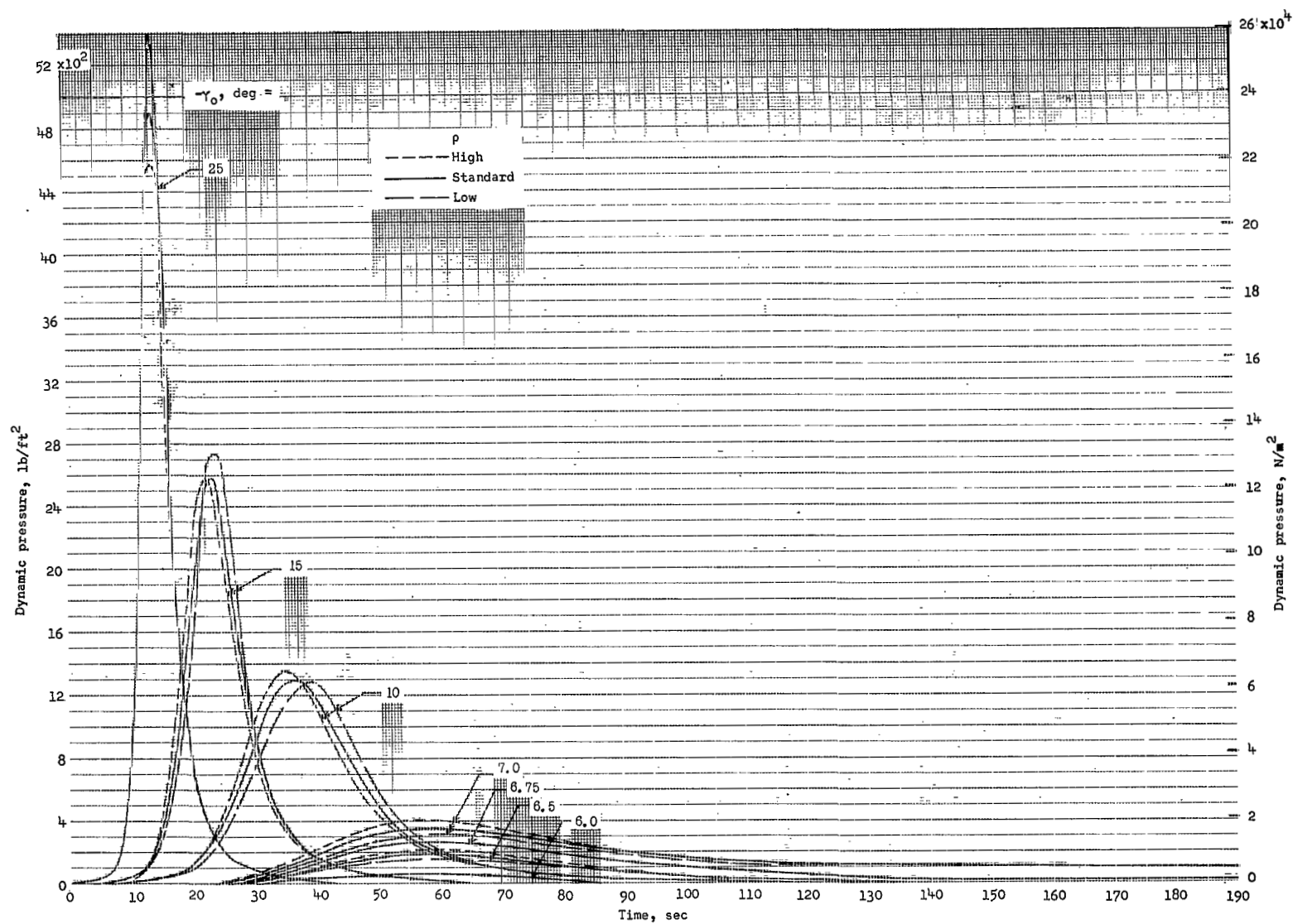(b) $\frac{W}{C_D A}$ = 60 lbf/ft^2 (2873 N/m^2).

Figure 25.- Concluded.

(a) $\dfrac{W}{C_D A}$ = 20 lbf/ft^2 $\left(958 \text{ N/m}^2\right)$.

Figure 26.- Effect of atmospheric-density perturbations on the time history of dynamic pressure for various initial reentry angles. V_0 = 50 000 ft/sec (15 240 m/sec).
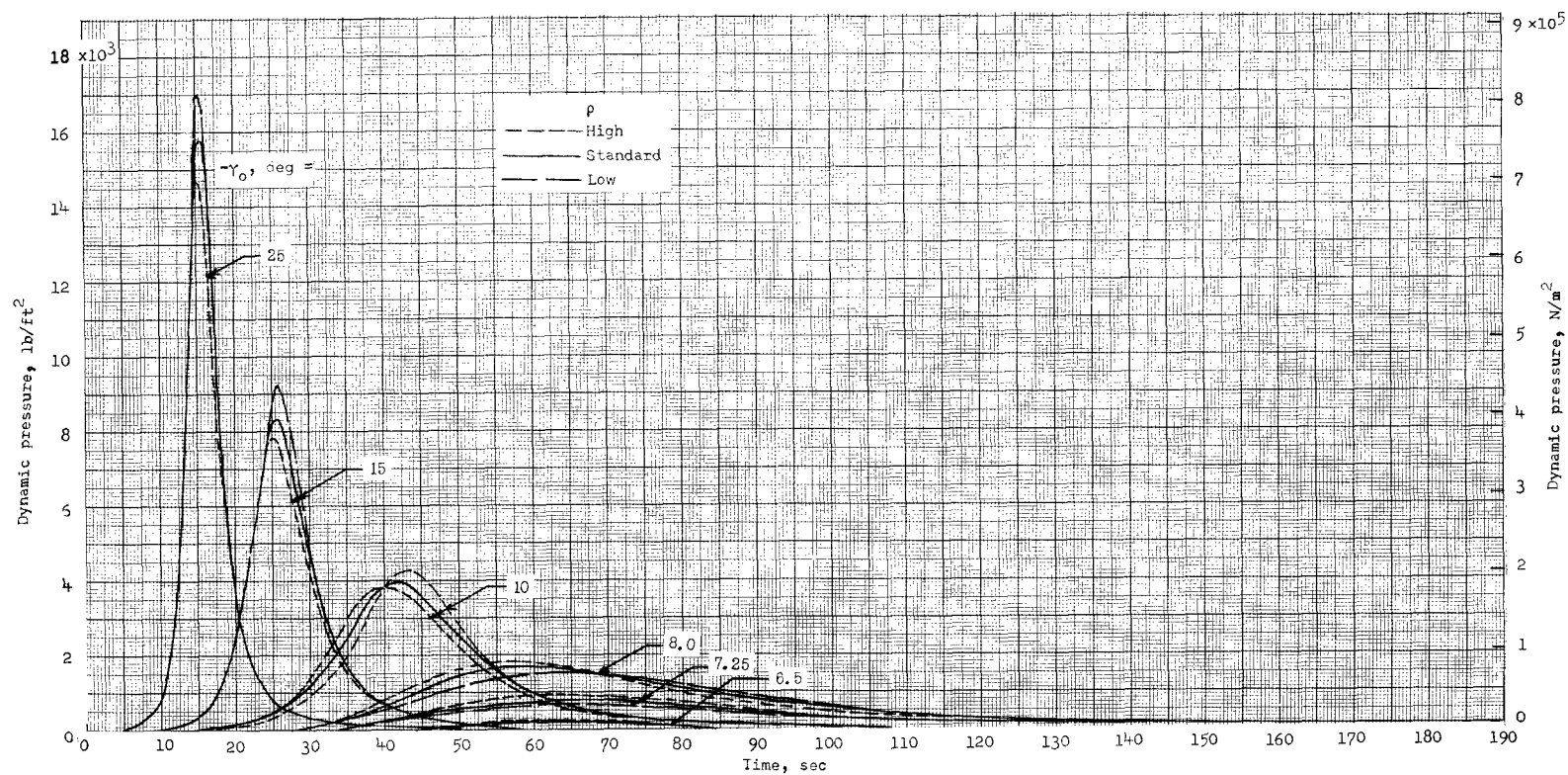
(b) $\dfrac{W}{C_D A} = 60 \ \mathrm{lbf/ft^2} \ \left(2873 \ \mathrm{N/m^2}\right)$.

Figure 26.- Concluded.

"The aeronautical and space activities of the United States shall be conducted so as to contribute . . . to the expansion of human knowledge of phenomena in the atmosphere and space. The Administration shall provide for the widest practicable and appropriate dissemination of information concerning its activities and the results thereof."

—NATIONAL AERONAUTICS AND SPACE ACT OF 1958

NASA SCIENTIFIC AND TECHNICAL PUBLICATIONS

TECHNICAL REPORTS: Scientific and technical information considered important, complete, and a lasting contribution to existing knowledge.

TECHNICAL NOTES: Information less broad in scope but nevertheless of importance as a contribution to existing knowledge.

TECHNICAL MEMORANDUMS: Information receiving limited distribution because of preliminary data, security classification, or other reasons.

CONTRACTOR REPORTS: Scientific and technical information generated under a NASA contract or grant and considered an important contribution to existing knowledge.

TECHNICAL TRANSLATIONS: Information published in a foreign language considered to merit NASA distribution in English.

SPECIAL PUBLICATIONS: Information derived from or of value to NASA activities. Publications include conference proceedings, monographs, data compilations, handbooks, sourcebooks, and special bibliographies.

TECHNOLOGY UTILIZATION PUBLICATIONS: Information on technology used by NASA that may be of particular interest in commercial and other non-aerospace applications. Publications include Tech Briefs, Technology Utilization Reports and Notes, and Technology Surveys.

Details on the availability of these publications may be obtained from:

SCIENTIFIC AND TECHNICAL INFORMATION DIVISION

NATIONAL AERONAUTICS AND SPACE ADMINISTRATION

Washington, D.C. 20546